Probing New Physics Beyond the Neutrinoless Double-Beta Decay of Ge-76

Sofia Calgaro – for the GERDA collaboration

sofia.calgaro@pd.infn.it

XX NeuTel 2023, October 25, 2023

Searching for $0\nu 2\beta$

Signature

- $2\nu 2\beta$ (SM): continuous, broad spectrum
- $0\nu 2\beta$ (BSM): peak at $Q_{\beta\beta}$ (electrons energy)

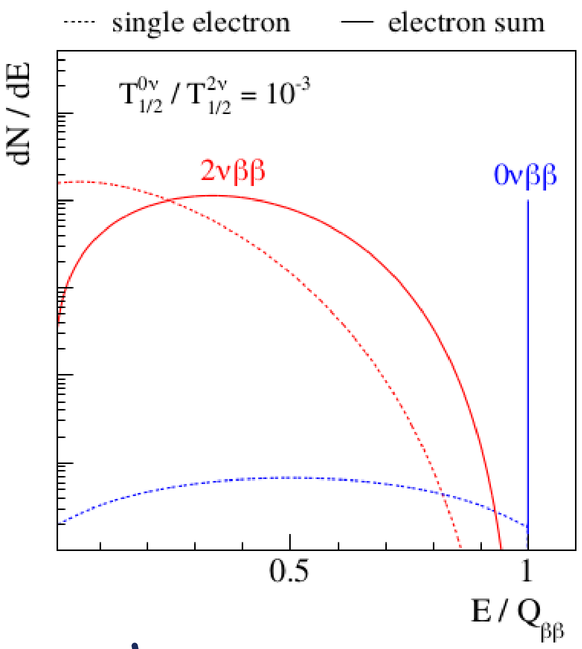

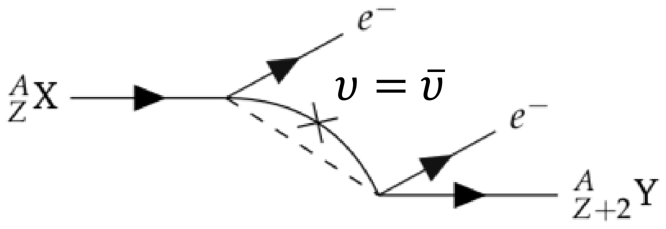

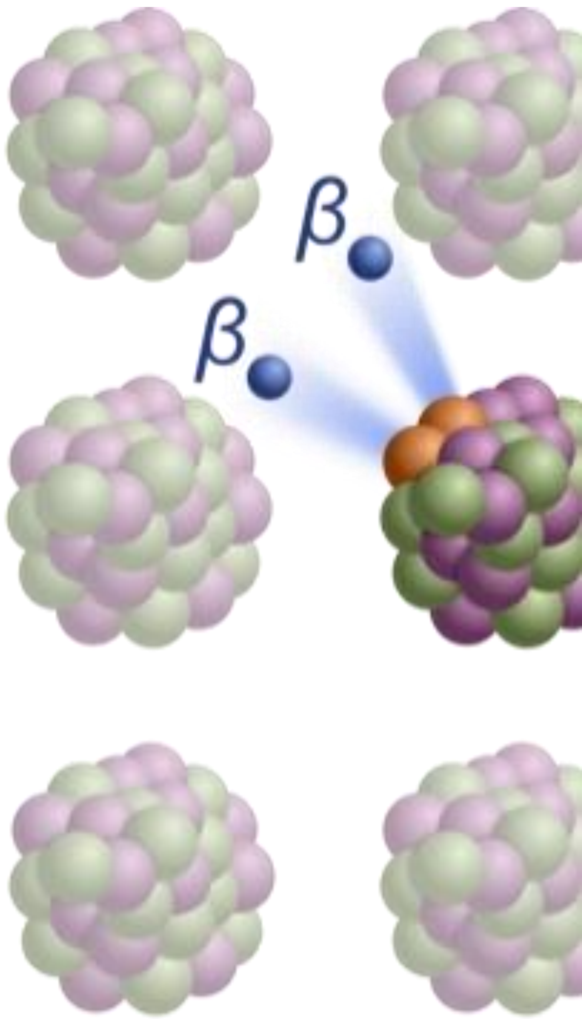

Physics Implications

- Violation of lepton number
- Nature of neutrinos (Dirac/Majorana)
- Neutrino mass scale & ordering (normal/inverted)
- Matter-antimatter asymmetry in the Universe

Searching for $0\nu2\beta$

$0\nu2\beta$ half-life

Phase-space integral

$$\left(T_{1/2}^{0\nu}\right)^{-1} = G^{0\nu}(Q_{\beta\beta}, Z)|M^{0\nu}|^2 \left(\frac{m_{\beta\beta}}{m_e}\right)^2$$

Nuclear Matrix Element

$m_{\beta\beta} = \left|\sum_i U_{ei}^2 m_i\right|$ → to compare results obtained with different isotopes

Effective Majorana neutrino Mass

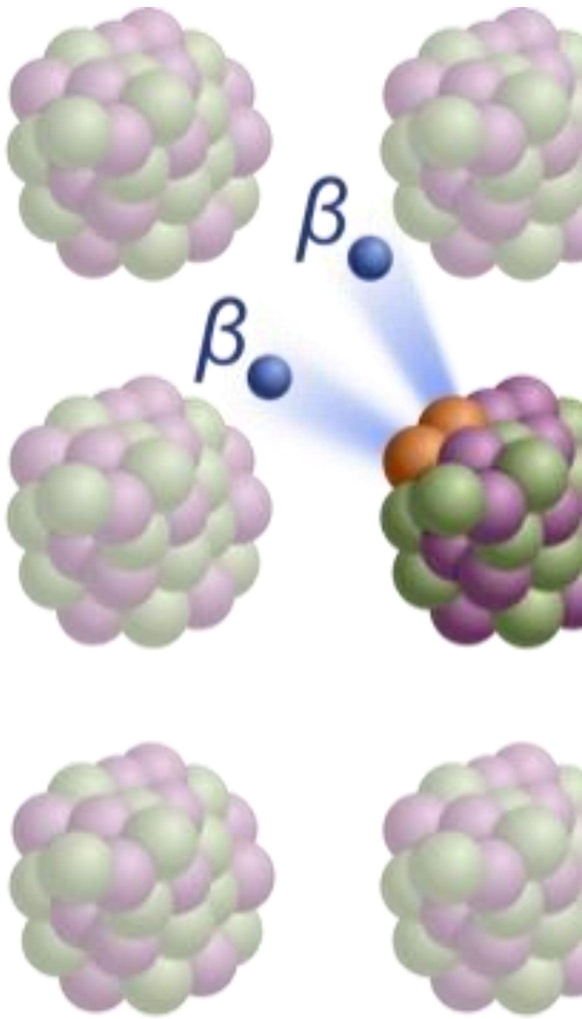

Searching for $0\nu2\beta$

$0\nu2\beta$ half-life

Phase-space integral

$$\left(T^{0\nu}_{1/2}\right)^{-1} = G^{0\nu}(Q_{\beta\beta}, Z)\,|M^{0\nu}|^2 \left(\frac{m_{\beta\beta}}{m_e}\right)^2$$

Nuclear Matrix Element

$m_{\beta\beta} = \left|\sum_i U_{ei}^2 m_i\right|$ → to compare results obtained with different isotopes

Effective Majorana neutrino Mass

GERmanium Detector Array
demonstrated that operating
<u>bare germanium detectors in LAr</u>
is feasible and leads to a significant bkg reduction

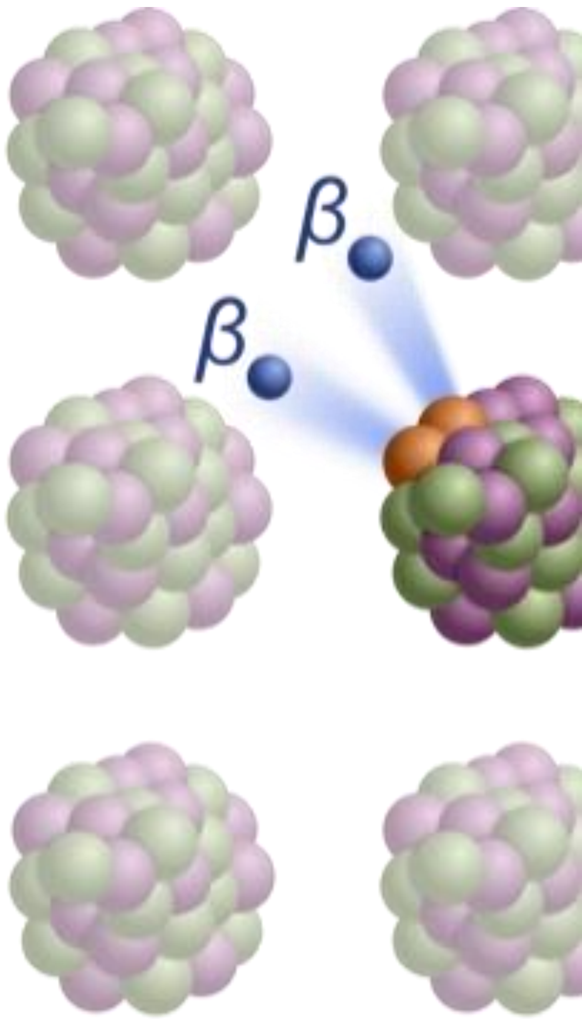

Searching for $0\nu2\beta$

$0\nu2\beta$ half-life

Phase-space integral

$$\left(T_{1/2}^{0\nu}\right)^{-1} = G^{0\nu}(Q_{\beta\beta}, Z)|M^{0\nu}|^2 \left(\frac{m_{\beta\beta}}{m_e}\right)^2$$

Nuclear Matrix Element

$m_{\beta\beta} = |\sum_i U_{ei}^2 m_i|$ → to compare results obtained with different isotopes

Effective Majorana neutrino Mass

GERmanium Detector Array
demonstrated that operating
<u>bare germanium detectors in LAr</u>
is feasible and leads to a significant bkg reduction

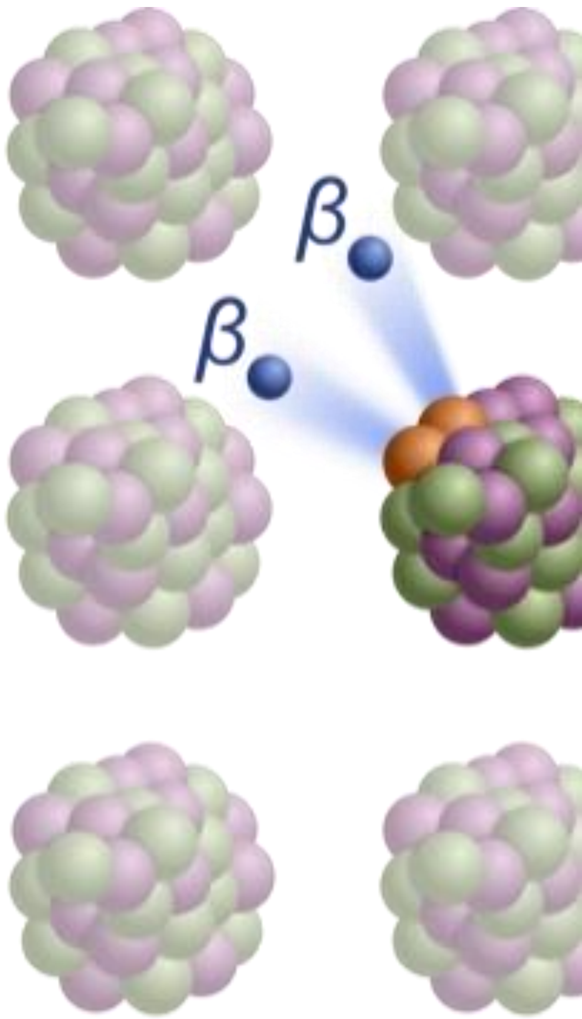

$0\nu2\beta$ half-life sensitivity

$$T_{1/2}^{0\nu} \propto \begin{cases} \epsilon \cdot f \cdot \sqrt{\dfrac{\varepsilon}{BI \cdot \Delta E}} & \text{with bkg} \\ \epsilon \cdot f \cdot \varepsilon & \text{without bkg} \end{cases}$$

ϵ: efficiency
f: isotopic fraction
$\varepsilon = M \cdot t$: exposure
ΔE: energetic resolution at $Q_{\beta\beta}$
BI: bkg index

GERDA Approach

GERMANIUM, $^{76}_{32}\mathbf{Ge} \rightarrow {}^{76}_{34}\mathbf{Se} + \mathbf{2e^-}\ [+\mathbf{2\bar{\nu}_e}]$

$Q_{\beta\beta}(^{76}\mathrm{Ge}) = 2039.061 \pm 0.007\ \mathrm{keV}$

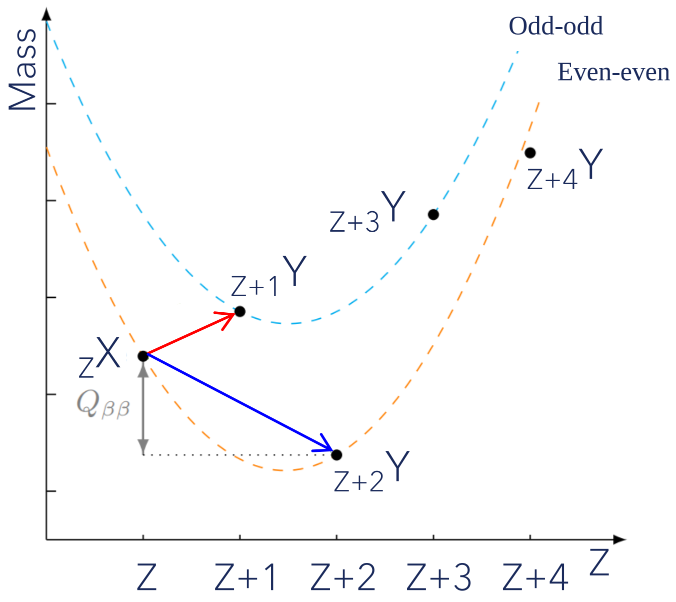

GERDA Approach

GERMANIUM, $^{76}_{32}\mathbf{Ge} \rightarrow {}^{76}_{34}\mathbf{Se} + \mathbf{2e^-}\ [+\mathbf{2\bar{\nu}_e}]$

$$Q_{\beta\beta}(^{76}\text{Ge}) = 2039.061 \pm 0.007\ \text{keV}$$

- Source ≡ detector ⟹ high detection efficiency
- Ge: high purity ⟹ low intrinsic background
- Excellent energetic resolution ⟹ $\mathbf{FWHM \sim 0.1\%}$ @ $Q_{\beta\beta}$

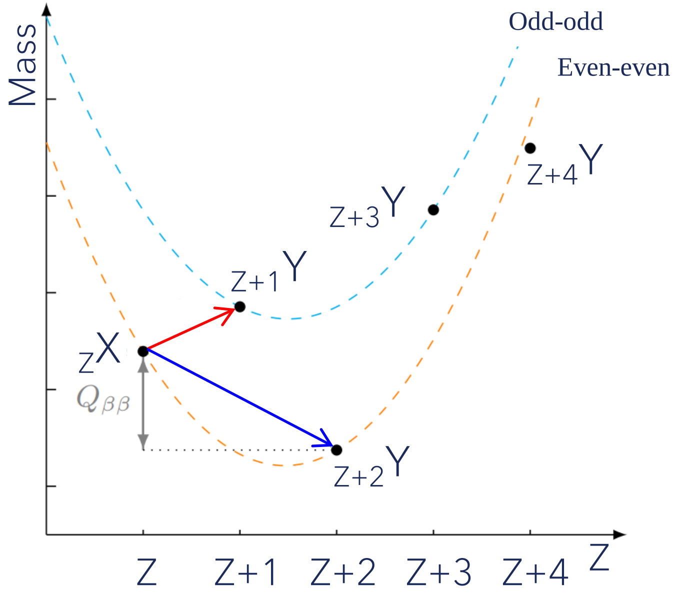

GERDA Approach

GERMANIUM, $^{76}_{32}\mathbf{Ge} \rightarrow {}^{76}_{34}\mathbf{Se} + \mathbf{2e^-}\ [+\mathbf{2\bar{\nu}_e}]$

$Q_{\beta\beta}(^{76}\text{Ge}) = 2039.061 \pm 0.007\ \text{keV}$

- Source ≡ detector ⟹ high detection efficiency
- Ge: high purity ⟹ low intrinsic background
- Excellent energetic resolution ⟹ $\mathbf{FWHM \sim 0.1\%}$ @ $Q_{\beta\beta}$
- Low $\boldsymbol{Q_{\beta\beta}}$ ⟹ difficult to reach low bkg levels
- $\boldsymbol{f_{76}^{nat}}$~**8%** ⟹ enrichment in Ge-76 is necessary

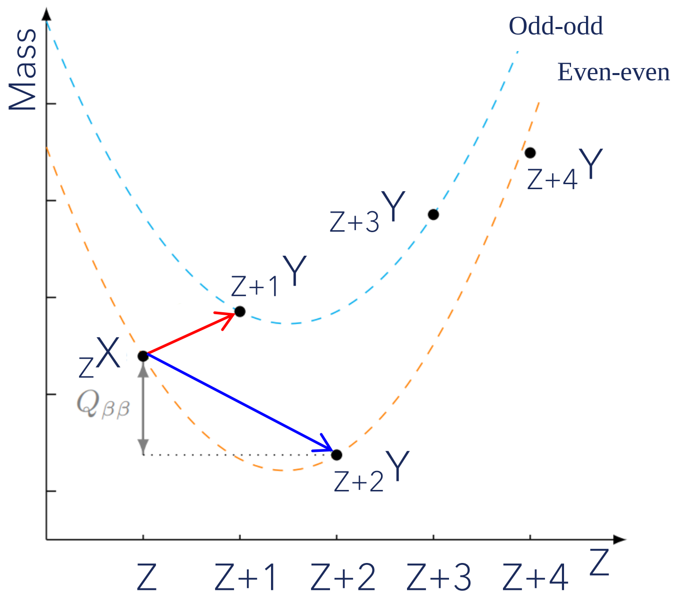

GERDA Approach

GERMANIUM, $^{76}_{32}\mathbf{Ge} \rightarrow {}^{76}_{34}\mathbf{Se} + 2\mathbf{e}^- \; [+2\bar{\nu}_\mathbf{e}]$

$$Q_{\beta\beta}(^{76}\text{Ge}) = 2039.061 \pm 0.007\ \text{keV}$$

- Source ≡ detector ⟹ high detection efficiency
- Ge: high purity ⟹ low intrinsic background
- Excellent energetic resolution ⟹ $\mathbf{FWHM \sim 0.1\%\ @\ } Q_{\beta\beta}$
- Low $\boldsymbol{Q_{\beta\beta}}$ ⟹ difficult to reach low bkg levels
- $\boldsymbol{f_{76}^{nat}}$~**8%** ⟹ enrichment in Ge-76 is necessary

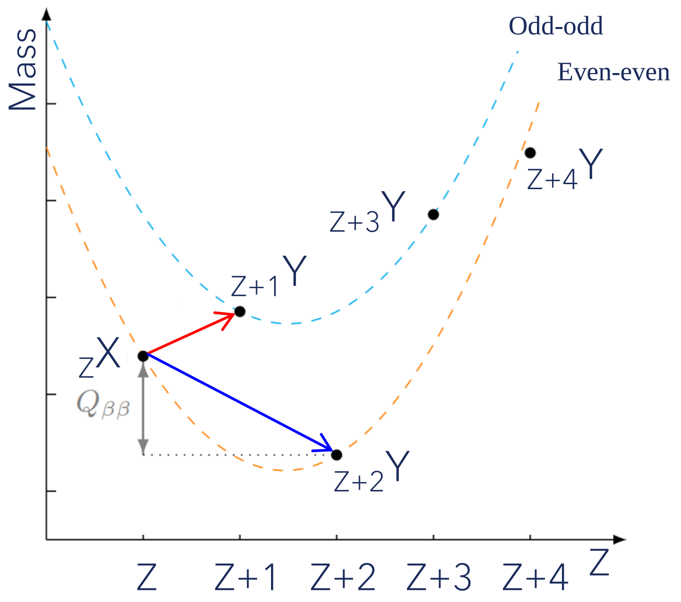

- p+ (implanted B) & n+ (diffused Li), passivated groove
- Fully depleted crystals
- Different geometries: BEGe, coaxials, IC
- Mass: ~0.4-3 kg
- Event topology discrimination: Pulse Shape Discrimination (PSD)

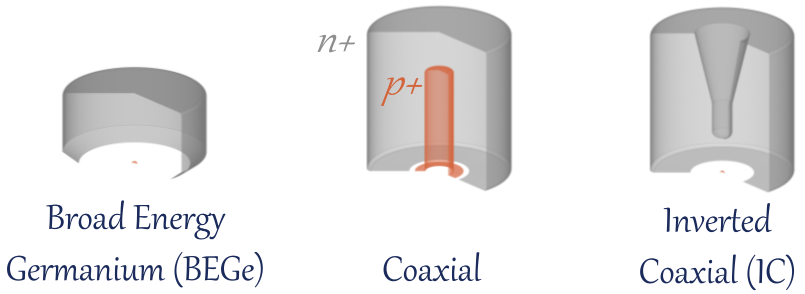

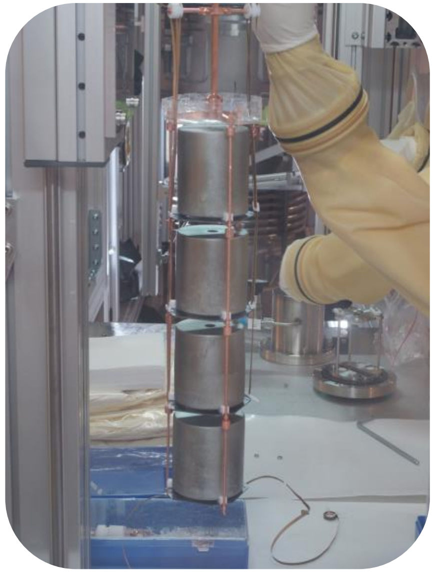

GERDA Approach

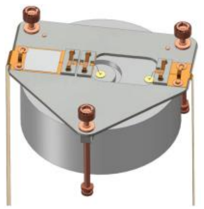

Ge-76 enriched detectors
(f_{76}~87%)

Detectors array
(7 strings)

GERDA Approach

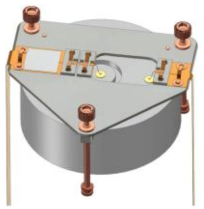

Ge-76 enriched detectors (f_{76}~87%)

Detectors array (7 strings)

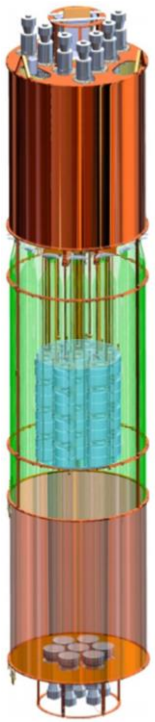

LAr veto

- SiPMs coupled to WLS fibers
- 9 + 7 PMTs

GERDA Approach

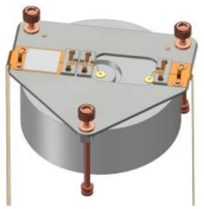

Ge-76 enriched detectors
(f_{76}~87%)

Detectors array
(7 strings)

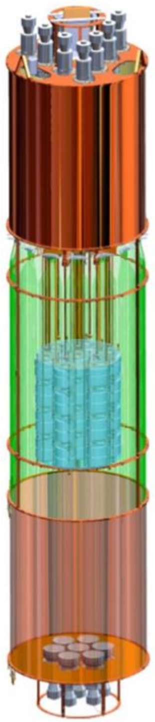

LAr veto
- SiPMs coupled to WLS fibers
- 9 + 7 PMTs

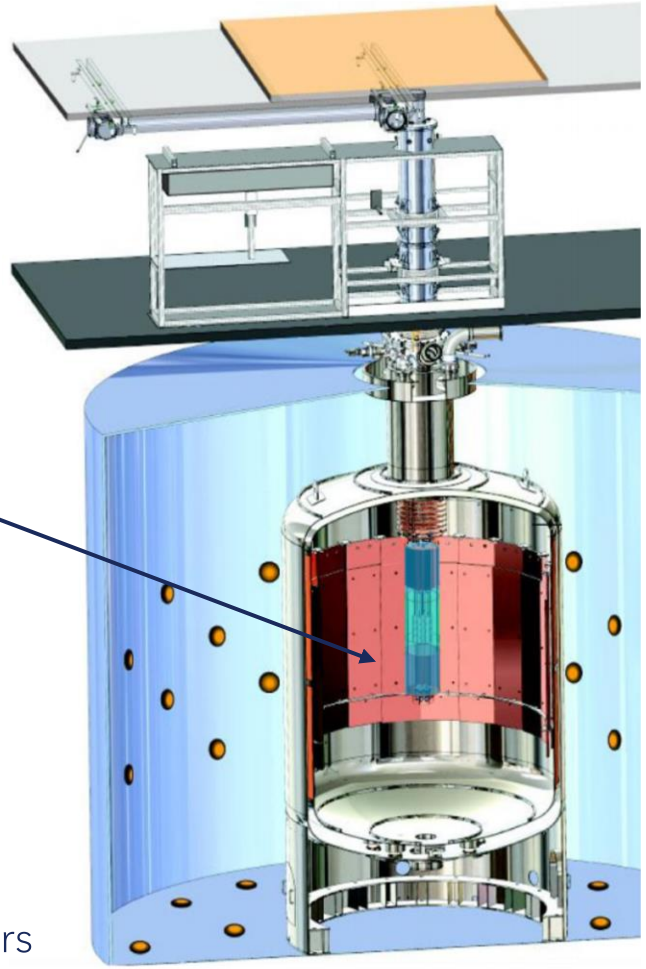

LAr cryostat
- 64 m^3, Ø 4m, H 5.88m

GERDA Approach

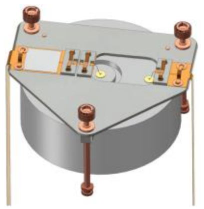

Ge-76 enriched detectors
(f_{76}~87%)

Detectors array
(7 strings)

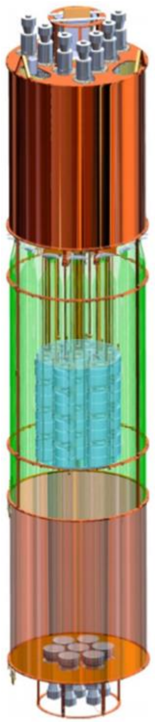

LAr veto
- SiPMs coupled to WLS fibers
- 9 + 7 PMTs

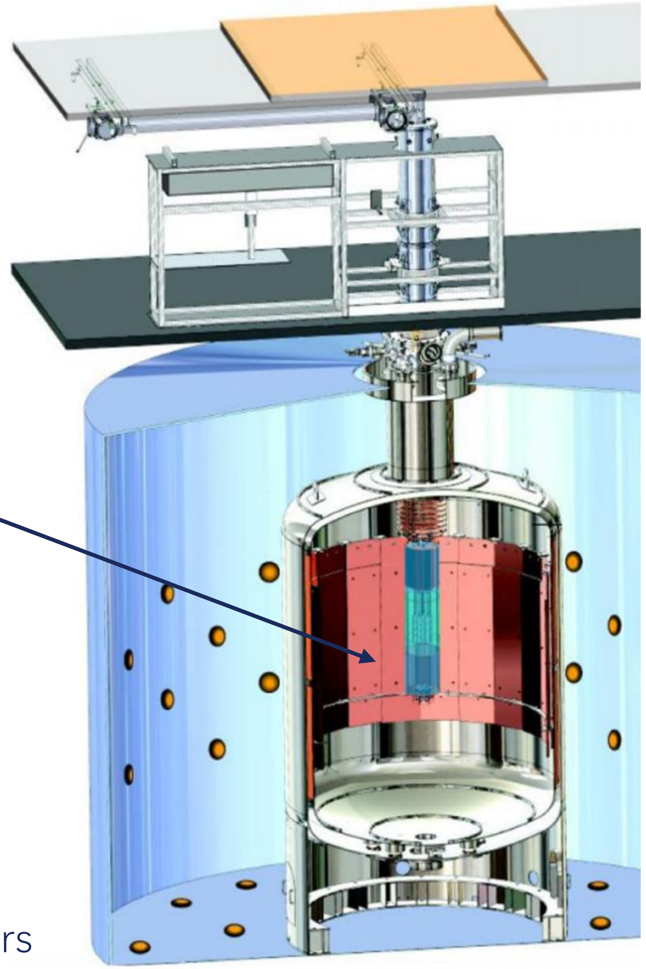

LAr cryostat
- 64 m^3, Ø 4m, H 5.88m

Ultrapure water tank
- 66 PMTs + plastic scintillators
- 590 m^3, Ø 10m, H 8.5 m

GERDA Approach

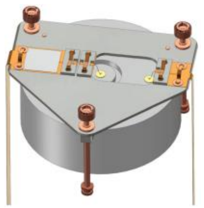

Ge-76 enriched detectors (f_{76}~87%)

Detectors array (7 strings)

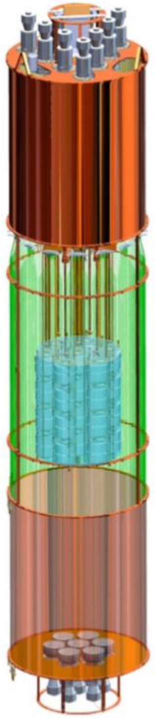

LAr veto
- SiPMs coupled to WLS fibers
- 9 + 7 PMTs

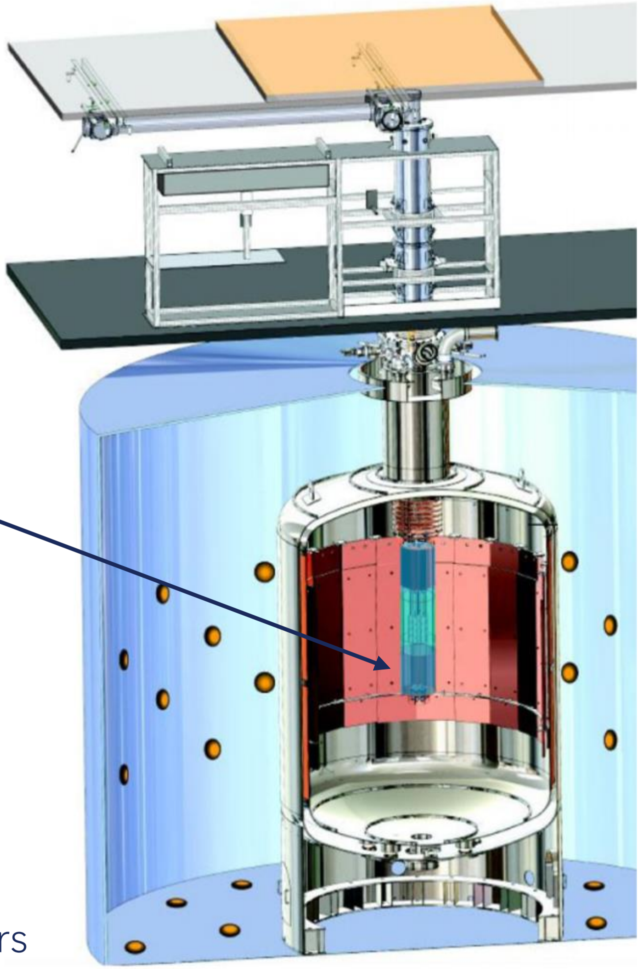

LAr cryostat
- 64 m^3, Ø 4m, H 5.88m

Ultrapure water tank
- 66 PMTs + plastic scintillators
- 590 m^3, Ø 10m, H 8.5 m

muon flux ~1.25/m^{2}h

Background Reduction Efficiencies

Analysis Cuts

- Quality cuts (no baselines, test pulses R=0.05 Hz, pile-ups) ~99.9%

Background Reduction Efficiencies

Analysis Cuts

- Quality cuts (no baselines, test pulses R=0.05 Hz, pile-ups) ~99.9%
- Muon veto ~99%
- LAr veto ~98%

Background Reduction Efficiencies

Analysis Cuts

- Quality cuts (no baselines, test pulses R=0.05 Hz, pile-ups) ~99.9%
- Muon veto ~99%
- LAr veto ~98%
- Multiplicity (M) 1 events ~100%

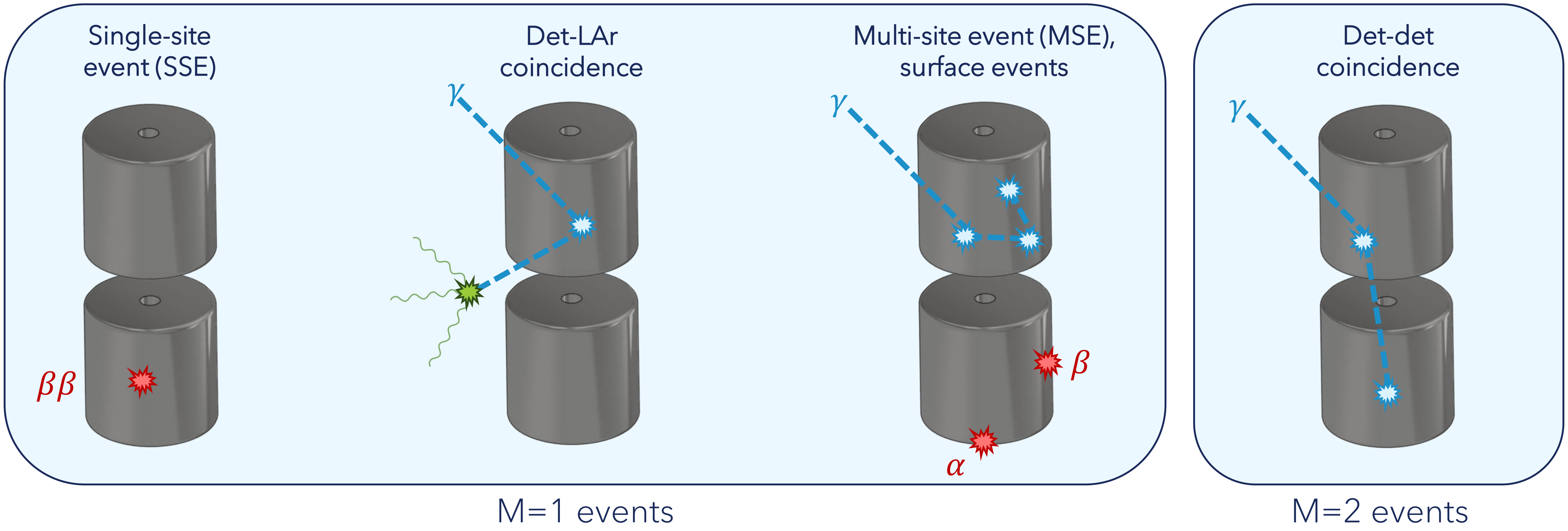

Background Reduction Efficiencies

Analysis Cuts

- Quality cuts (no baselines, test pulses R=0.05 Hz, pile-ups) ~99.9%
- Muon veto ~99%
- LAr veto ~98%
- Multiplicity (M) 1 events ~100%
- PSD cut for $0\nu2\beta$ ~69-90%

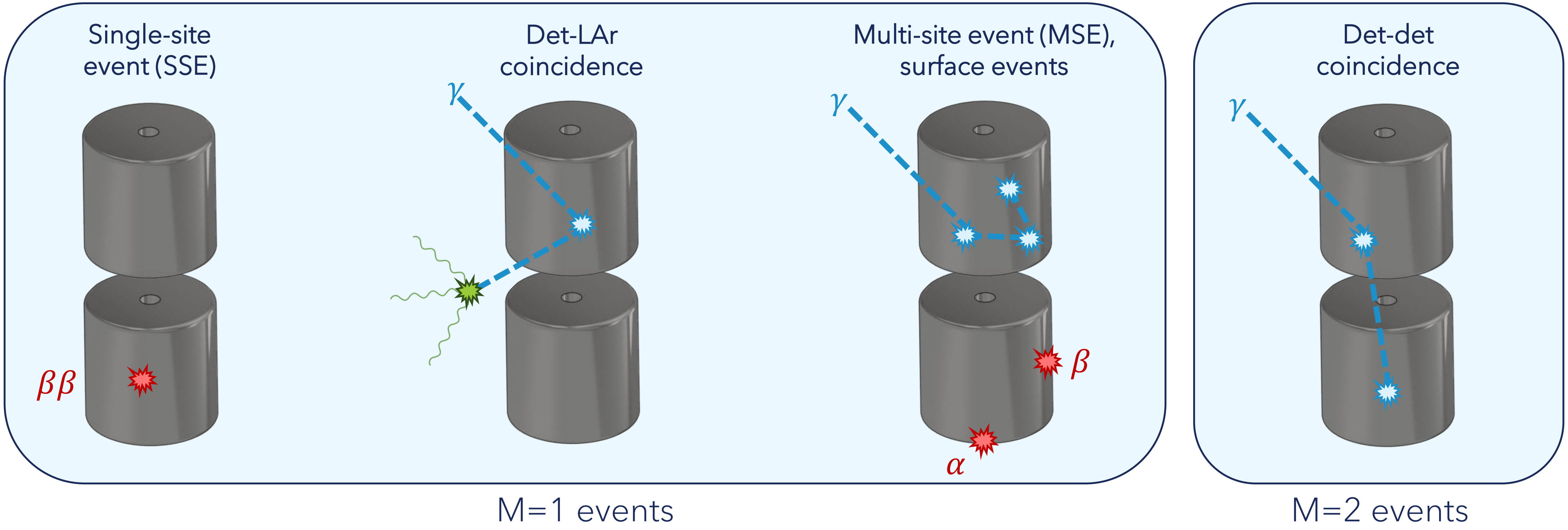

Exposure

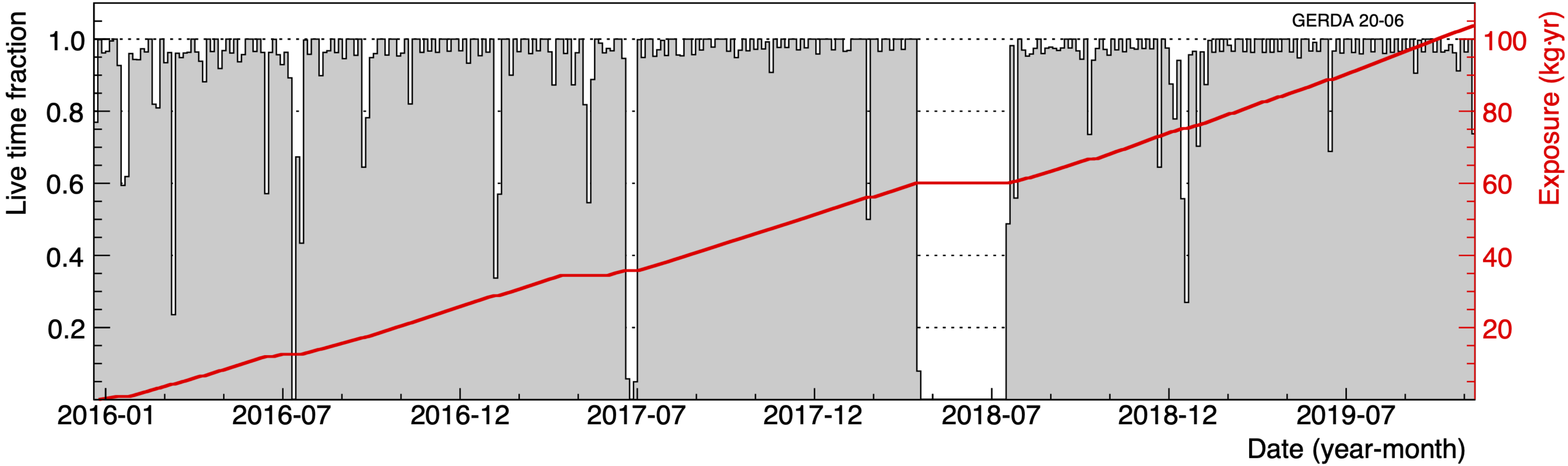

Phase I (Nov. 2011 – Sep. 2013): 23.5 kg yr
Phase II (Dec. 2015 – Nov. 2019): 103.7 kg yr
Total: 127.2 kg yr

Exposure

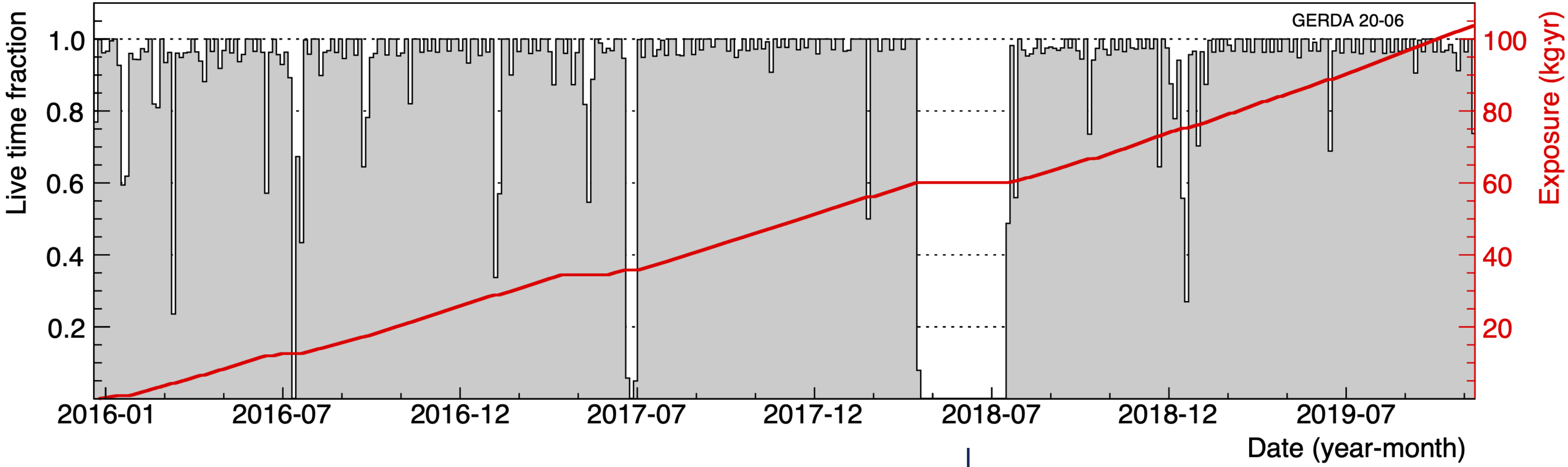

Upgrade in summer 2018 (Phase "II+")

+ inner fiber shroud

+ 5 new ICs

Phase I (Nov. 2011 – Sep. 2013): 23.5 kg yr
Phase II (Dec. 2015 – Nov. 2019): 103.7 kg yr
Total: 127.2 kg yr

Exposure

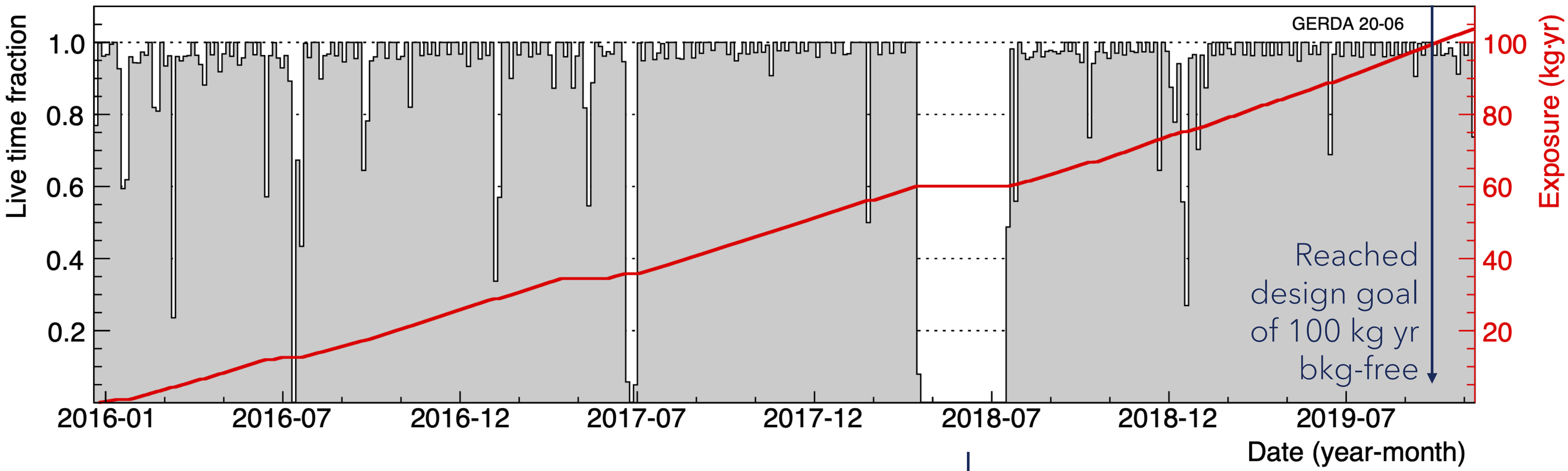

Phase I (Nov. 2011 – Sep. 2013): 23.5 kg yr
Phase II (Dec. 2015 – Nov. 2019): 103.7 kg yr
Total: 127.2 kg yr

Upgrade in summer 2018 (Phase "II+")

+ inner fiber shroud

+ 5 new ICs

Final 0ν2β Results

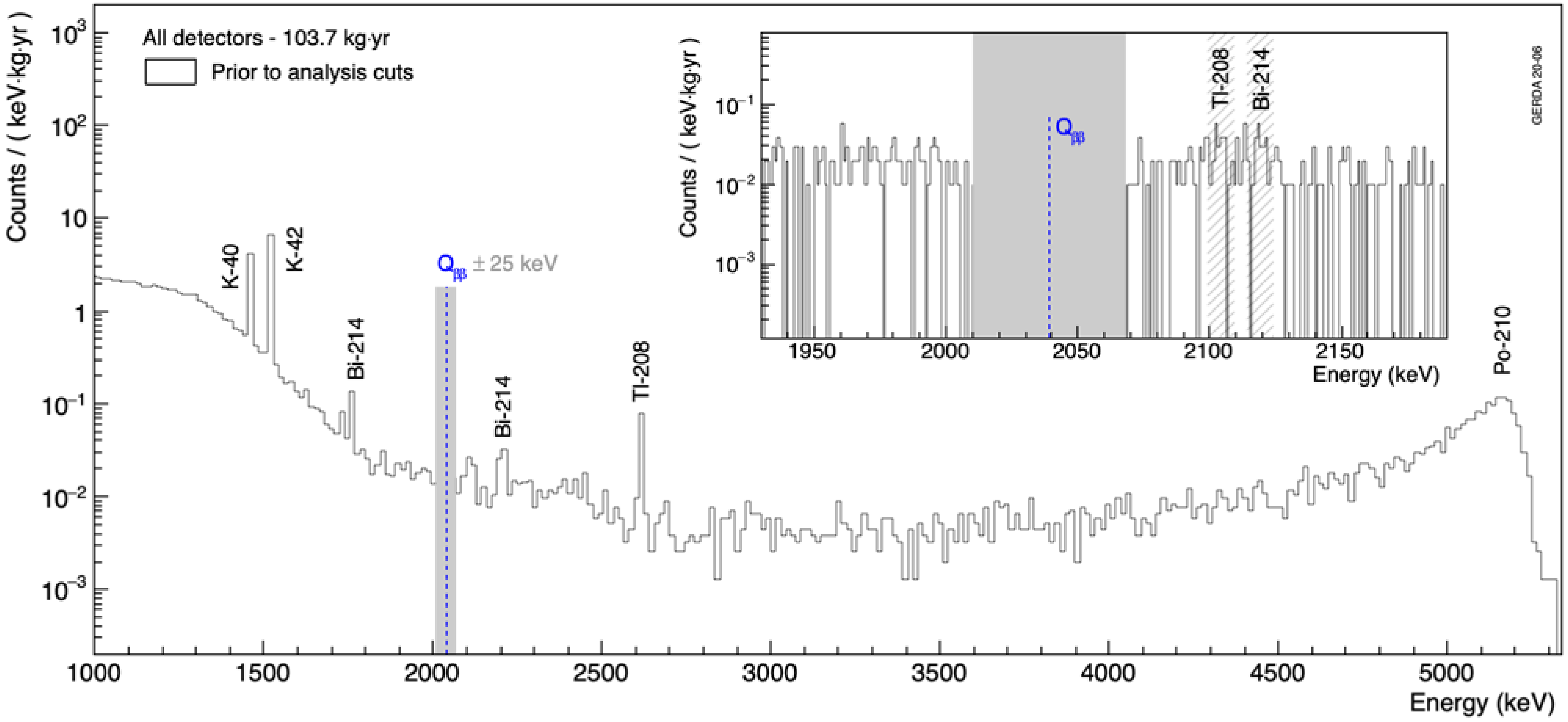

Blind analysis in $Q_{\beta\beta}(^{76}\mathrm{Ge}) \pm 25$ keV

PRL 125 (2020) 252502

Final $0\nu2\beta$ Results

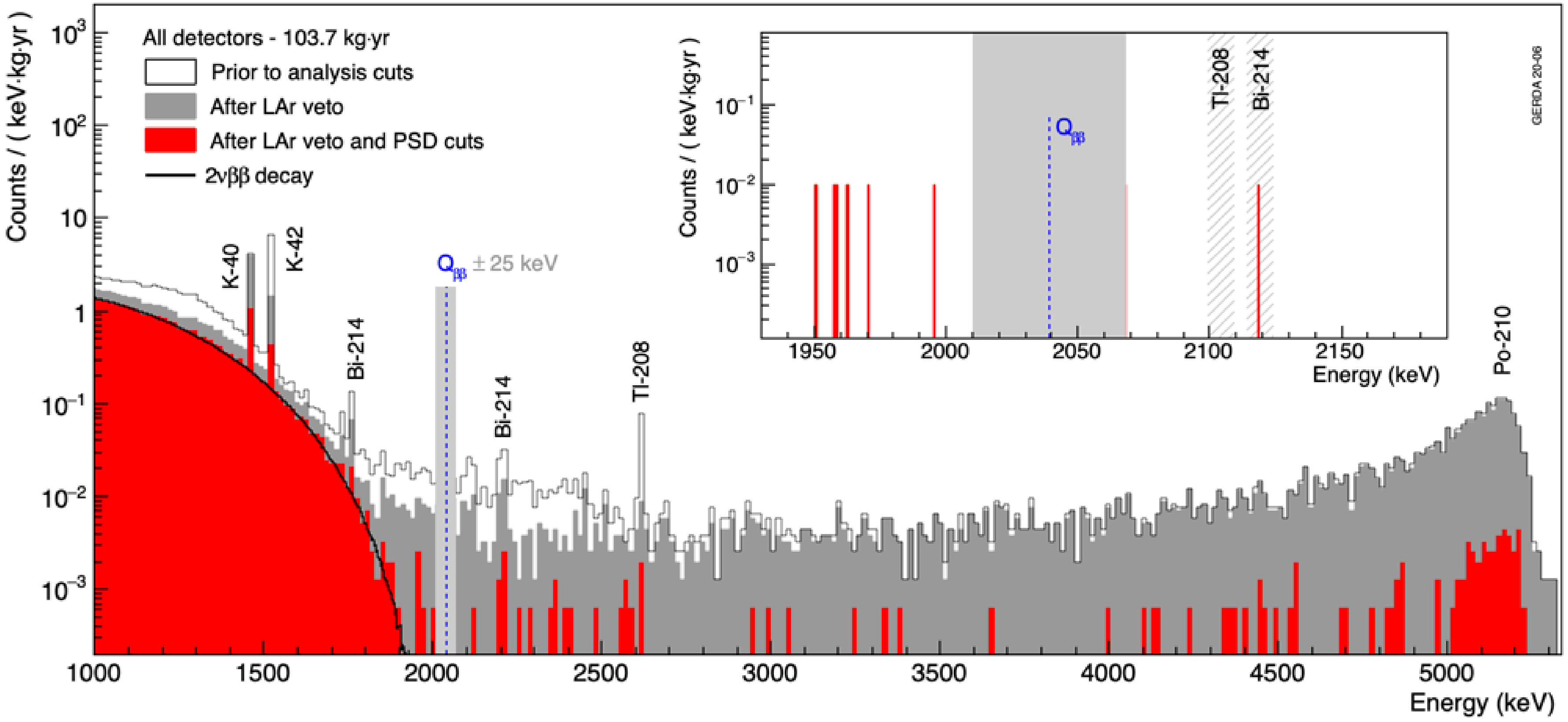

Blind analysis in $Q_{\beta\beta}(^{76}\mathrm{Ge}) \pm 25$ keV

PRL 125 (2020) 252502

Final 0ν2β Results

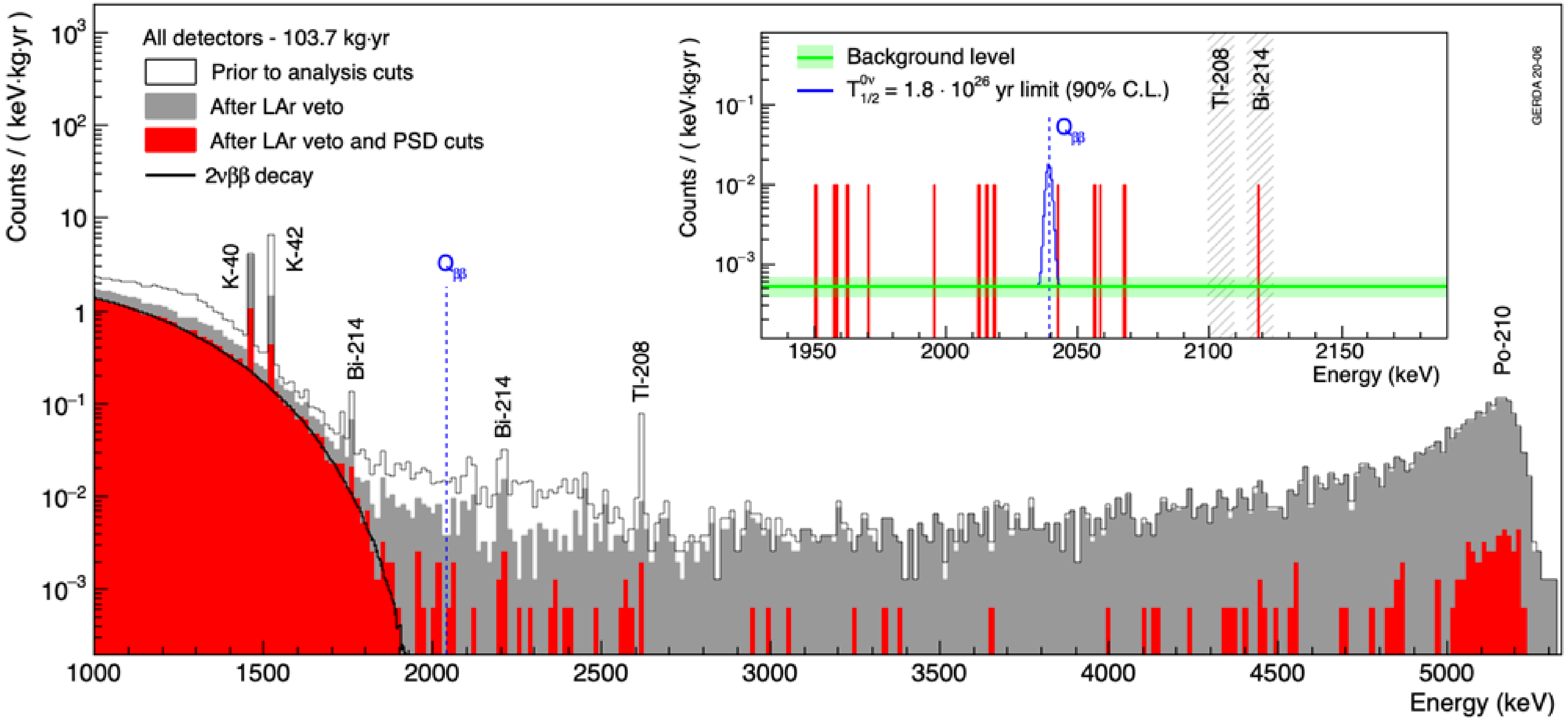

PRL 125 (2020) 252502

Final $0\nu2\beta$ Results

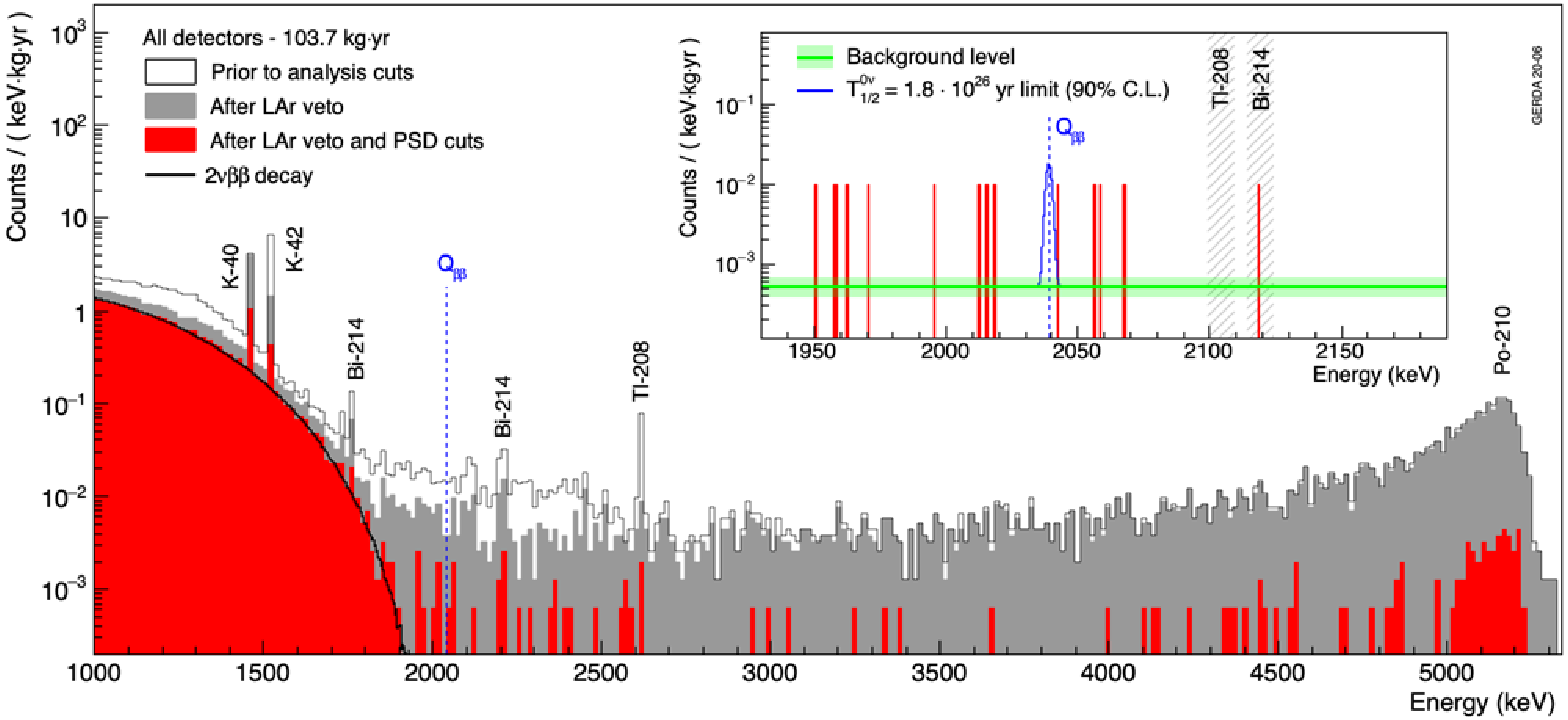

	Goal	Results
Background	$< 10^{-3}$ cts/(keV · kg · yr)	$5.2^{+1.6}_{-1.3} \cdot 10^{-4}$ cts/(keV · kg · yr)
Exposure	> 100 kg yr	103.7 kg yr
$T_{1/2}$ sensitivity	10^{26} yr	1.8×10^{26} yr @ 90% CL $m_{\beta\beta} < 79 - 180$ meV @ 90% CL

PRL 125 (2020) 252502

Final 0ν2β Results

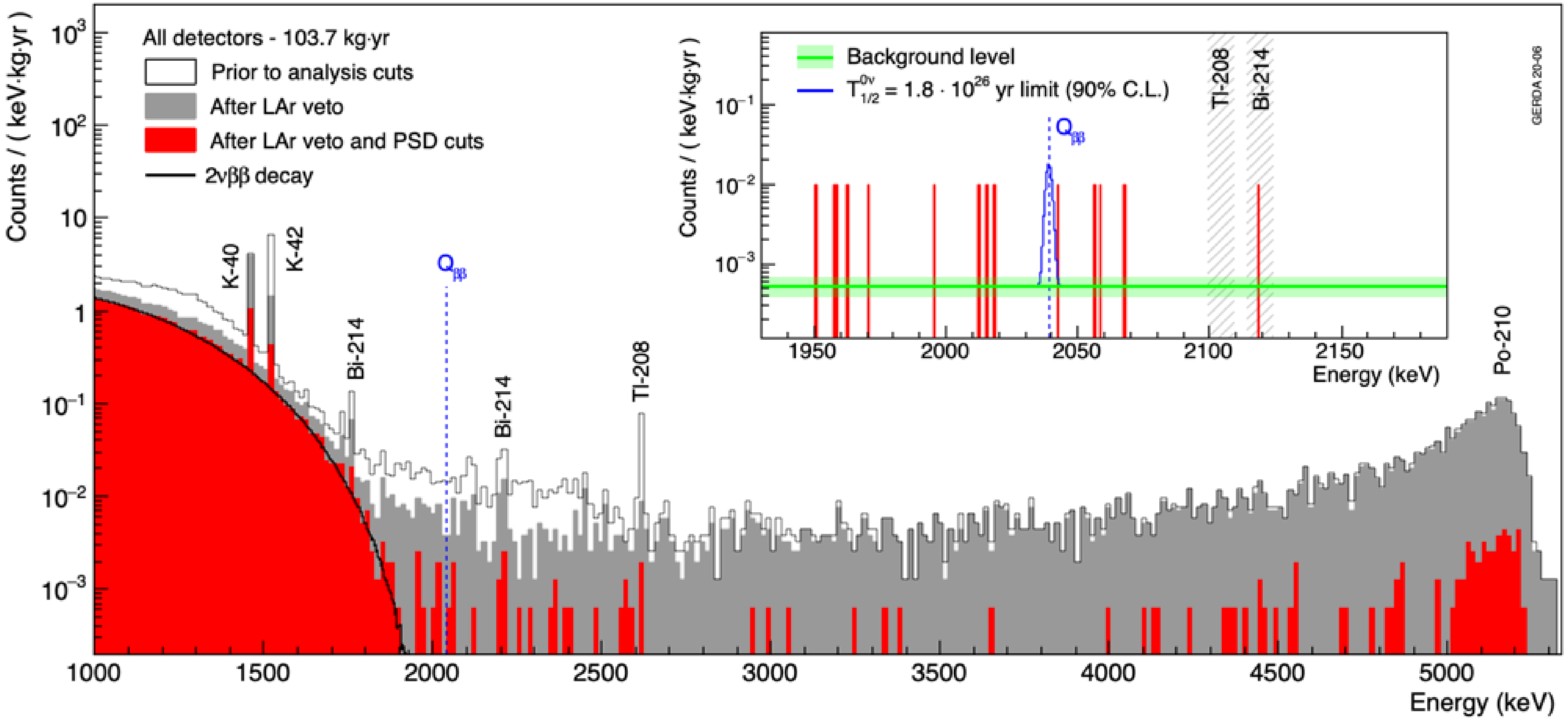

	Goal	Results
Background	$< 10^{-3}$ cts/(keV · kg · yr)	$5.2^{+1.6}_{-1.3} \cdot 10^{-4}$ cts/(keV · kg · yr)
Exposure	> 100 kg yr	103.7 kg yr
$T_{1/2}$ sensitivity	10^{26} yr	1.8×10^{26} yr @ 90% CL $m_{\beta\beta} < 79 - 180$ meV @ 90% CL

All design goals were reached and surpassed

PRL 125 (2020) 252502

Exotic Searches in $2\nu2\beta$ Decays

$$T^{2\nu}_{\frac{1}{2}}(^{76}\text{Ge}) = (2.022 \pm 0.018_{\text{stat}} \pm 0.038_{\text{syst}}) \times 10^{21}\ \text{yr}$$

PRL 131 (2023) 142501

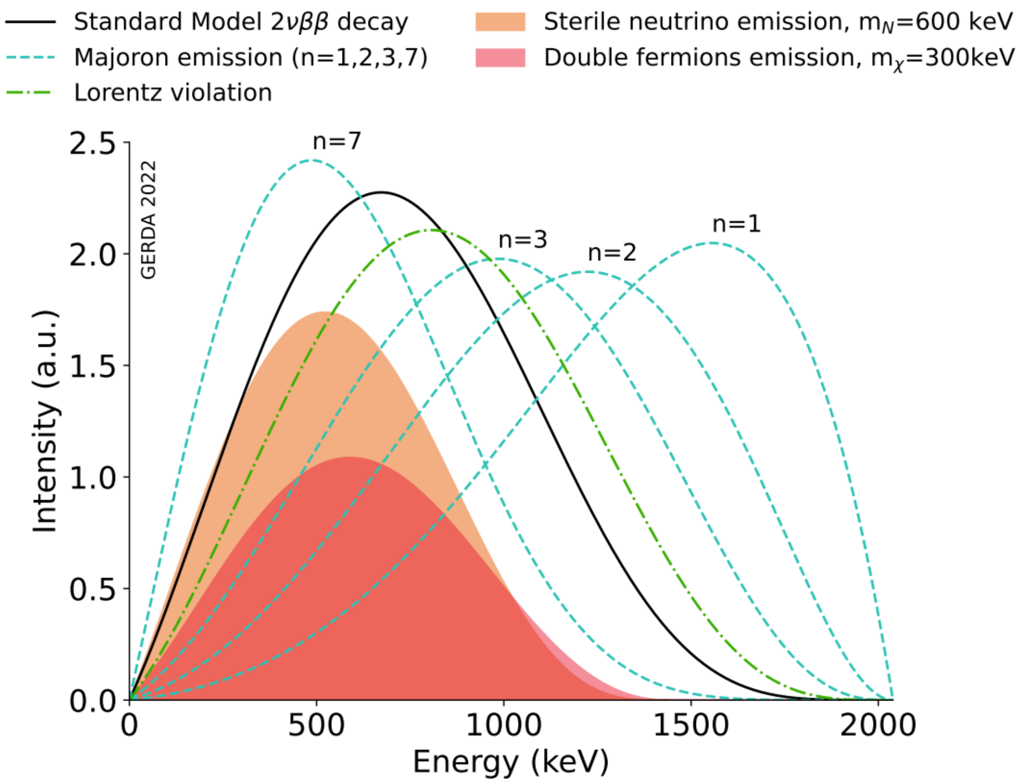

JCAP 12 (2022) 012

Exotic Searches in $2\nu2\beta$ Decays

$$T^{2\nu}_{\frac{1}{2}}(^{76}\mathrm{Ge}) = (2.022 \pm 0.018_{\mathrm{stat}} \pm 0.038_{\mathrm{syst}}) \times 10^{21}\ \mathrm{yr}$$

PRL 131 (2023) 142501

- Study of $\beta\beta$ decay modes with different final states:
  $$2n \rightarrow 2p + 2e^{-} + X$$

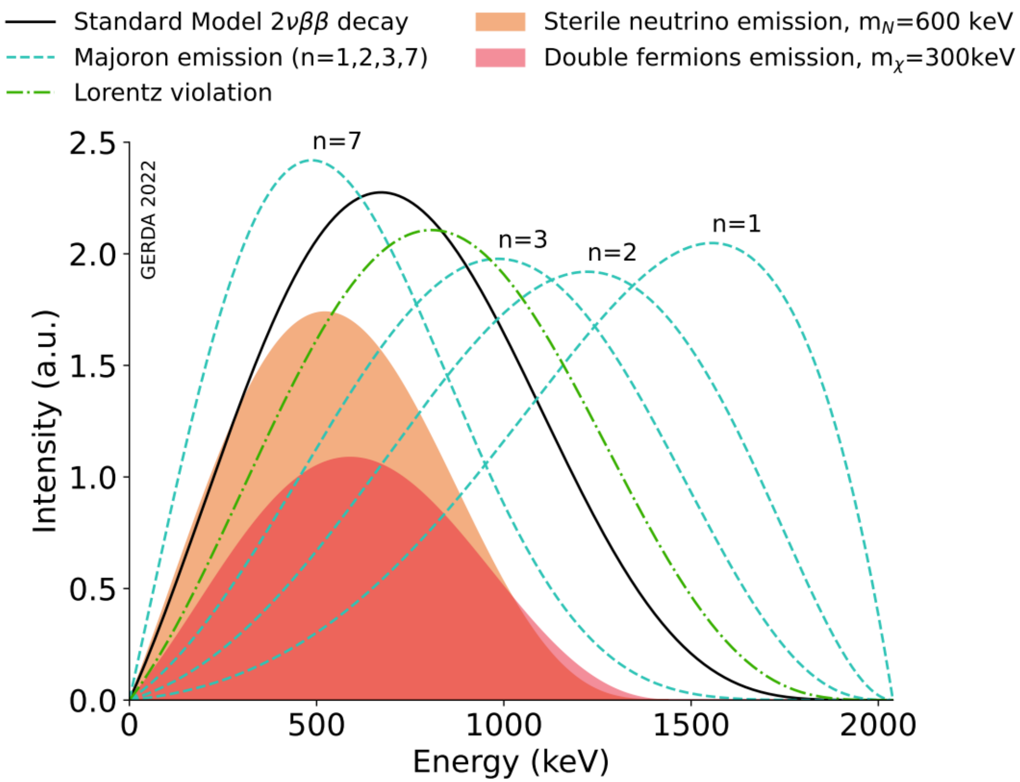

JCAP 12 (2022) 012

Exotic Searches in $2\nu2\beta$ Decays

$$T^{2\nu}_{\frac{1}{2}}(^{76}\text{Ge}) = (2.022 \pm 0.018_{\text{stat}} \pm 0.038_{\text{syst}}) \times 10^{21}\ \text{yr}$$

PRL 131 (2023) 142501

- Study of $\beta\beta$ decay modes with different final states:
  $$2n \rightarrow 2p + 2e^- + X$$
- Continuous distribution in [0;$Q_{\beta\beta}$]:
  $$2n \rightarrow 2p + 2e^- + 2\overline{\nu}_e$$

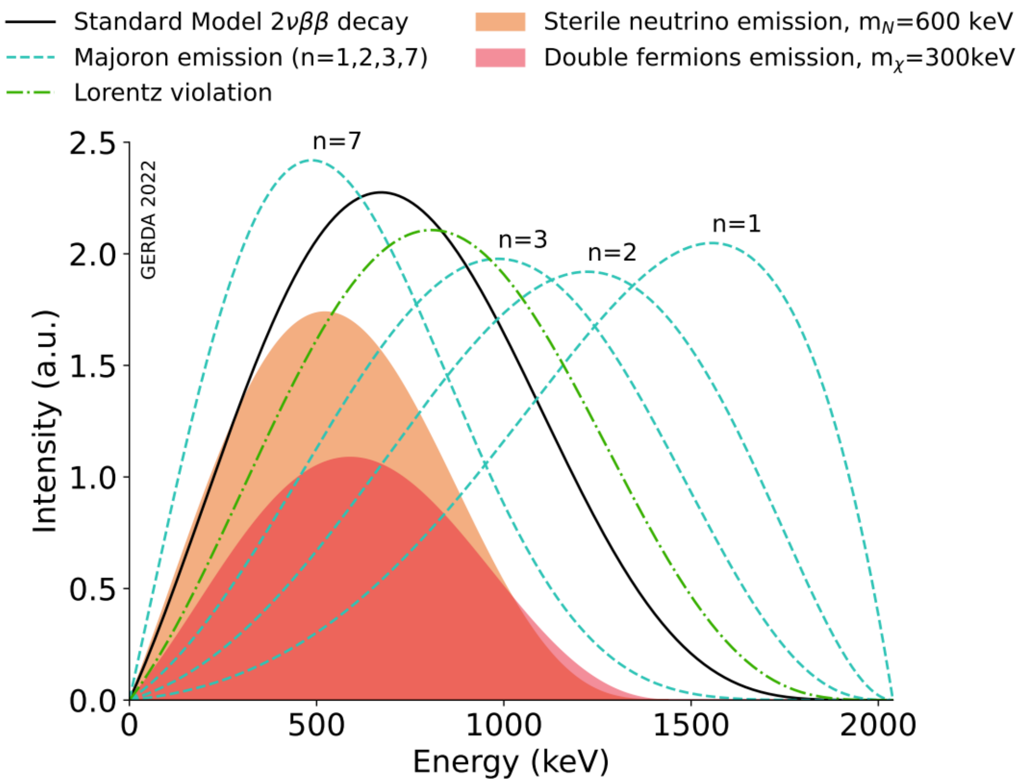

JCAP 12 (2022) 012

Exotic Searches in $2\nu2\beta$ Decays

$$T^{2\nu}_{\frac{1}{2}}(^{76}\text{Ge}) = (2.022 \pm 0.018_{\text{stat}} \pm 0.038_{\text{syst}}) \times 10^{21}\ \text{yr}$$

PRL 131 (2023) 142501

- Study of $\beta\beta$ decay modes with different final states:
$$2n \rightarrow 2p + 2e^- + X$$
- Continuous distribution in $[0;Q_{\beta\beta}]$:
$$2n \rightarrow 2p + 2e^- + 2\overline{\nu}_e$$
- Different distributions depending on the nature of the emitted X that deviate from the SM prediction

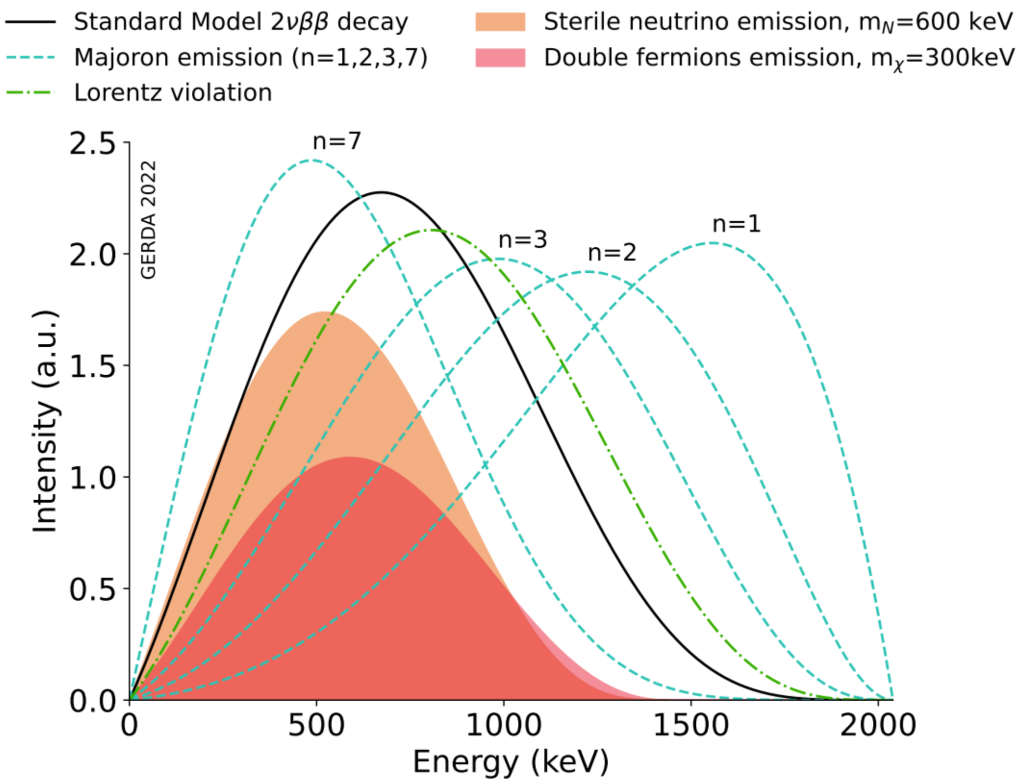

JCAP 12 (2022) 012

Exotic Searches in $2\nu2\beta$ Decays

- Majoron emissions

$2n \rightarrow 2p + 2e^- + J\ (JJ)$

Phase space factor $G \sim (Q_{\beta\beta} - E)^n$, n=spectral index

J, n = (1, 2, 3) : $T_{1/2} > (6.4,\ 2.9,\ 1.2) \times 10^{23}$ yr

$g_J < (1.8 - 4.4) \times 10^{-5}$, -, 0.017

JJ, n = (3, 7) : $T_{1/2} > (1.2, 1.0) \times 10^{23}$ yr

$g_J < 1.2, 1.0$

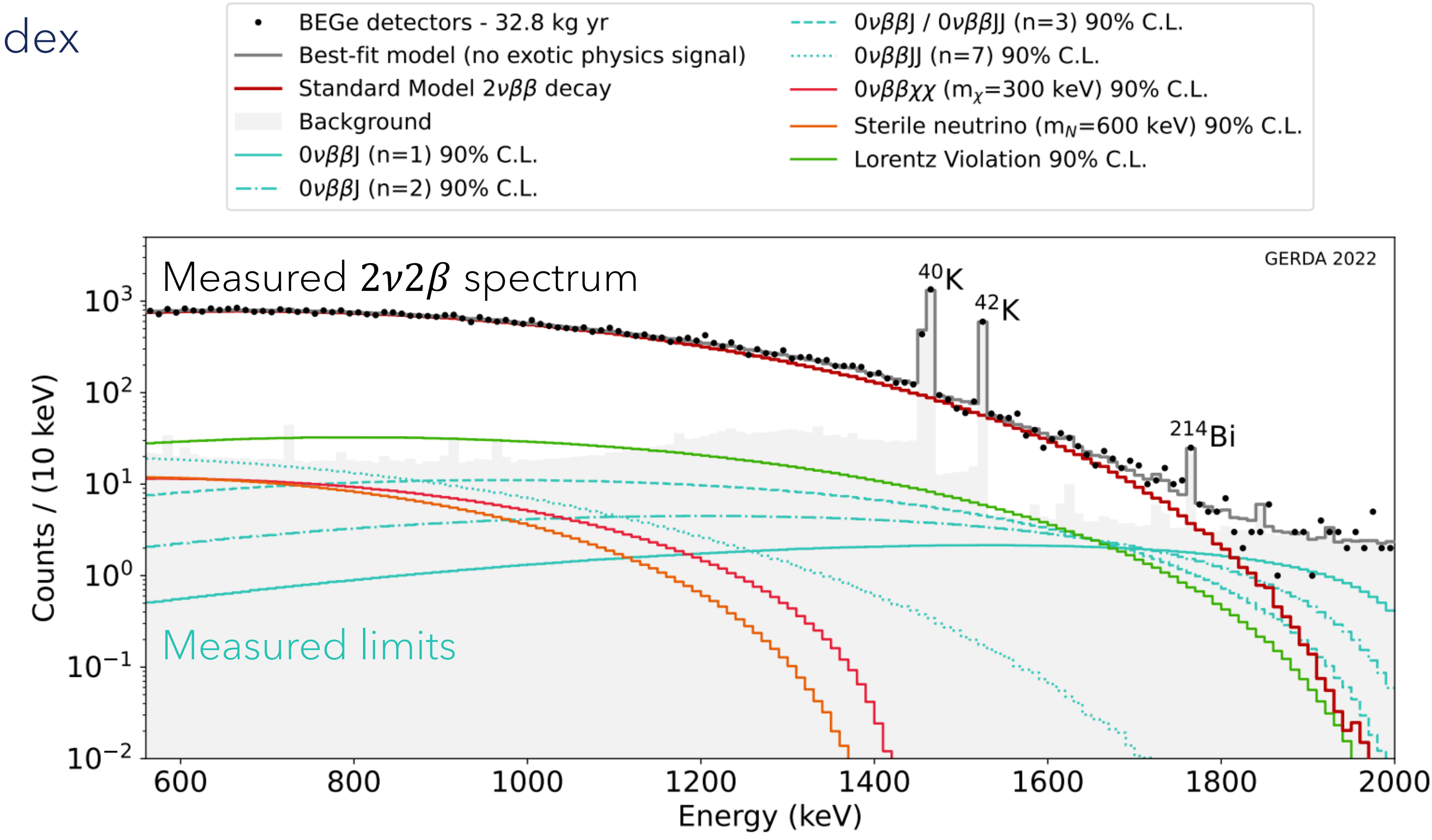

Results shown as 90% CL limits

JCAP 12 (2022) 012

Exotic Searches in $2\nu2\beta$ Decays

- Majoron emissions

$2n \rightarrow 2p + 2e^- + J\ (JJ)$

Phase space factor $G \sim (Q_{\beta\beta} - E)^n$, n=spectral index

J, n = (1, 2, 3) : $T_{1/2} > (6.4,\ 2.9,\ 1.2) \times 10^{23}$ yr

$g_J < (1.8 - 4.4) \times 10^{-5}$, -, 0.017

JJ, n = (3, 7) : $T_{1/2} > (1.2, 1.0) \times 10^{23}$ yr

$g_J < 1.2, 1.0$

✓ Improvement of a factor ~10^2 compared to previous GERDA Phase I result (EPJ C 75 (2015) 416)

✓ Results comparable with limits obtained with other $\beta\beta$ decay isotopes (~^{136}Xe, ^{100}Mo, ^{116}Cd)

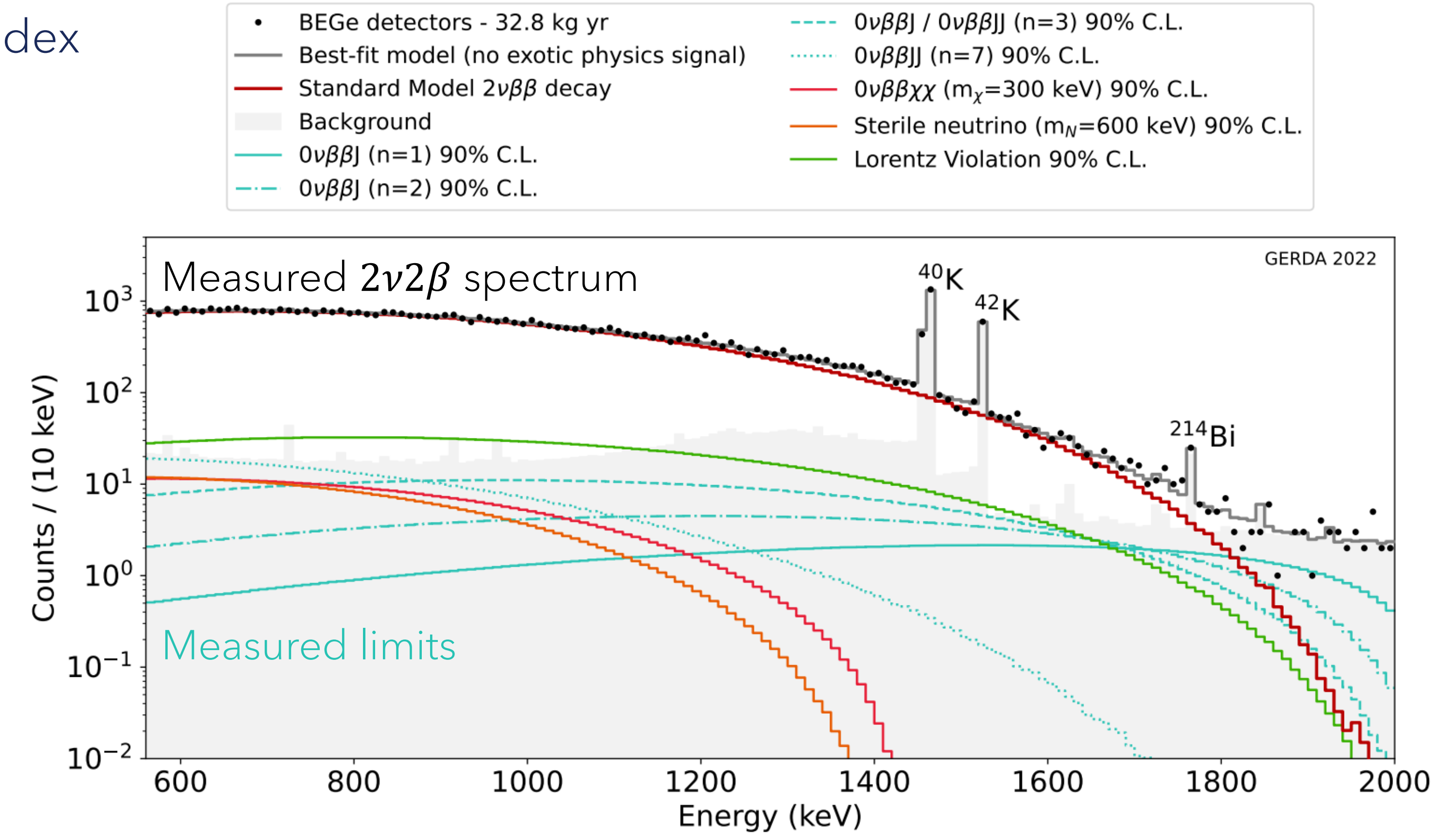

Results shown as 90% CL limits

JCAP 12 (2022) 012

Exotic Searches in $2\nu2\beta$ Decays

- Z$_2$-odd fermion emission

$2n \rightarrow 2p + 2e^- + 2\chi$

$m_\chi = 100$ keV: $T_{1/2} > 0.18 \times 10^{23}$ yr

$g_\chi < (1.4 - 3.2) \times 10^{-3}$ MeV^{-2}

$m_\chi = 700$ keV: $T_{1/2} > 0.25 \times 10^{23}$ yr

$g_\chi < (7.4 - 17) \times 10^{-3}$ MeV^{-2}

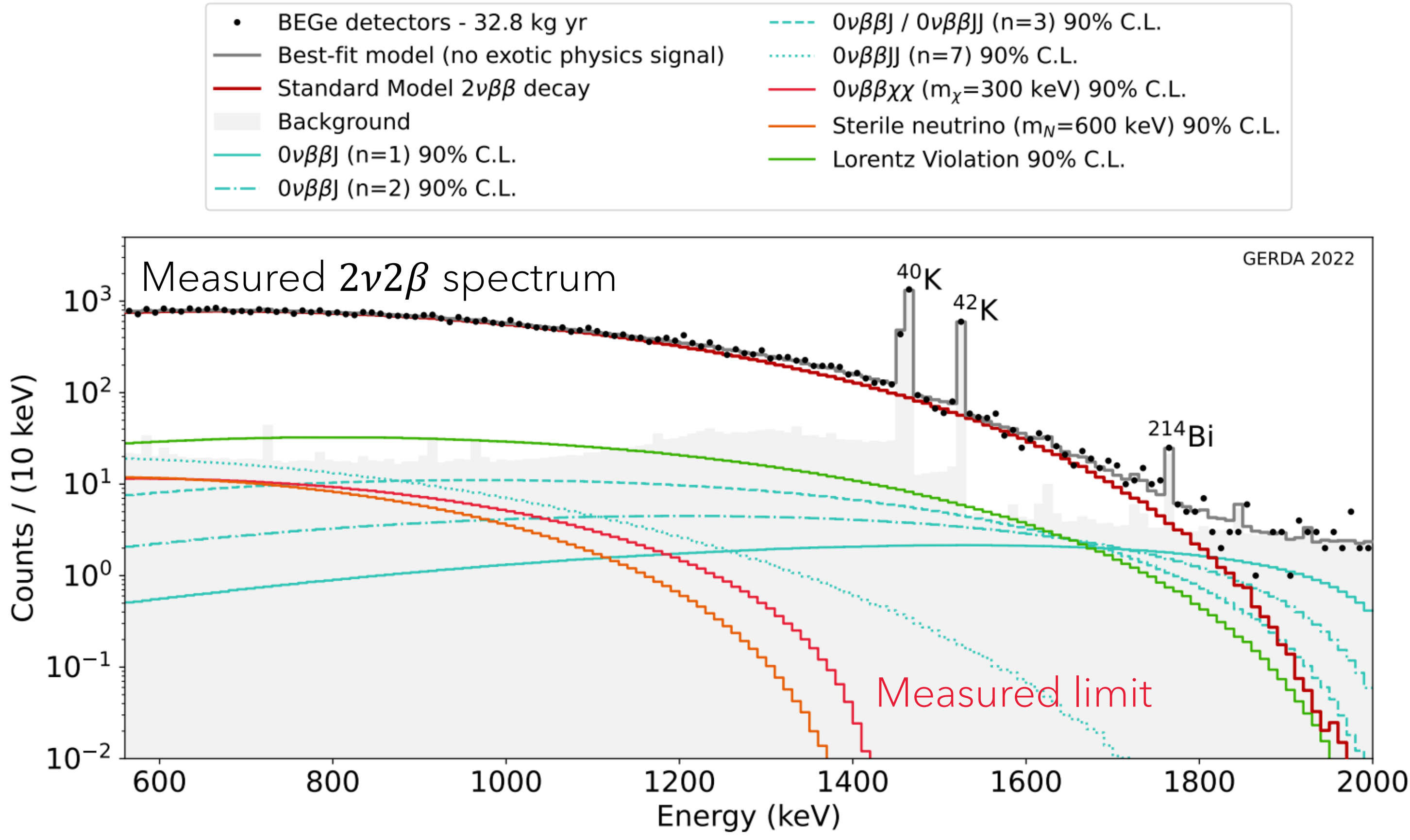

✓ First experimental constraints on light exotic fermions

Results shown as 90% CL limits

JCAP 12 (2022) 012

- Sterile neutrino emission

$2n \rightarrow 2p + 2e^- + \bar{\nu_e} + N$

$m_N = 100 \text{ keV} \Longrightarrow \sin^2\theta < 0.15$

$m_N = 900 \text{ keV} \Longrightarrow \sin^2\theta < 0.05$

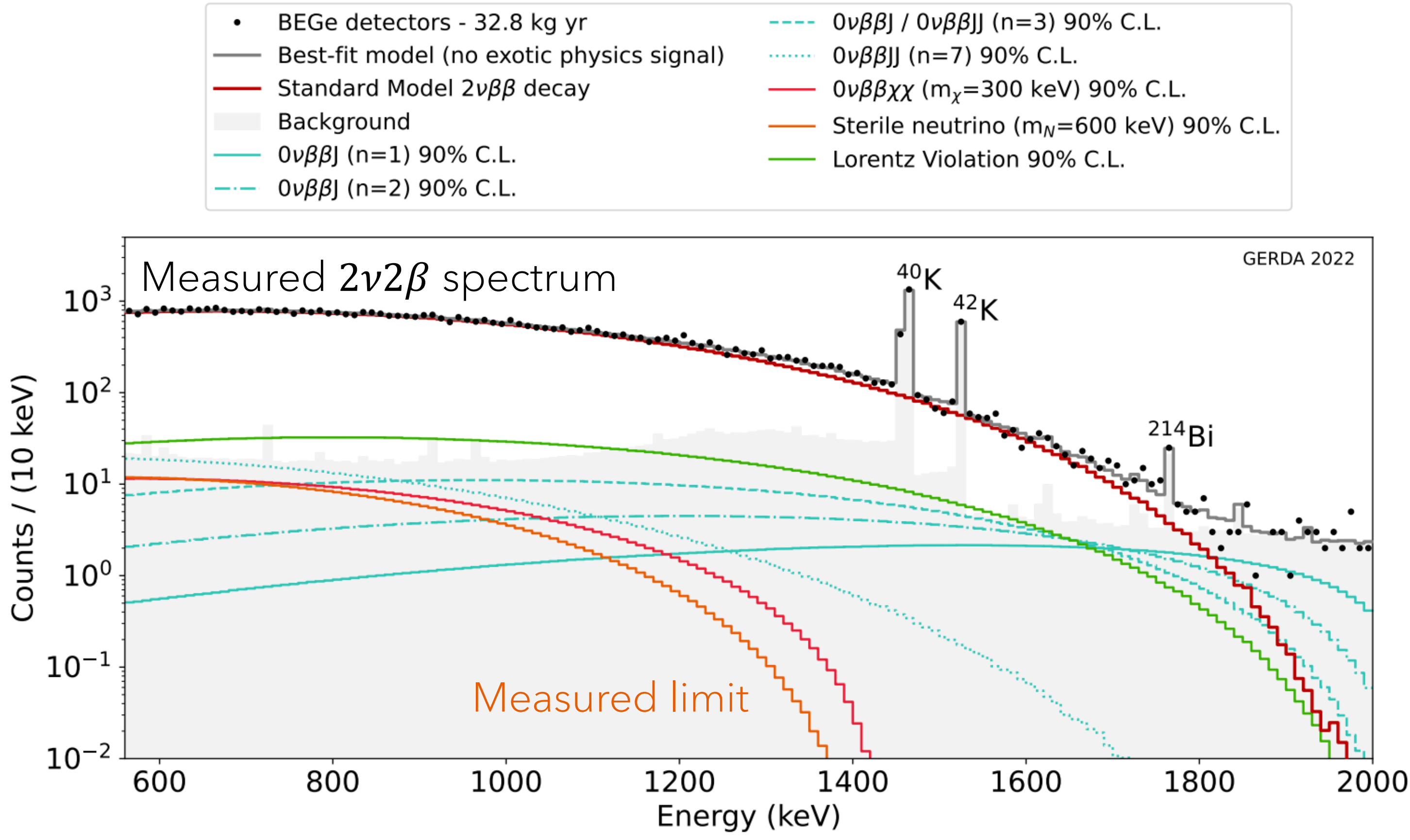

Results shown as 90% CL limits

JCAP 12 (2022) 012

Exotic Searches in 2ν2β Decays

- Sterile neutrino emission

$$2n \rightarrow 2p + 2e^- + \bar{\nu_e} + N$$

$$m_N = 100\ \text{keV} \Longrightarrow \sin^2\theta < 0.15$$

$$m_N = 900\ \text{keV} \Longrightarrow \sin^2\theta < 0.05$$

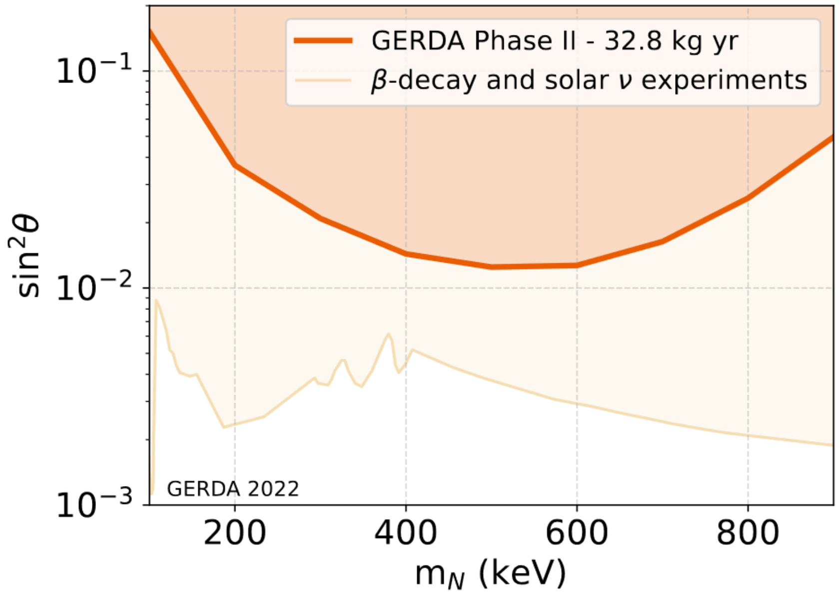

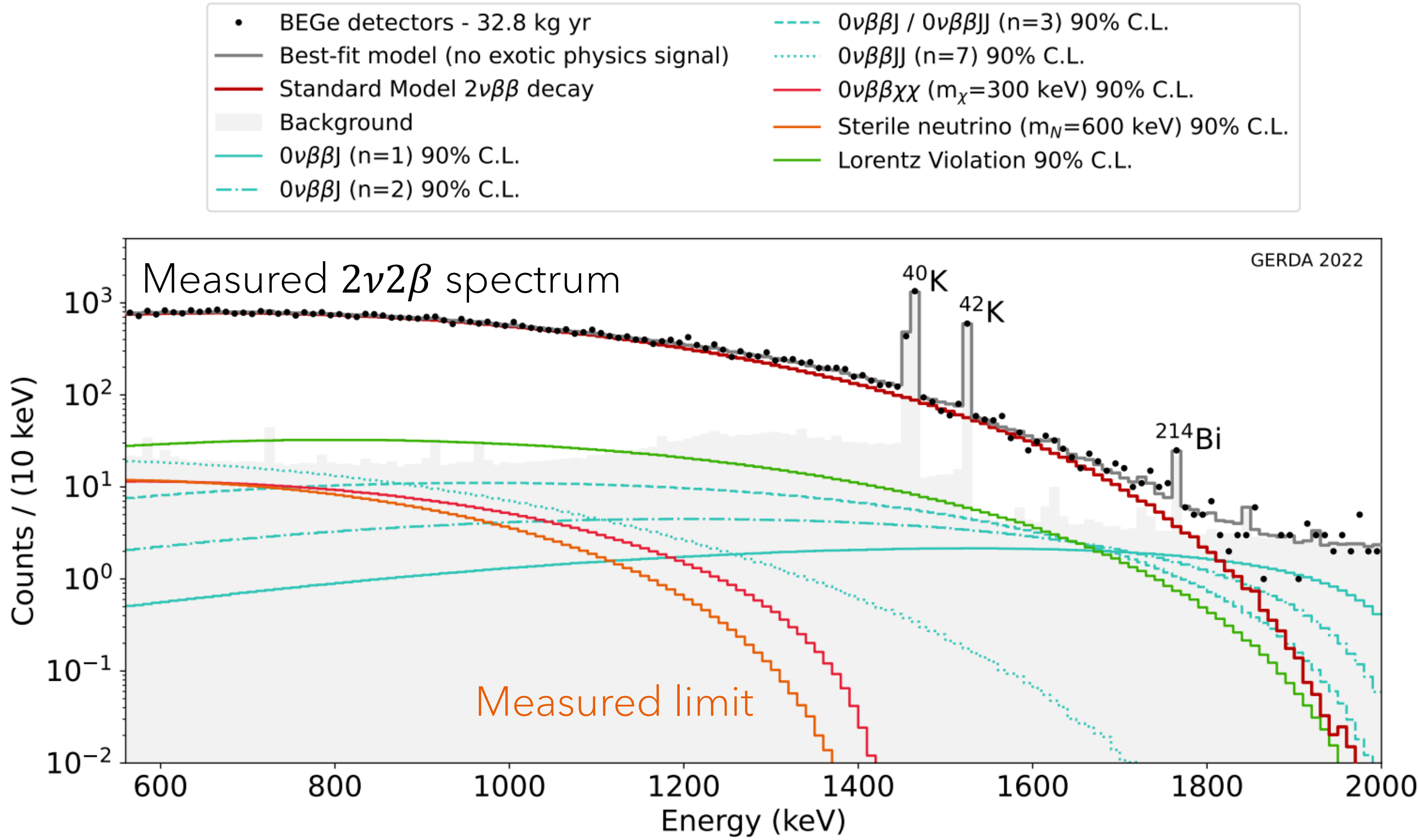

- ✓ Constraints are not competitive with single-β decay on sterile neutrinos
- ✓ Potential of $\beta\beta$ decay experiments to search for sterile nutrinos

Results shown as 90% CL limits

JCAP 12 (2022) 012

Exotic Searches in $2\nu2\beta$ Decays

- <u>Lorentz violation in neutrino sector</u>

$2n \rightarrow 2p + 2e^- + 2\bar{\nu}_{LV}$

Coefficient $a_{of}^{(3)}$ affecting the kinematics (n=4) and regulating the size of the breaking

$\left(-2.7 < a_{of}^{(3)} < 6.2\right) \times 10^{-6}$ GeV

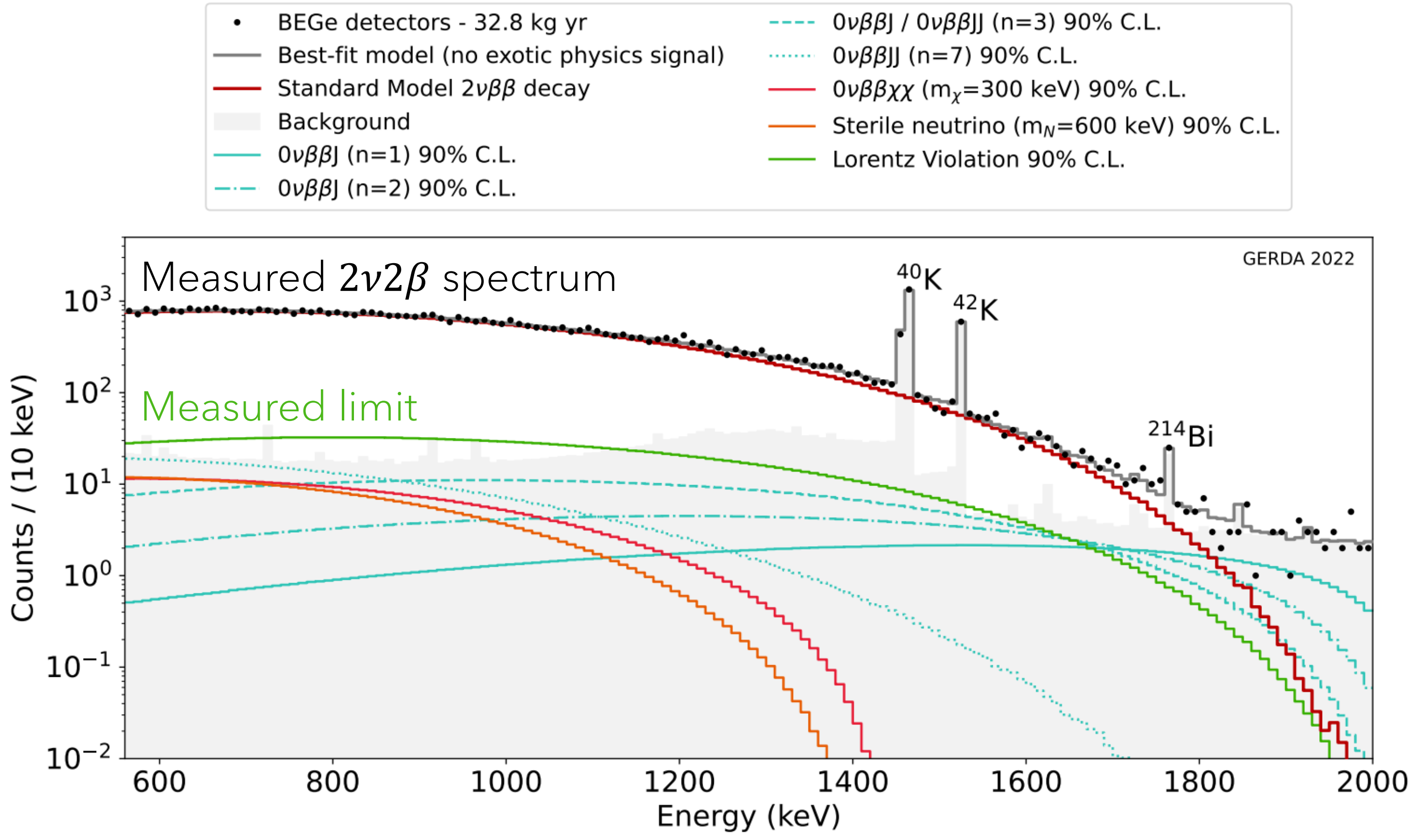

- ✓ First constraint with Ge-76
- ✓ Results comparable to limits obtained with other $\beta\beta$ decay isotopes (^{136}Xe, ^{100}Mo, ^{116}Cd, ^{82}Se)
- ✓ Single-β decay experiments ~10^{-8} GeV

Results shown as 90% CL limits

JCAP 12 (2022) 012

BSM Decays

Probes of baryon number, charge, lepton number conservation

EPJ C 83 (2023) 778

BSM Decays

Probes of baryon number, charge, lepton number conservation

- Inclusive tri-nucleon decays (ppp, ppn, pnn, nnn) of ^{76}Ge

66.7 keV γ from de-excitation in ^{73}Ge following β decay(s)

$\tau_{ppp,ppn,pnn} > 1.2 \times 10^{26}$ yr @ 90% CI

$\tau_{nnn} > k \times 10^{26}$ yr @ 90% CI

k = fraction of states decaying to the 66.7 keV state

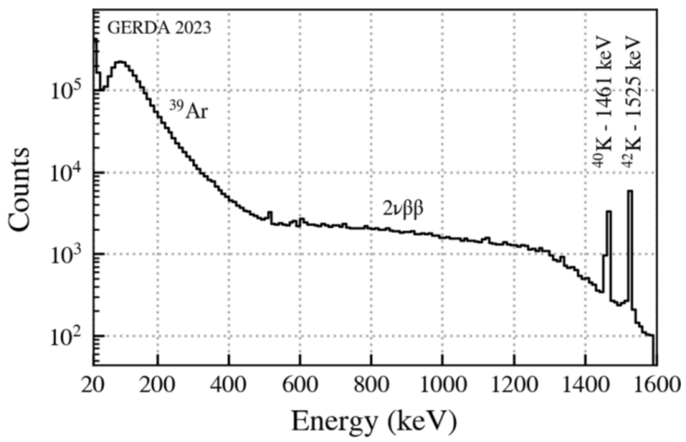

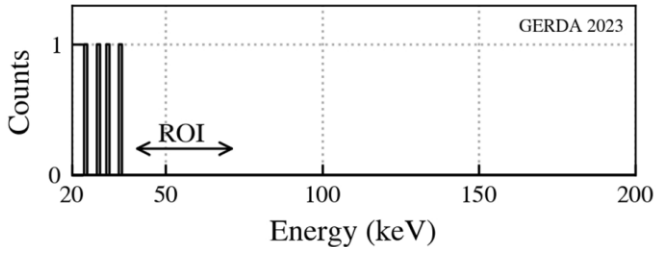

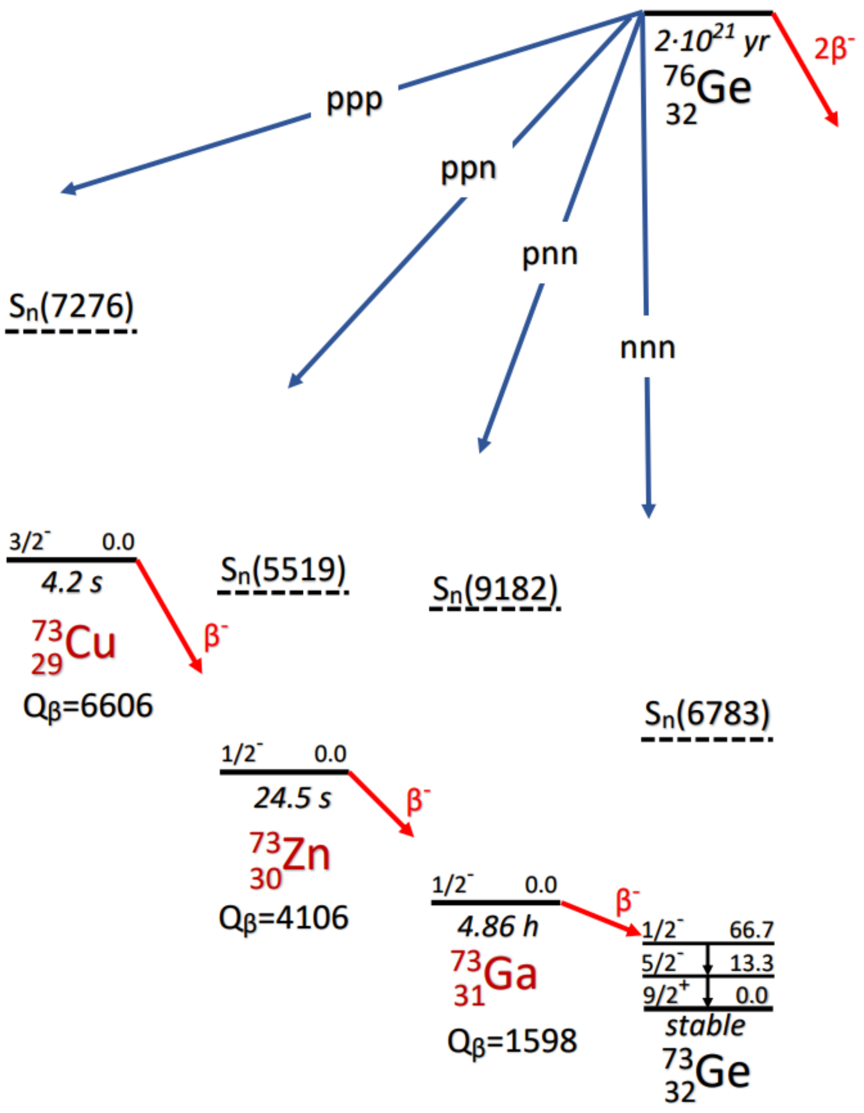

EPJ C 83 (2023) 778

BSM Decays

Probes of baryon number, charge, lepton number conservation

- Inclusive tri-nucleon decays (ppp, ppn, pnn, nnn) of ^{76}Ge

66.7 keV γ from de-excitation in ^{73}Ge following β decay(s)

$\tau_{ppp,ppn,pnn} > 1.2 \times 10^{26}$ yr @ 90% CI

$\tau_{nnn} > k \times 10^{26}$ yr @ 90% CI

k = fraction of states decaying to the 66.7 keV state

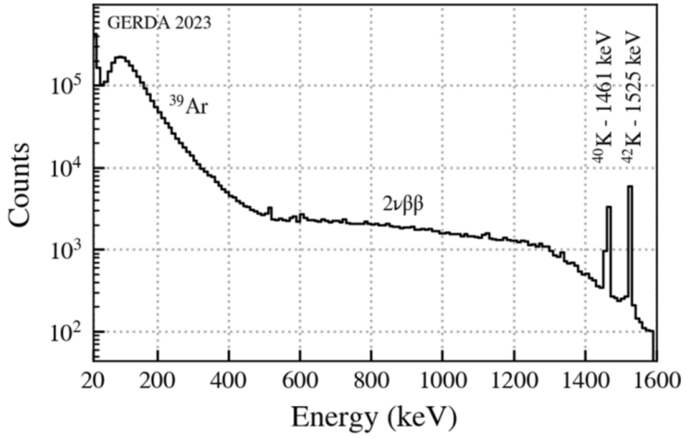

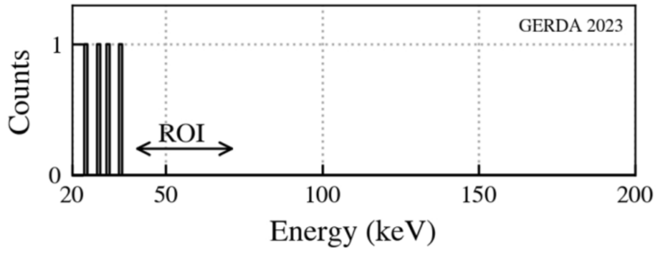

- ✓ Improvement of a factor ~10-10^3 compared to previous tri-nucleon limits
- ✓ First limits on the inclusive Zn and Ga channels
- ✓ Most stringent limits on inclusive tri-nucleon decays using γ cascade de-excitation in ^{73}Ge

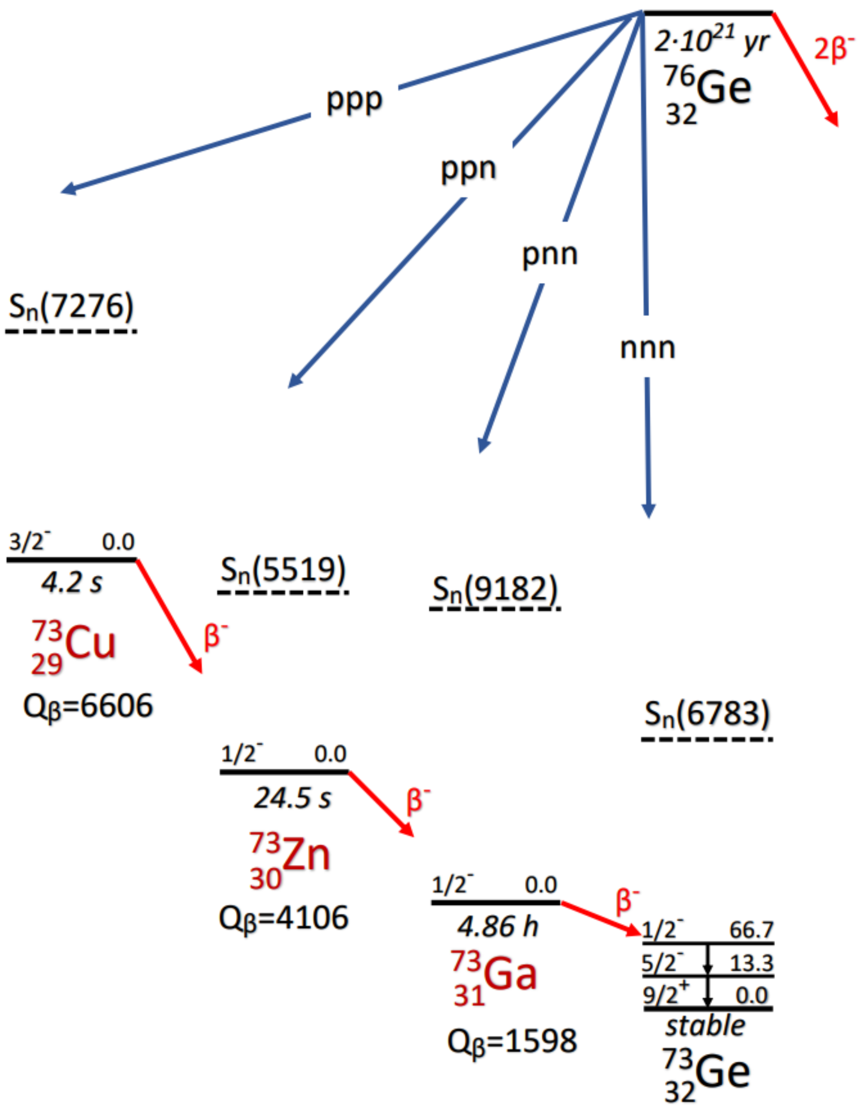

EPJ C 83 (2023) 778

Preliminary

Probes of baryon number, charge, lepton number conservation

- Radiative neutrinoless double electron capture (0νECEC) in ^{36}Ar

$^{36}\mathrm{Ar} \rightarrow {}^{36}\mathrm{S} + \gamma + \mathrm{X_K}(2.47\ \mathrm{keV}) + \mathrm{X_L}(0.23\ \mathrm{keV})$: γ-line signal at ~429 keV

$T_{1/2} > 1.5 \times 10^{22}$ yr @ 90% CL

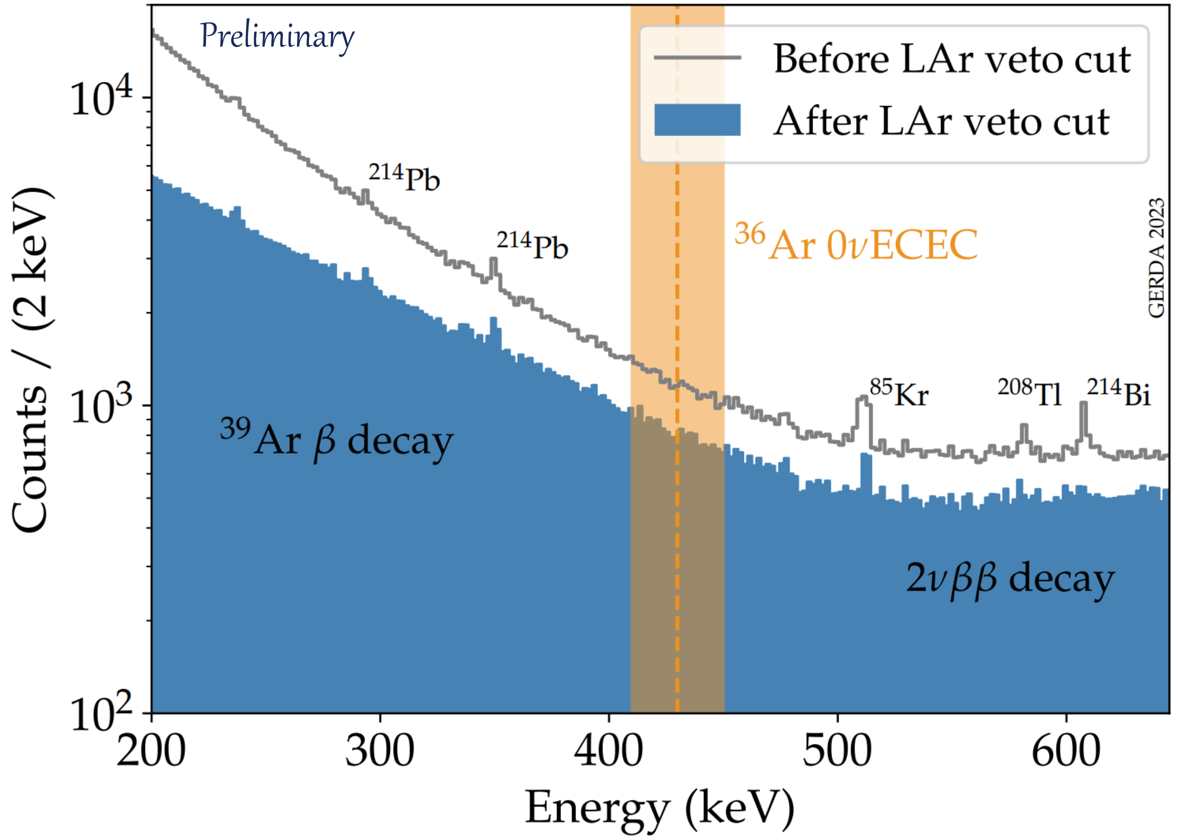

Paper submitted to EPJ C

Preliminary

Probes of baryon number, charge, lepton number conservation

- Radiative neutrinoless double electron capture (0νECEC) in ^{36}Ar

$^{36}\mathrm{Ar} \rightarrow {}^{36}\mathrm{S} + \gamma + \mathrm{X_K}(2.47\ \mathrm{keV}) + \mathrm{X_L}(0.23\ \mathrm{keV})$: γ-line signal at ~429 keV

$T_{1/2} > 1.5 \times 10^{22}$ yr @ 90% CL

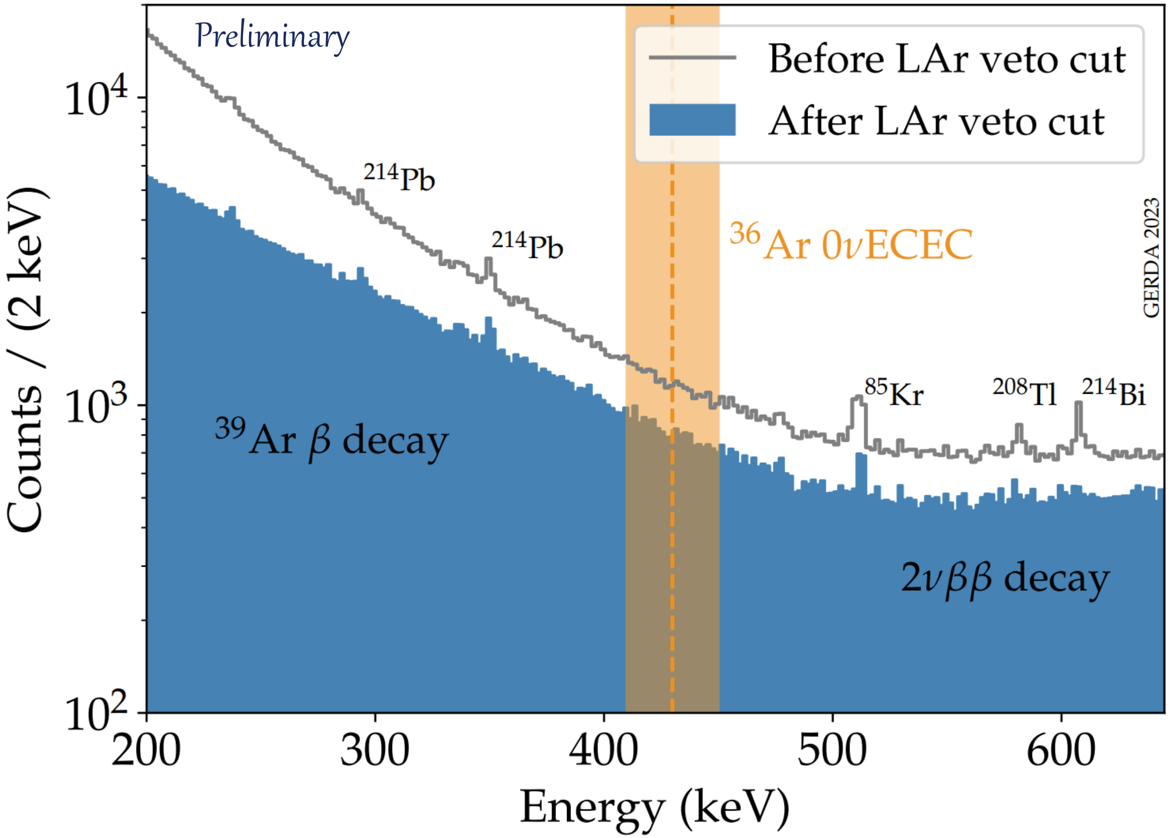

- ✓ Improvement of a factor ~4 compared to previous GERDA Phase I result (EPJ C 76 (2016) 652)
- ✓ Most stringent limit on $T_{1/2}(0\nu\mathrm{ECEC})$ of ^{36}Ar

Paper submitted to EPJ C

BSM Decays

Probes of baryon number, charge, lepton number conservation

- Inclusive neutron/proton decays of ^{76}Ge

(n [16]: $^{76}Ge \rightarrow {}^{75}Ge$, p [14]: $^{76}Ge \rightarrow {}^{75}Ga \rightarrow {}^{75}Ge$)

e^- & γ signal from ^{75}Ge decay to ^{75}As + de-excitation

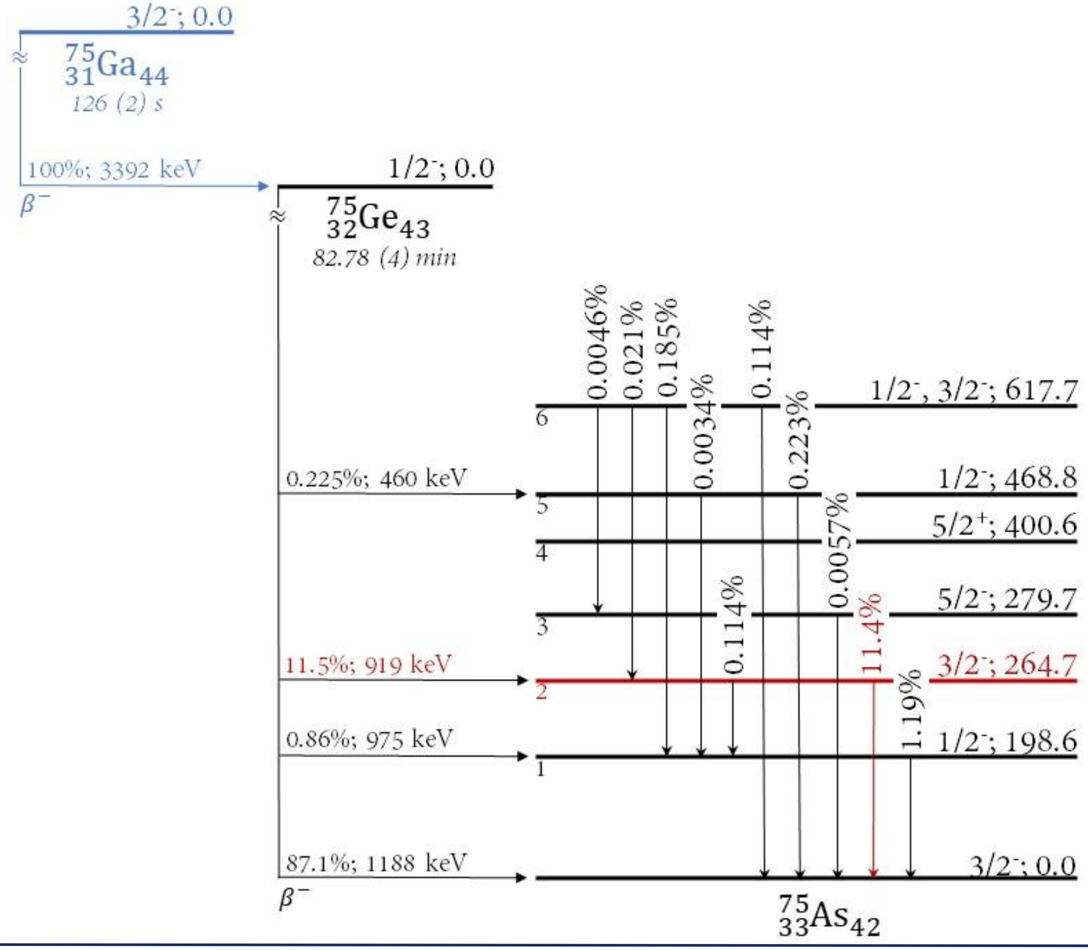

Preliminary

Paper in preparation

BSM Decays

Preliminary

Probes of baryon number, charge, lepton number conservation

- Inclusive neutron/proton decays of ^{76}Ge

(n [16]: $^{76}\text{Ge} \rightarrow {}^{75}\text{Ge}$, p [14]: $^{76}\text{Ge} \rightarrow {}^{75}\text{Ga} \rightarrow {}^{75}\text{Ge}$)

e^- & γ signal from ^{75}Ge decay to ^{75}As + de-excitation

Experiment	Decay	N_{eff}	τ_{low}, 90% CL (yr)
GERDA	$^{76}\text{Ge} \xrightarrow{n} {}^{75}\text{Ge} + X$	16	1.6×10^{24}, 1.5×10^{24} 90% CI
	$^{76}\text{Ge} \xrightarrow{p} {}^{75}\text{Ga} + X$	14	1.4×10^{24}, 1.3×10^{24} 90% CI
SNO [46] [a]	$^{16}\text{O} \xrightarrow{n} {}^{15}\text{O} + inv.$	8	1.9×10^{29}
	$^{16}\text{O} \xrightarrow{p} {}^{15}\text{N} + inv.$	8	2.1×10^{29}
SNO+ [47] [a]	$^{16}\text{O} \xrightarrow{n} {}^{15}\text{O} + inv.$	8	2.5×10^{29}
	$^{16}\text{O} \xrightarrow{p} {}^{15}\text{N} + inv.$	8	3.6×10^{29}
Borexino [48] [b]	$^{12}\text{C} \xrightarrow{n} {}^{11}\text{C} + inv.$	4	1.8×10^{25}
	$^{13}\text{C} \xrightarrow{p} {}^{12}\text{B} + inv.$	4	1.1×10^{26}
DAMA/LXe [37]	$^{136}\text{Xe} \xrightarrow{n} {}^{135}\text{Xe} + X$	32	3.3×10^{23}
	$^{136}\text{Xe} \xrightarrow{p} {}^{135}\text{I} + X$	26	4.5×10^{23}
DAMA [38]	$^{129}\text{Xe} \xrightarrow{p} {}^{128}\text{I} + X$	24	1.9×10^{24}
NaI(Tl) [39]	$^{127}\text{I} \xrightarrow{n} {}^{126}\text{I} + X$	34	1.5×10^{24}
	$^{127}\text{I} \xrightarrow{p} {}^{126}\text{Te} + X$	20	3.0×10^{24}
Geochemical [40, 49]	$^{130}\text{Te} \xrightarrow{n} {}^{129}\text{Te} + X$	28	8.6×10^{24}
	$^{130}\text{Te} \xrightarrow{p} {}^{129}\text{Sb} + X$	24	7.4×10^{24}

[a] Searches for γ rays coming from the de-excitation of a residual excited nucleus following the disappearance of a nucleon in ^{16}O.
[b] Searches for decays of unstable nuclei left after nucleon decays of parent ^{12}C, ^{13}C nuclei.

Paper in preparation

Preliminary

Probes of baryon number, charge, lepton number conservation

- Semi-visible electron decay, $e^- \to \nu_e \gamma$

Ge&Ar Doppler-broadened γ-line signal at ~256 keV

Author	Mode	τ_e, 90% CL (yr)
GERDA	$e^- \to \nu_e \gamma$	1.6×10^{26}
		8.5×10^{25} 90% CI
Borexino [52]	$e^- \to \nu_e \gamma$	6.7×10^{28}
H.V. Klapdor et al. [14]	$e^- \to \nu_e \gamma$	9.4×10^{25}
MAJORANA [53]	$e^- \to 3\nu_e$	1.2×10^{24}
EDELWEISS-III [29]	$e^- \to 3\nu_e$	1.2×10^{24}

Paper in preparation

Bosonic Dark Matter Interactions

Preliminary

- Bosonic dark matter candidates
  - **vector DM** (*dark photons*), $\mathcal{L}_V = g_V V_\mu \bar{\psi} \gamma^\mu \psi$
  - **pseudoscalar DM** (*axion-like particles*), $\mathcal{L}_a = g_a a \bar{\psi} i \gamma_5 \psi$

- Mass range 65-1022 keV/c^2

Results shown as
90% CI limits

Paper in preparation

Bosonic Dark Matter Interactions

Preliminary

- Bosonic dark matter candidates
  - **vector DM** (*dark photons*), $\mathcal{L}_V = g_V V_\mu \bar{\psi} \gamma^\mu \psi$
  - **pseudoscalar DM** (*axion-like particles*), $\mathcal{L}_a = g_a a \bar{\psi} i \gamma_5 \psi$

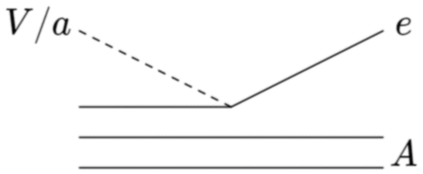

- Mass range 65-1022 keV/c^2

- Search for full energy depositions
  - e^-: **photoelectric-like absorption** PRL 125, 011801, 2020

Results shown as 90% CI limits

Paper in preparation

Bosonic Dark Matter Interactions

Preliminary

- Bosonic dark matter candidates
  - **vector DM** (*dark photons*), $\mathcal{L}_V = g_V V_\mu \bar{\psi} \gamma^\mu \psi$
  - **pseudoscalar DM** (*axion-like particles*), $\mathcal{L}_a = g_a a \bar{\psi} i \gamma_5 \psi$

- Mass range 65-1022 keV/c^2

- Search for full energy depositions
  - $\boldsymbol{e^-}$: **photoelectric-like absorption** PRL 125, 011801, 2020
  - $\boldsymbol{e^- + \gamma}$: **dark Compton scattering**

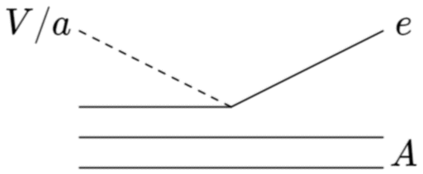

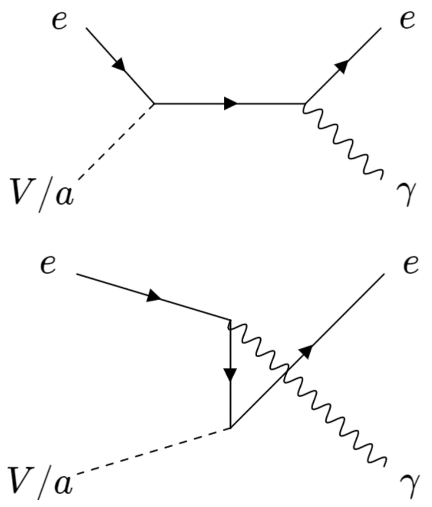

Results shown as
90% CI limits

Paper in preparation

Bosonic Dark Matter Interactions

- Bosonic dark matter candidates
  - **vector DM** (*dark photons*), $\mathcal{L}_V = g_V V_\mu \bar{\psi}\gamma^\mu\psi$
  - **pseudoscalar DM** (*axion-like particles*), $\mathcal{L}_a = g_a a\bar{\psi}i\gamma_5\psi$
- Mass range 65-1022 keV/c^2
- Search for full energy depositions
  - e^-: photoelectric-like absorption PRL 125, 011801, 2020
  - $e^- + \gamma$: dark Compton scattering

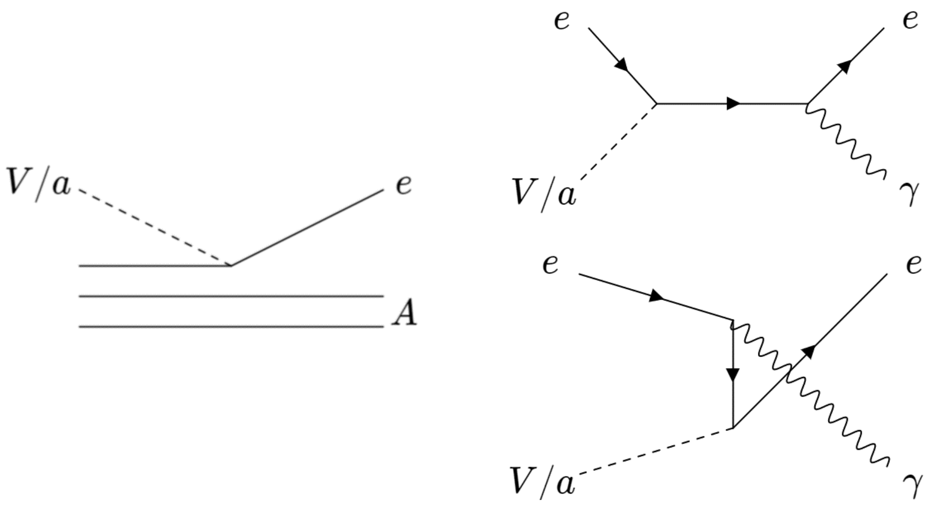

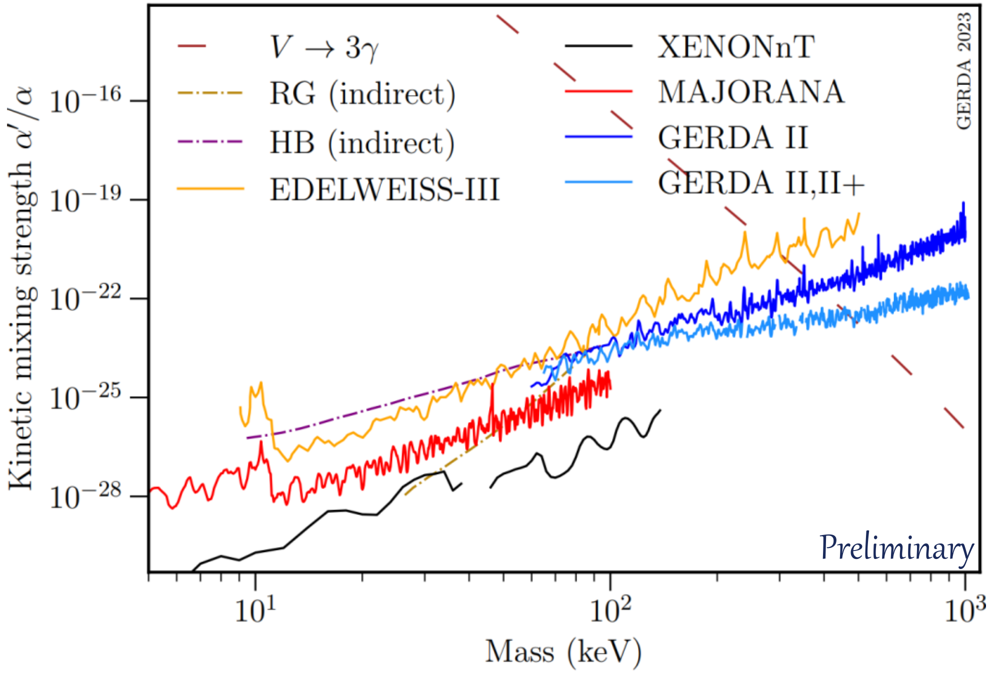

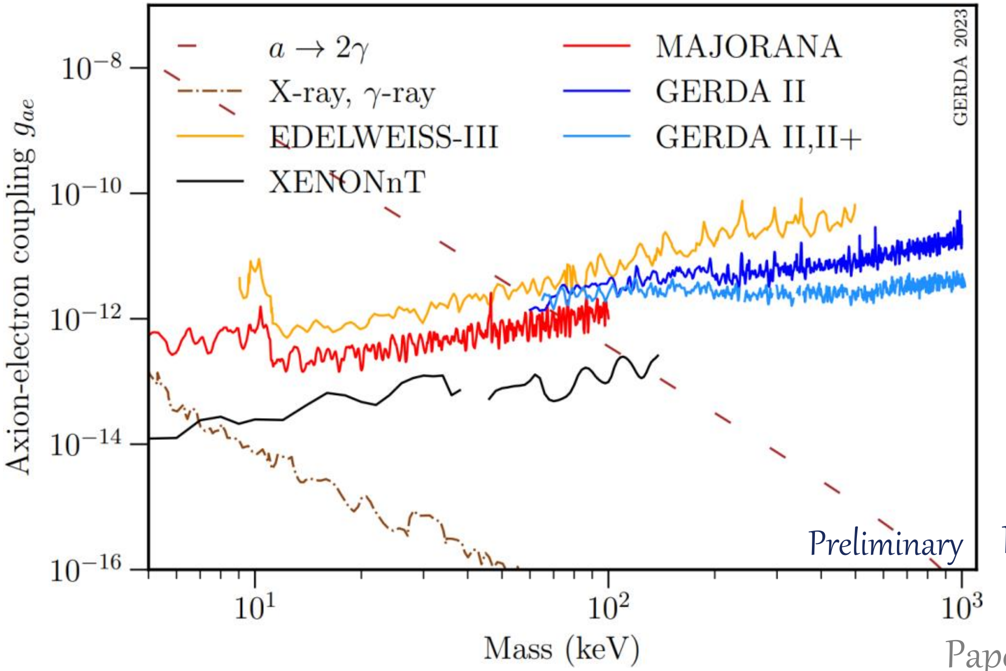

Results shown as 90% CI limits

Paper in preparation

Preliminary

Conclusions

- GERDA: up to 43.6 kg of HPGe detectors enriched in Ge-76 to search for $0\nu2\beta$
  - $T_{1/2} > 1.8 \times 10^{26}$ yr @ 90% CL
  - $m_{\beta\beta} < 79 - 180$ meV @ 90% CL

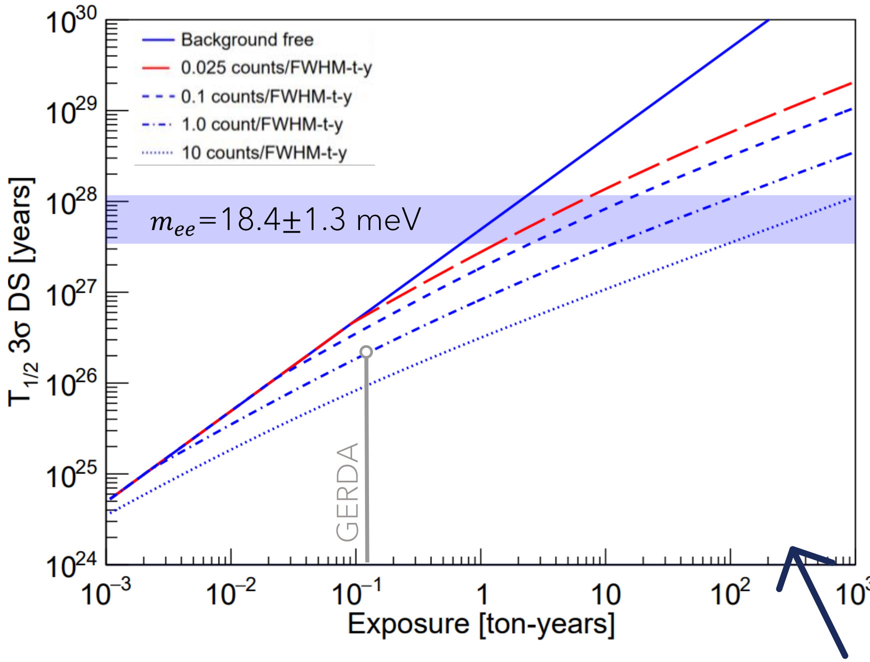

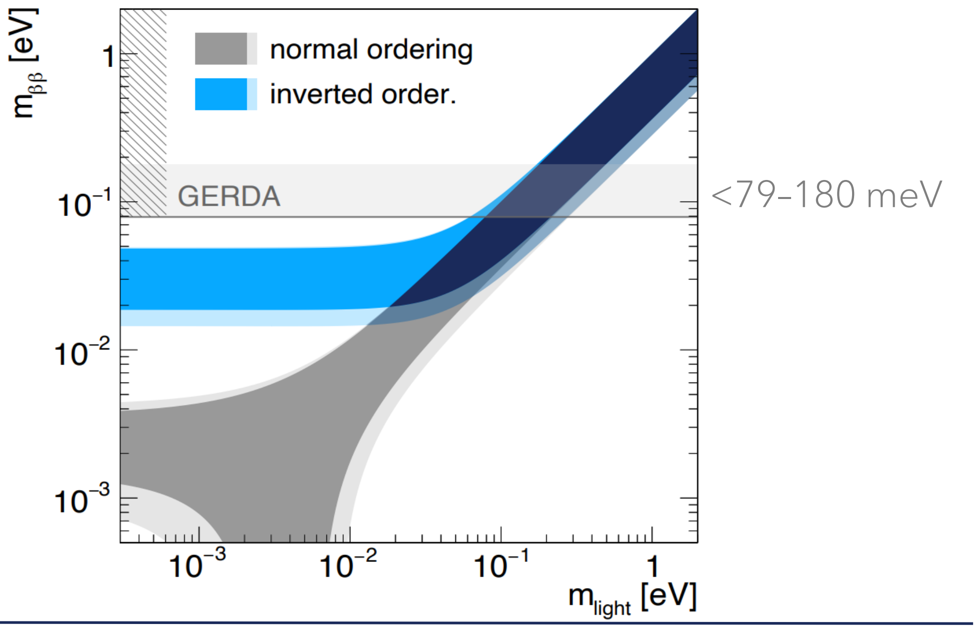

Conclusions

- GERDA: up to 43.6 kg of HPGe detectors enriched in Ge-76 to search for $0\nu 2\beta$
  - $T_{1/2} > 1.8 \times 10^{26}$ yr @ 90% CL
  - $m_{\beta\beta} < 79 - 180$ meV @ 90% CL

- Excellent energy resolution + low background level = ideal environment to probe other BSM physics

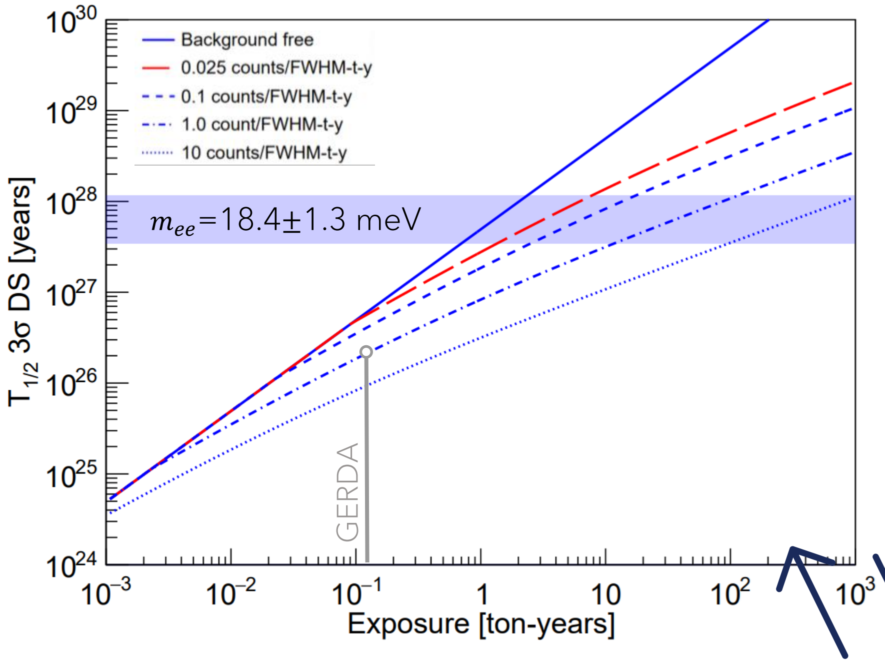

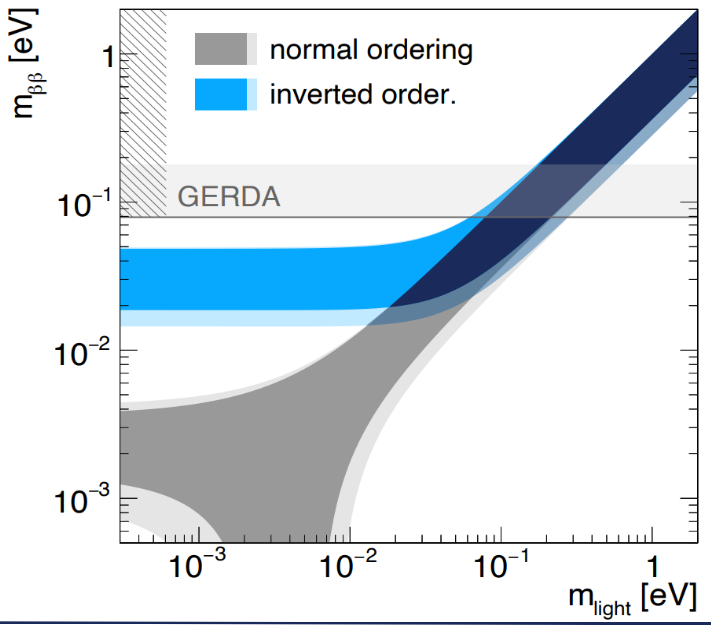

<79–180 meV

Conclusions

- GERDA: up to 43.6 kg of HPGe detectors enriched in Ge-76 to search for $0\nu2\beta$
  - $T_{1/2} > 1.8 \times 10^{26}$ yr @ 90% CL
  - $m_{\beta\beta} < 79 - 180$ meV @ 90% CL
- Excellent energy resolution + low background level = ideal environment to probe other BSM physics
- BSM physics: exotic particle emissions or decays + DM interactions

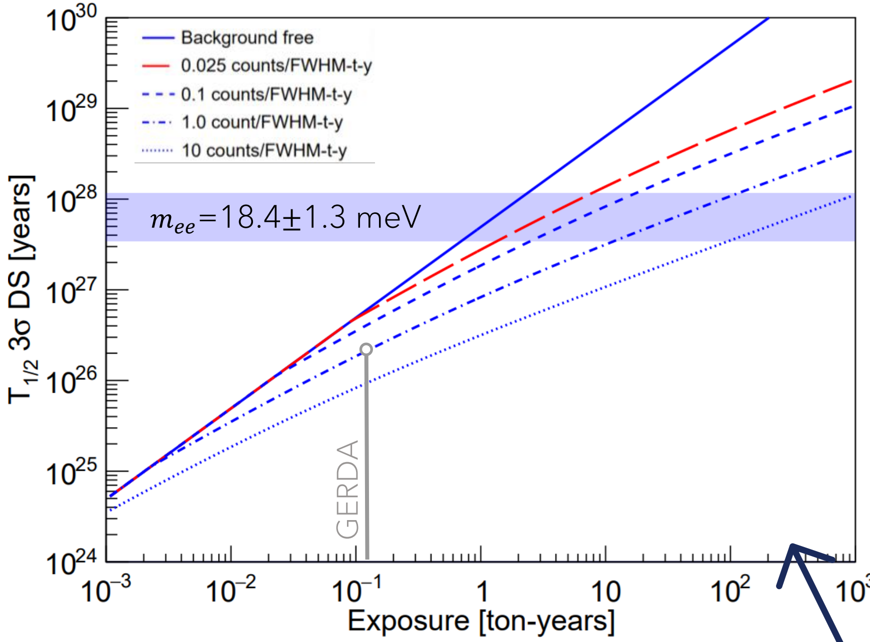

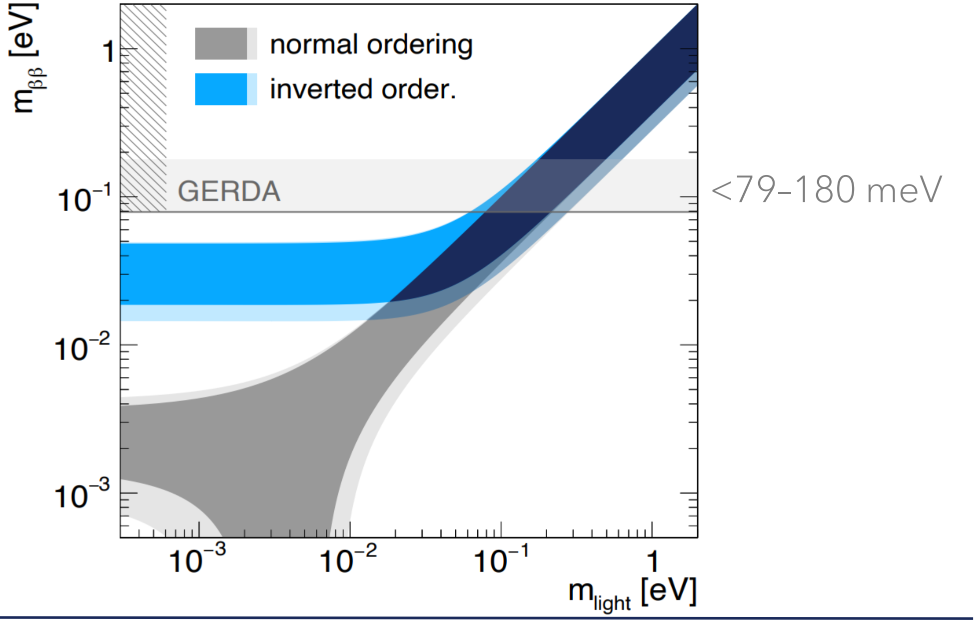

Conclusions

- GERDA: up to 43.6 kg of HPGe detectors enriched in Ge-76 to search for $0\nu2\beta$
  - $T_{1/2} > 1.8 \times 10^{26}$ yr @ 90% CL
  - $m_{\beta\beta} < 79 - 180$ meV @ 90% CL
- Excellent energy resolution + low background level = ideal environment to probe other BSM physics
- BSM physics: exotic particle emissions or decays + DM interactions
- LEGEND: up to 200 kg and 1000 kg of HPGe detectors in two stages, probing $T_{1/2}(0\nu2\beta)$ sensitivities beyond $10^{27,28}$ yr

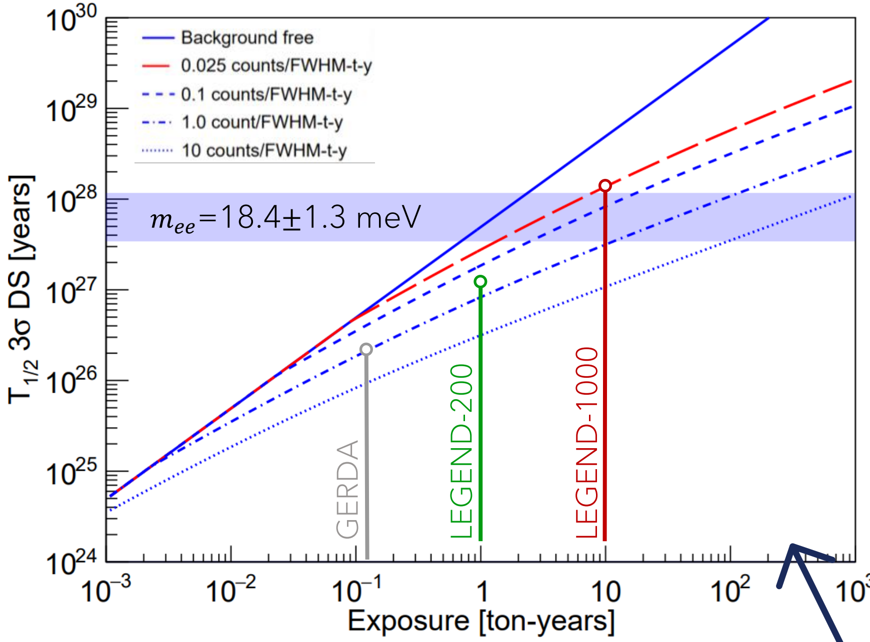

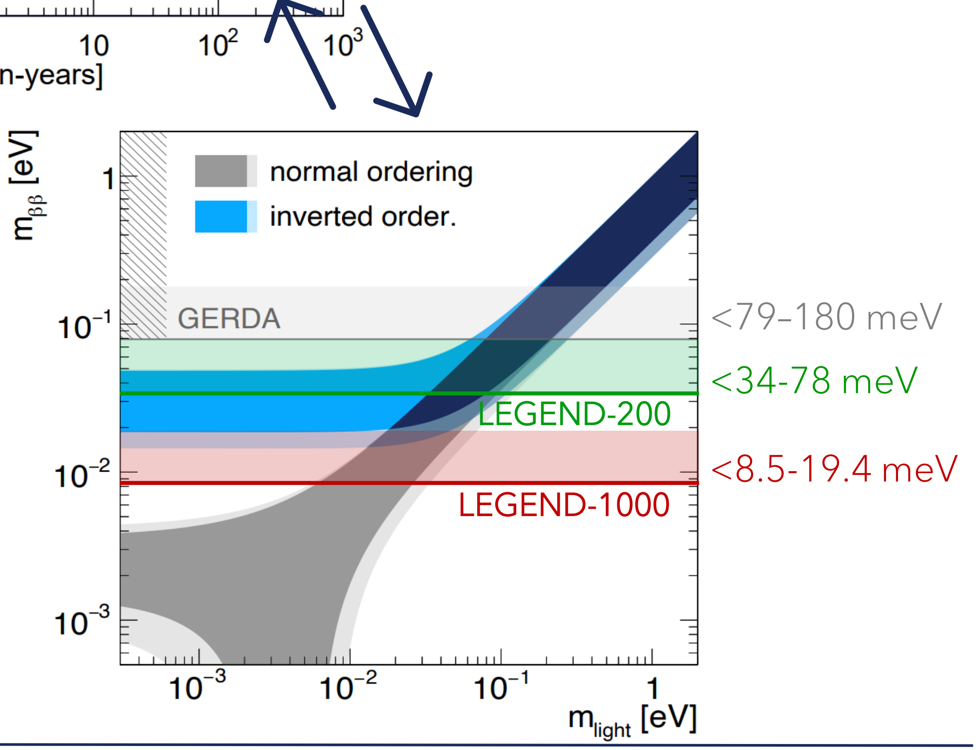

THANK YOU!

BACKUP SLIDES

Energy Resolution

Energy resolution

$$FWHM \simeq 2.355\sqrt{a + b \cdot E}$$

a → electronic noise
b → statistical fluctuations

Detector type	Period	a [keV^2]	b [10^{-4} keV]
BEGe	pre upgrade	0.681 ± 0.001	4.27 ± 0.01
	post upgrade	0.363 ± 0.001	4.32 ± 0.01
	all Phase II	0.551 ± 0.001	4.294 ± 0.009
Coaxial	pre upgrade	1.025 ± 0.002	6.47 ± 0.02
	post upgrade	0.898 ± 0.006	20.00 ± 0.06
	all Phase II	0.985 ± 0.002	10.73 ± 0.02
IC	all Phase II	0.280 ± 0.002	5.83 ± 0.02

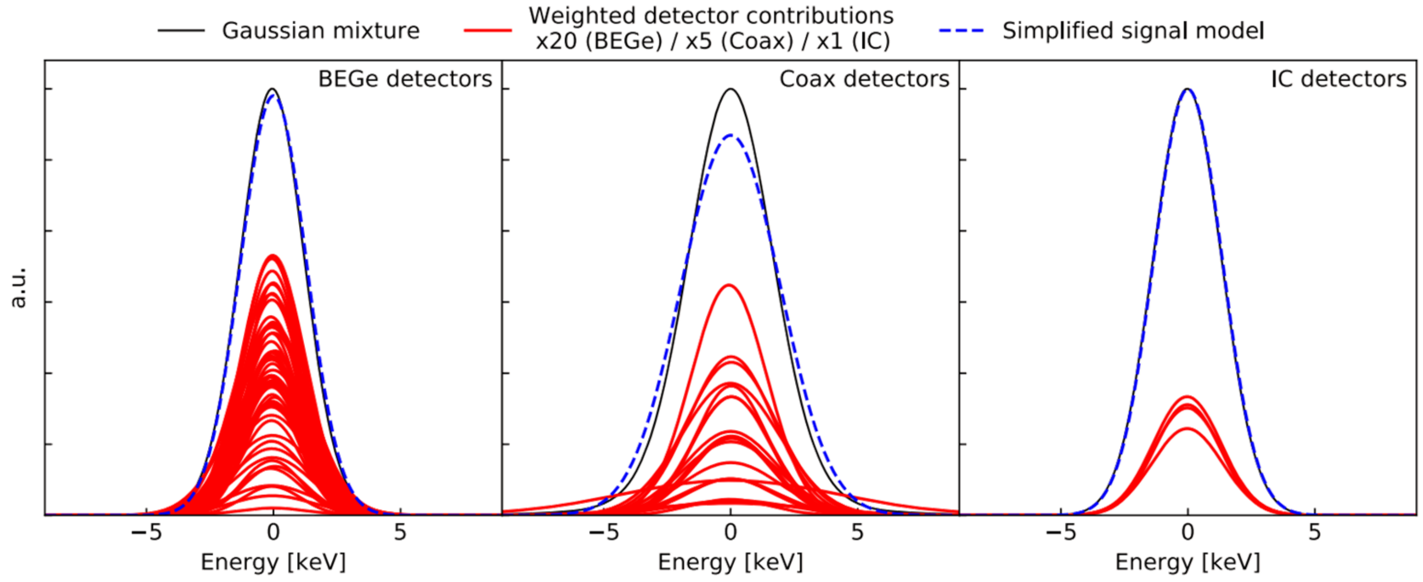

Gaussian mixture models to determine resolution per detector type

EPJ C 81 8 (2021) 682

Calibration Procedure

- **Weekly calibrations** with **3 Th-228** sources
- Use γ lines of known energies to pass from ADC to keV (physical unit)
- Peak fitting algorithm to extract each detector's resolution
- 3 terms:
  - Signal = gaussian
  - Bkg #1= linear + step (flat bkg below/above the peak derived from multiple Compton scatterings)
  - Bkg #2 = tail at low energies (due to incomplete charge collection effects + pile-up events residuals)

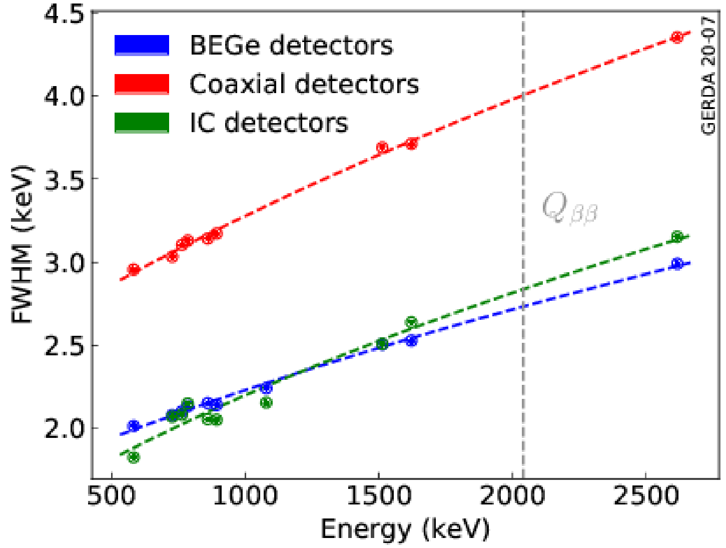

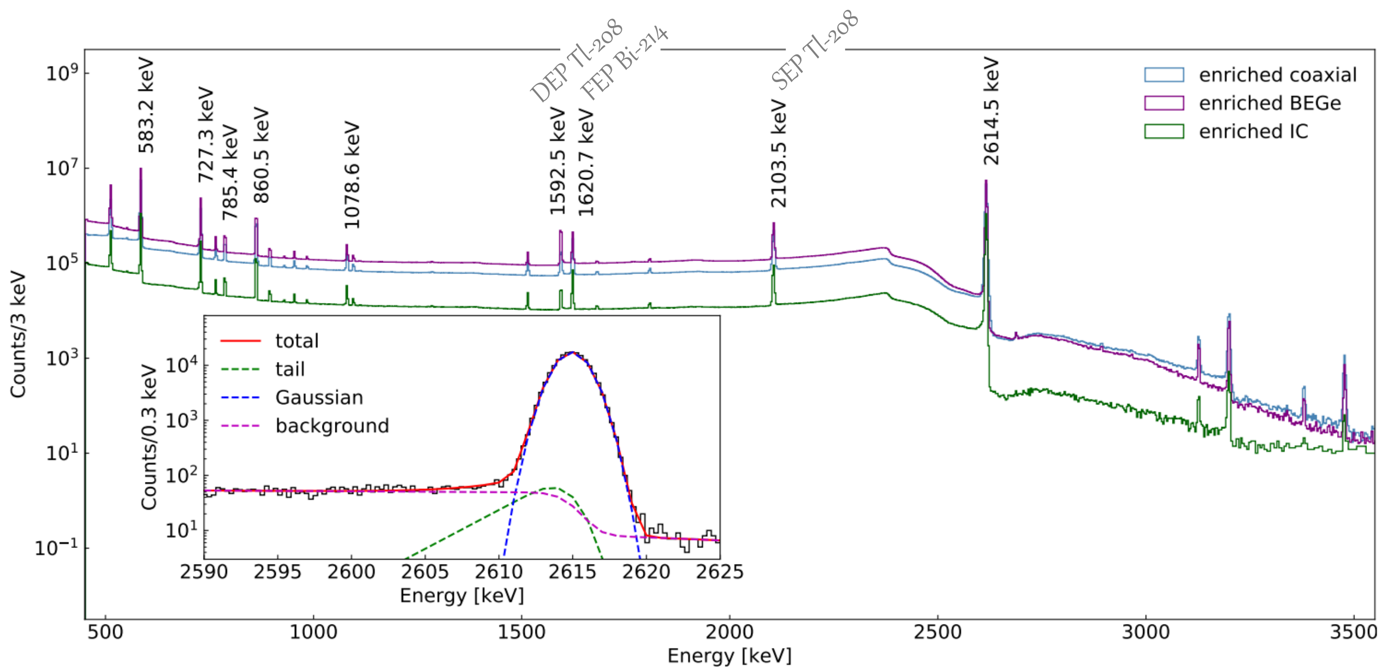

EPJ C 81 8 (2021) 682

Stability Over Time

FWHM

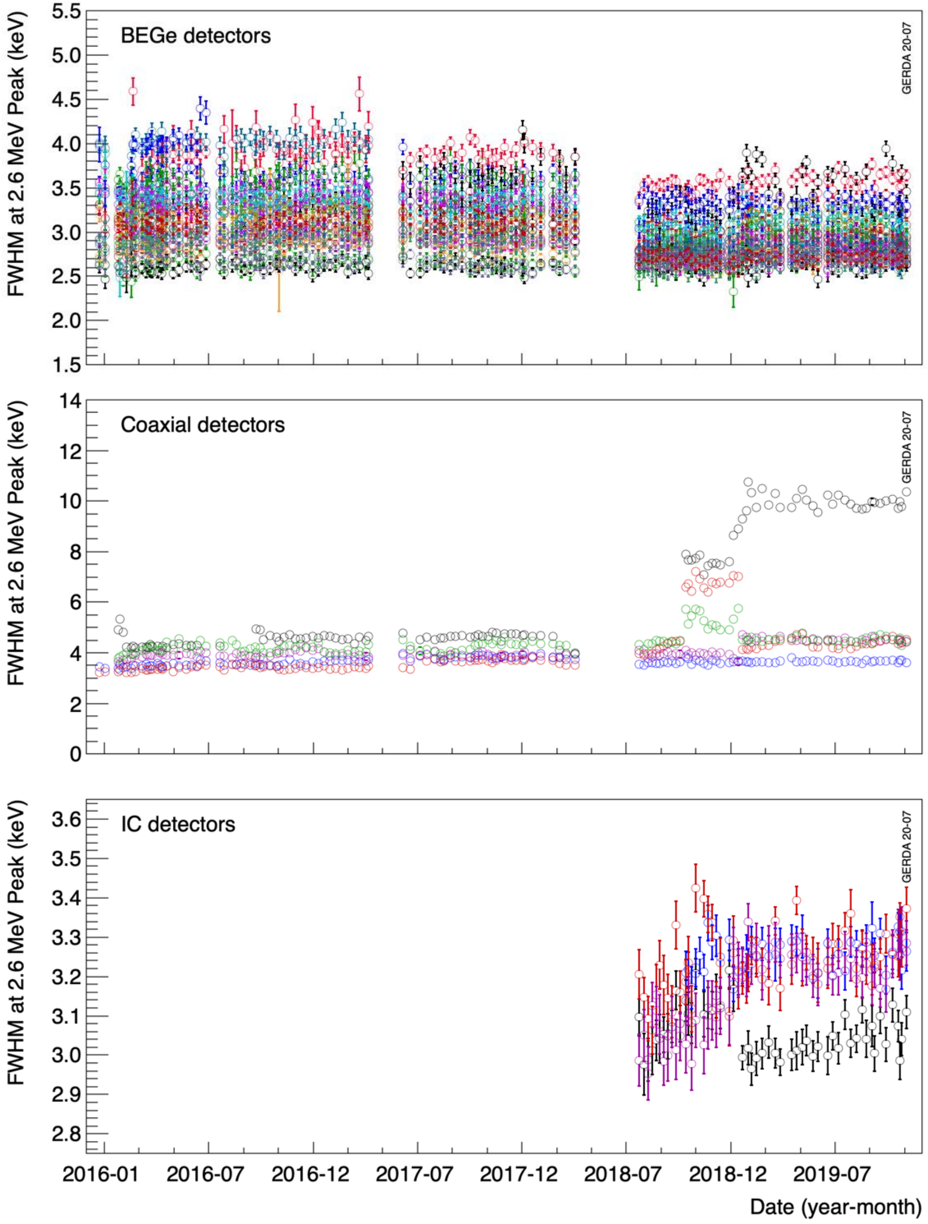

Energy shifts

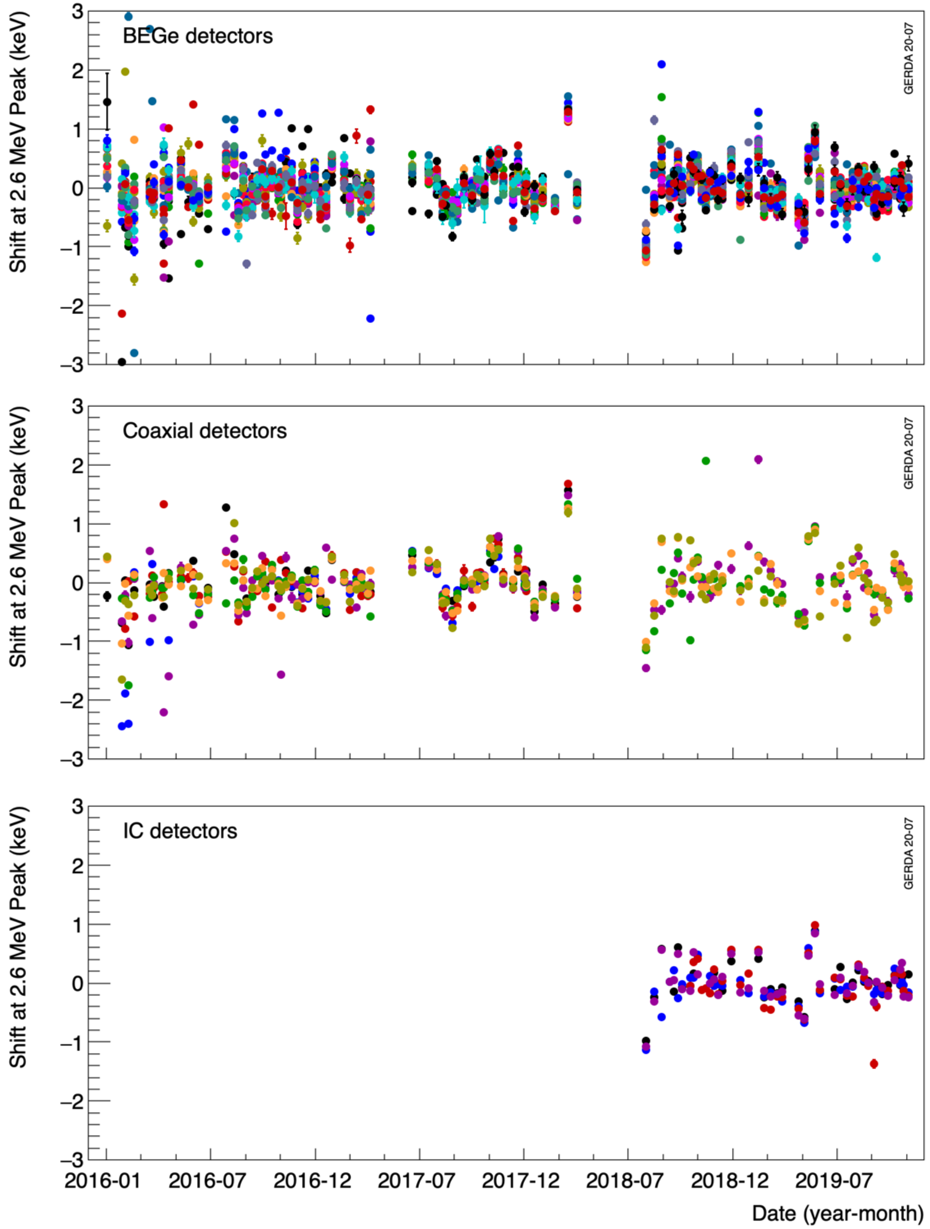

LAr Instrumentation

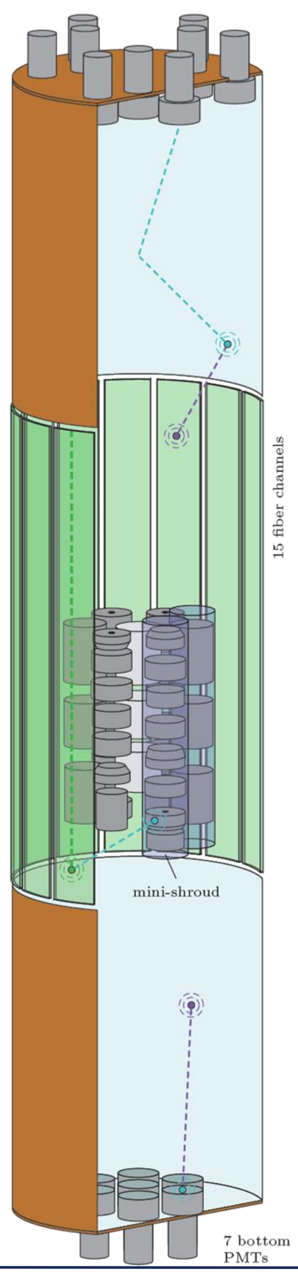

- Two barrels in LAr @ ~ 88K
  - ∅ 590 mm, H 1500 mm
  - 15 fiber channels
- Array of 6 SiPMs read in parallel
  - Ketek PM33100 3x3 mm^2
  - 405 WaveLength Shifting (WLS) fibers
- Nylon Mini-shrouds (MS)
  - Suppressiond of K-42 ions background
  - Transparent to LAr scintillation light (covered with TetraPhenyl Butadiene, TPB)
  - Nylon: low-background material
- Fiber shroud cylinder
  - ∅ 1375 mm, H 3000 mm
  - Reflected photons reach fibers without any LAr attenuation
  - Help to detect photons produced outside the barrels

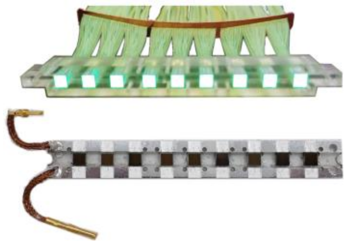

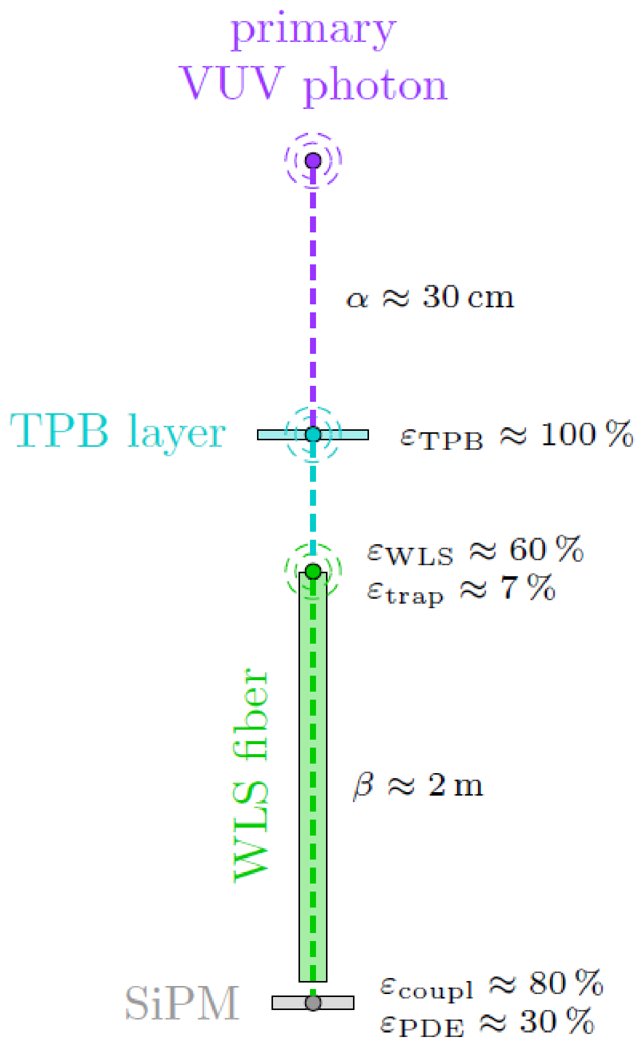

EPJ C 83 (2023) 319

LAr Veto Performance

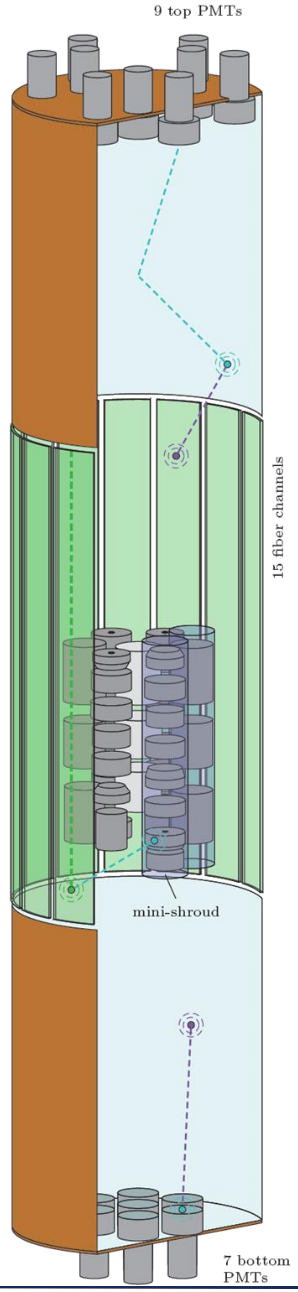

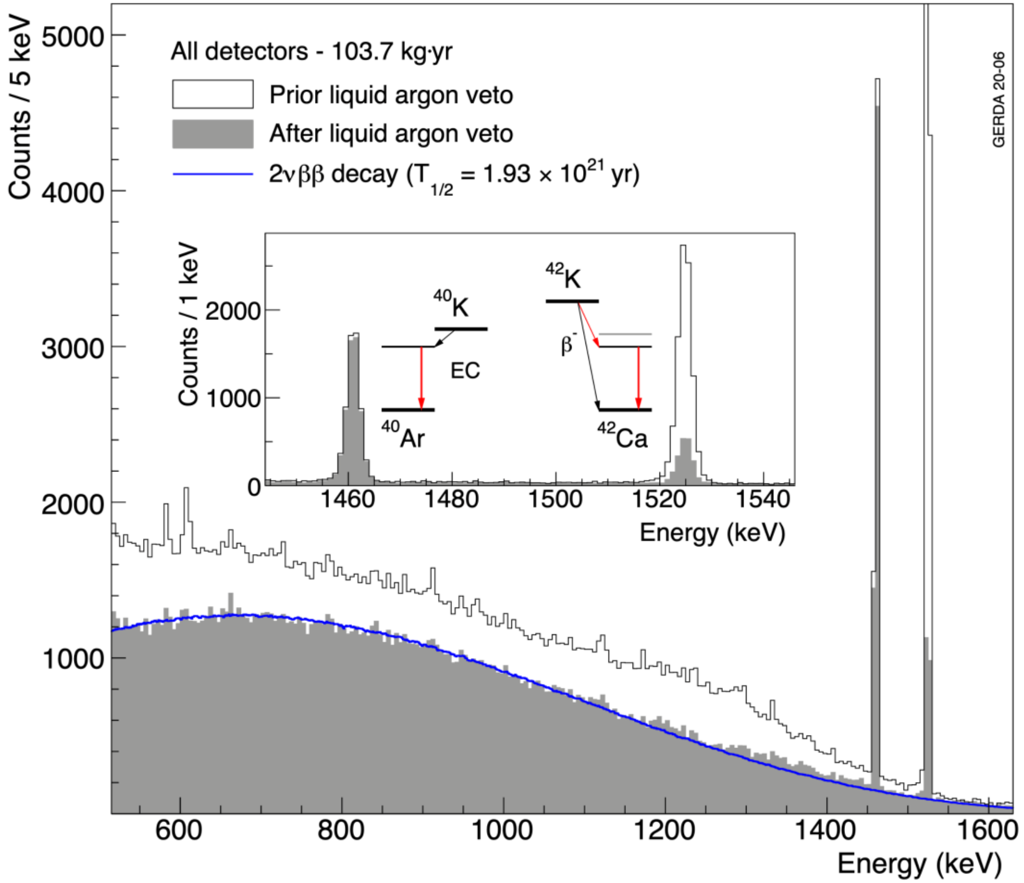

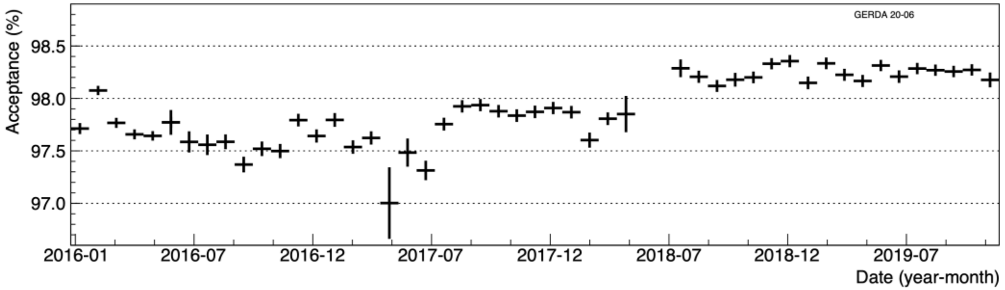

Phase II survival fraction

- K-40: 97.3 ± 0.2
- K-42: 19.7 ± 0.4

Efficiency LAr veto cut

- (97.7 ± 0.1)% in Phase II
- (98.2 ± 0.1)% in Phase II+

EPJ C 83 (2023) 319

PSD Performance

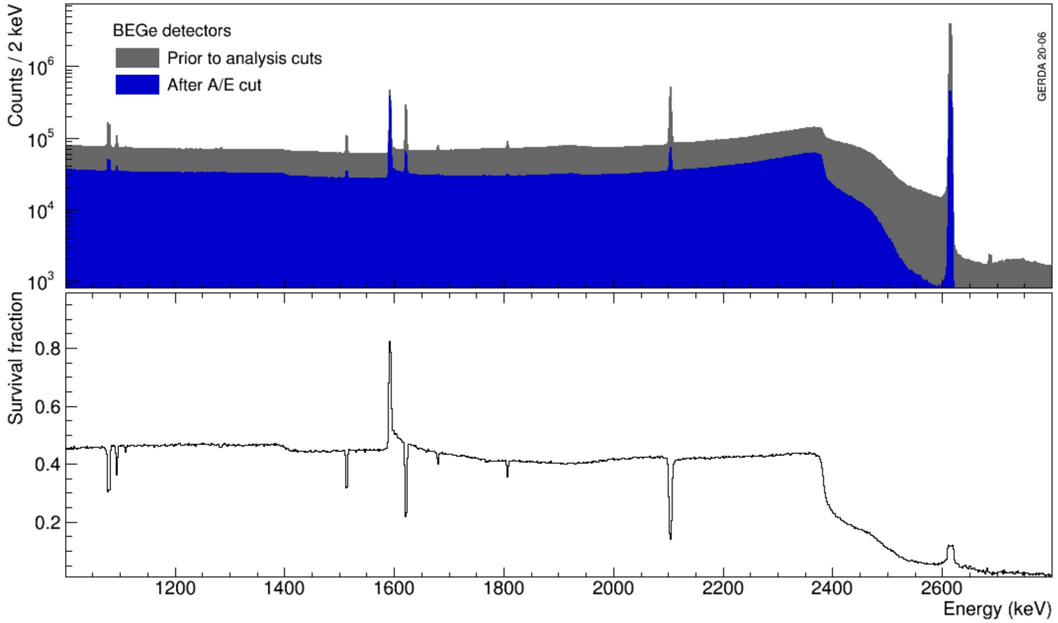

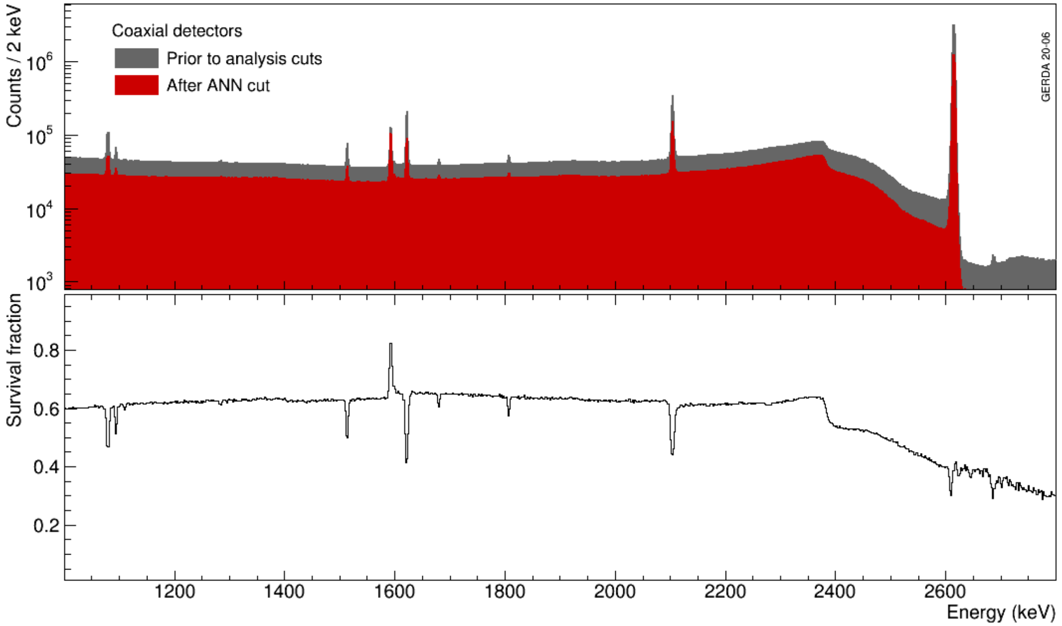

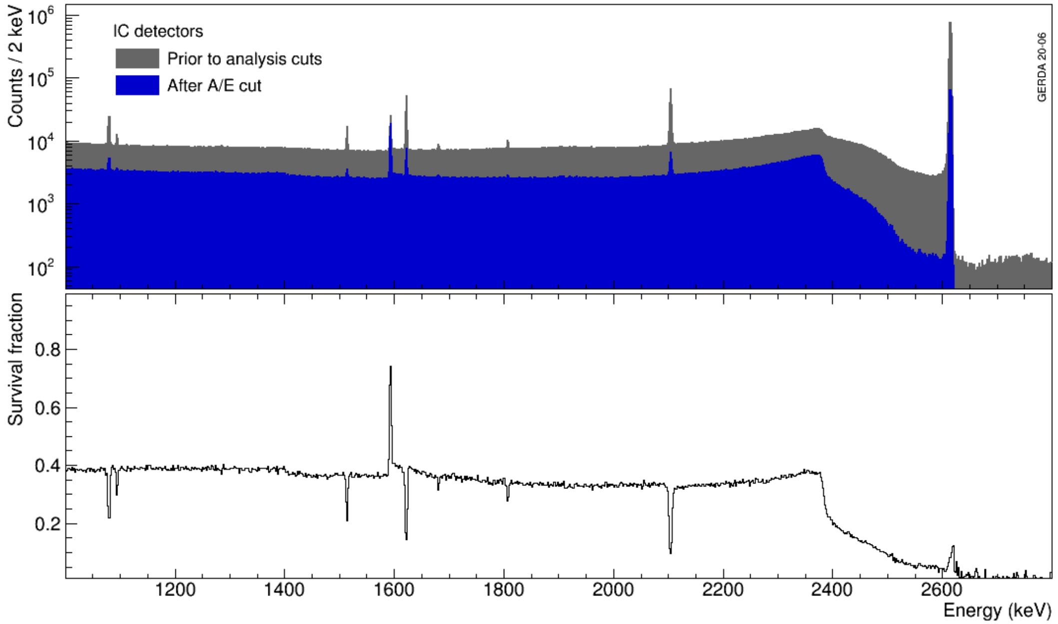

Survival fraction of calibration data events after applying PSD (A/E for BEGe/IC, ANN for COAX)

EPJ C 73 (2013) 2583, EPJ C 82 (2022) 284, PRL 125 (2020) 252502

PSD Performance

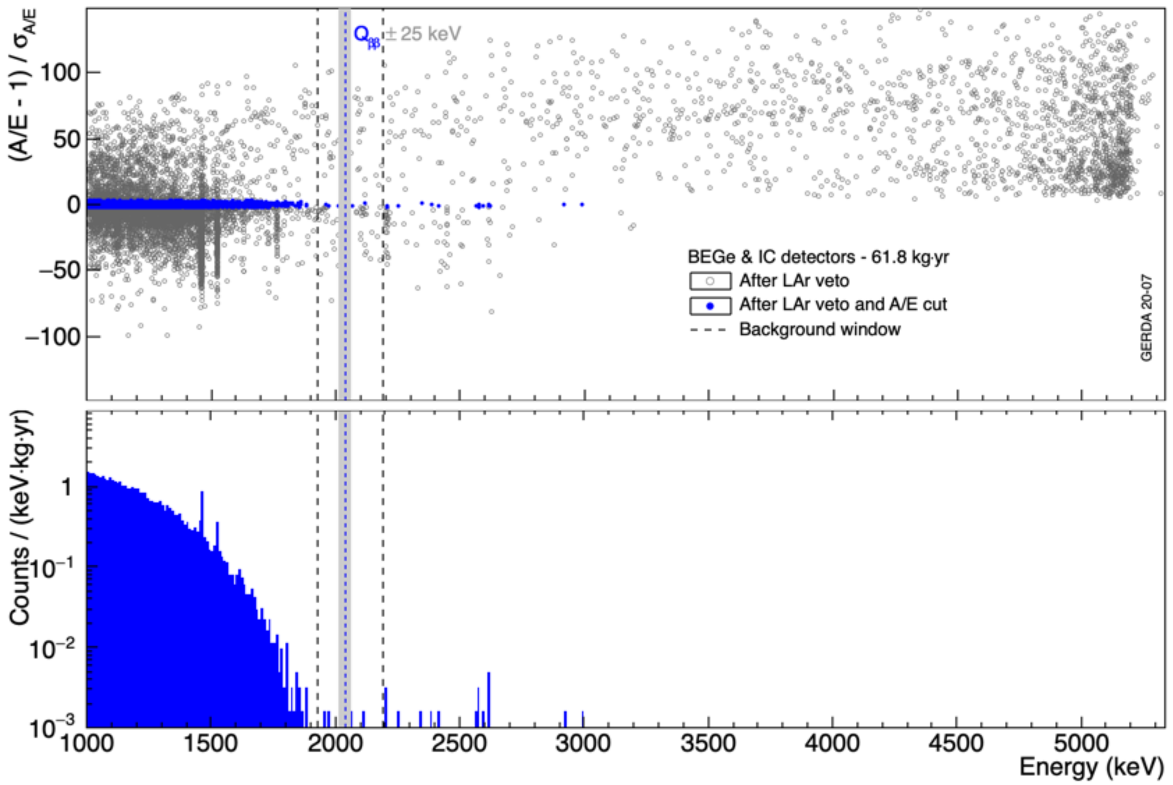

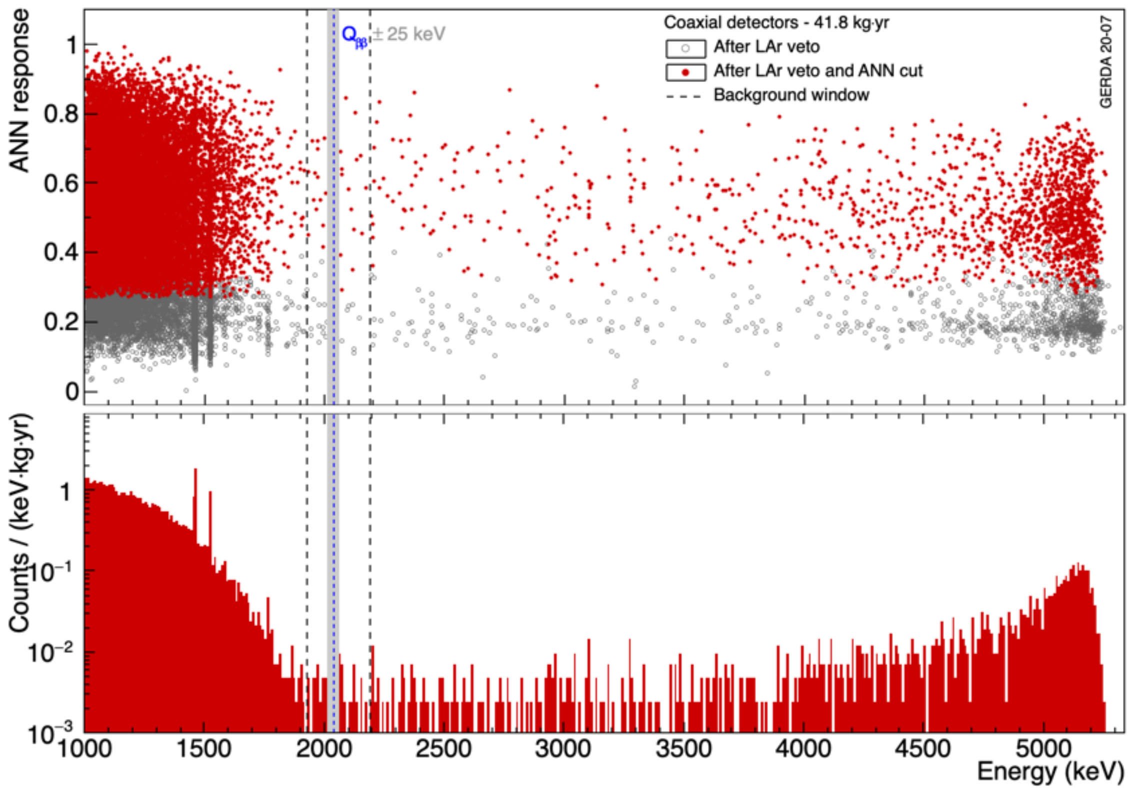

Efficiency $0\nu 2\beta$ PSD cut

Phase II (prior upgrade)

- BEGe: (88.2 ± 3.4)%
- COAX: (69.1 ± 5.6)%

Phase II+ (post upgrade)

- BEGe: (89.0 ± 4.1)%
- COAX: (68.8 ± 4.1)%
- IC: (90.0 ± 1.8)%

EPJ C 73 (2013) 2583, EPJ C 82 (2022) 284, PRL 125 (2020) 252502

GERDA Background Model

$Q_{\beta\beta}(^{76}\mathrm{Ge}) = 2039.061 \pm 0.007$ keV

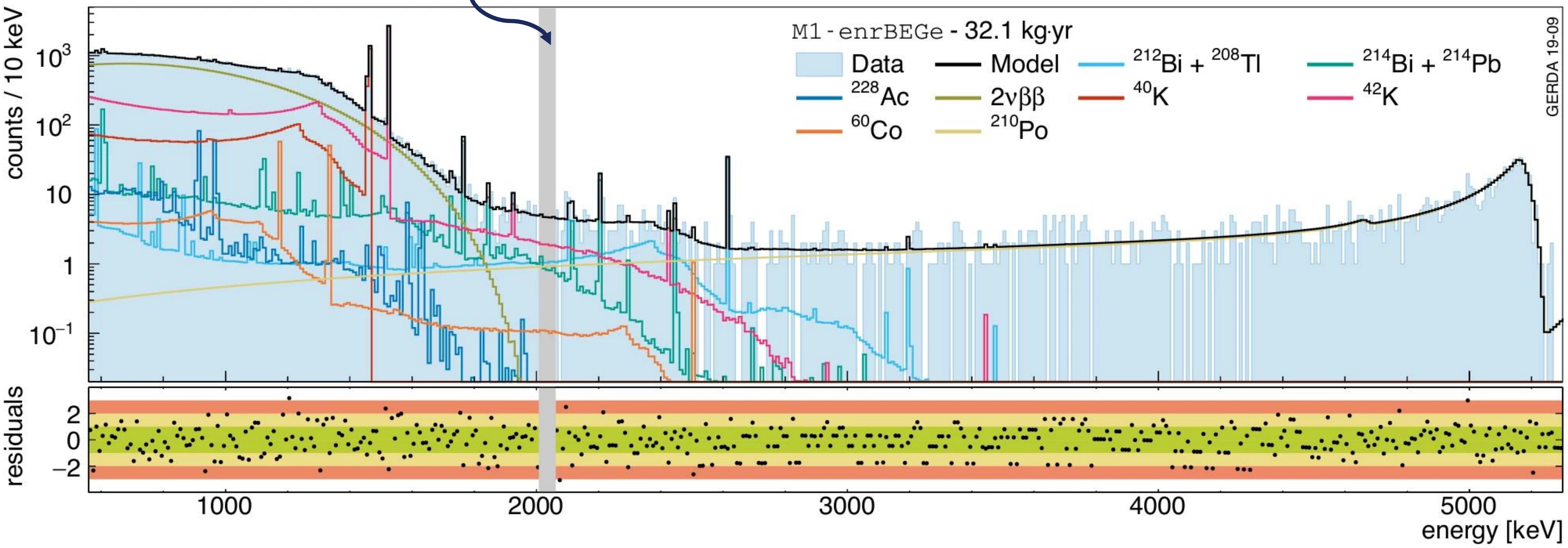

- Decomposition of the full-range energy spectrum
- Implementation of the detector array made with MaGe simulation framework
- Fundamental for
  - predicting the shape and composition of events in the $Q_{\beta\beta}$ ROI
  - identifying residual impurities and their location
  - finding alternative strategies to further reduce the background

J HEP. 2020, 139 (2020)

BSM Datasets

Search	Exposure [kg yr]	Phase	Motivation
Exotic Searches in $2\nu2\beta$ Decays	32.8	II - BEGe only	Minimize the systematic uncertainties; LAr instrumentation was upgraded but the changes were not included in the modelling of the LAr veto system
Tri-nucleon decays	61.9	(II,II+) - after 2017 only	Use data in which the detectors' trigger threshold was lowered to ~20 keV
Neutron & proton decays Electron decay Bosonic DM interactions	105.5	(II,II+)	Use data with LAr veto
$0\nu ECEC$ ^{36}Ar decay	2.81 + 8.401 *	I & (II,II+)	

(*) Product between the detection efficiency and the simulated mass of the LAr volume.
The value 2.81 kg yr for Phase I has been taken from EPJ C 76 (2016) 652

Comparison for Exotic Emissions

JCAP 12 (2022) 012

Majorons Emission

Decay mode / Isotope	$T_{1/2}$ (yr)	Ref.	G ($10^{-18}\,yr^{-1}$)	NME	g_J
$0\nu\beta\beta J$ ($n=1$)					
^{76}Ge	$> 6.4{\cdot}10^{23}$	present	44.2	(2.66 – 6.64)	$< (1.8 - 4.4){\cdot}10^{-5}$
^{136}Xe	$> 2.6{\cdot}10^{24}$	[54]	409	(1.11 – 4.77)	$< (0.4 - 1.7){\cdot}10^{-5}$
^{136}Xe	$> 4.3{\cdot}10^{24}$	[57]	409	(1.11 – 4.77)	$< (0.3 - 1.3){\cdot}10^{-5}$
^{100}Mo	$> 4.4{\cdot}10^{22}$	[55]	598	(3.84 – 6.59)	$< (1.8 - 3.1){\cdot}10^{-5}$
^{116}Cd	$> 8.2{\cdot}10^{21}$	[56]	569	(3.105 – 5.43)	$< (5.3 - 9.2){\cdot}10^{-5}$
$0\nu\beta\beta J$ ($n=2$)					
^{76}Ge	$> 2.9{\cdot}10^{23}$	present	–	–	–
^{136}Xe	$> 1.0{\cdot}10^{24}$	[54]	–	–	–
^{136}Xe	$> 9.8{\cdot}10^{23}$	[57]	–	–	–
^{100}Mo	$> 9.9{\cdot}10^{21}$	[28]	–	–	–
^{116}Cd	$> 4.1{\cdot}10^{21}$	[56]	–	–	–

Decay mode / Isotope	$T_{1/2}$ (yr)	Ref.	G ($10^{-18}\,yr^{-1}$)	NME	g_J
$0\nu\beta\beta J$ ($n=3$)					
^{76}Ge	$> 1.2{\cdot}10^{23}$	present	0.073	0.381	$< 1.7\cdot10^{-2}$
^{136}Xe	$> 4.5{\cdot}10^{23}$	[54]	1.47	0.160	$< 0.47\cdot10^{-2}$
^{136}Xe	$> 6.3{\cdot}10^{23}$	[57]	1.47	0.160	$< 0.40\cdot10^{-2}$
^{100}Mo	$> 4.4{\cdot}10^{21}$	[28]	2.42	0.263	$< 2.3\cdot10^{-2}$
^{116}Cd	$> 2.6{\cdot}10^{21}$	[56]	2.28	0.144	$< 5.6\cdot10^{-2}$
$0\nu\beta\beta JJ$ ($n=3$)					
^{76}Ge	$> 1.2{\cdot}10^{23}$	present	0.22	0.0026	< 1.21
^{136}Xe	$> 4.5{\cdot}10^{23}$	[54]	3.05	0.0011	< 0.69
^{136}Xe	$> 6.3{\cdot}10^{23}$	[57]	3.05	0.0011	< 0.64
^{100}Mo	$> 4.4{\cdot}10^{21}$	[28]	6.15	0.0019	< 1.41
^{116}Cd	$> 2.6{\cdot}10^{21}$	[56]	5.23	0.000945	< 2.37
$0\nu\beta\beta JJ$ ($n=7$)					
^{76}Ge	$> 1.0{\cdot}10^{23}$	present	0.42	0.0026	< 1.08
^{136}Xe	$> 1.1{\cdot}10^{22}$	[54]	12.5	0.0011	< 1.23
^{136}Xe	$> 5.1{\cdot}10^{22}$	[57]	12.5	0.0011	< 0.84
^{100}Mo	$> 1.2{\cdot}10^{21}$	[28]	50.8	0.0019	< 1.15
^{116}Cd	$> 8.9{\cdot}10^{20}$	[56]	33.9	0.000945	< 1.94

Sterile Neutrino Emission

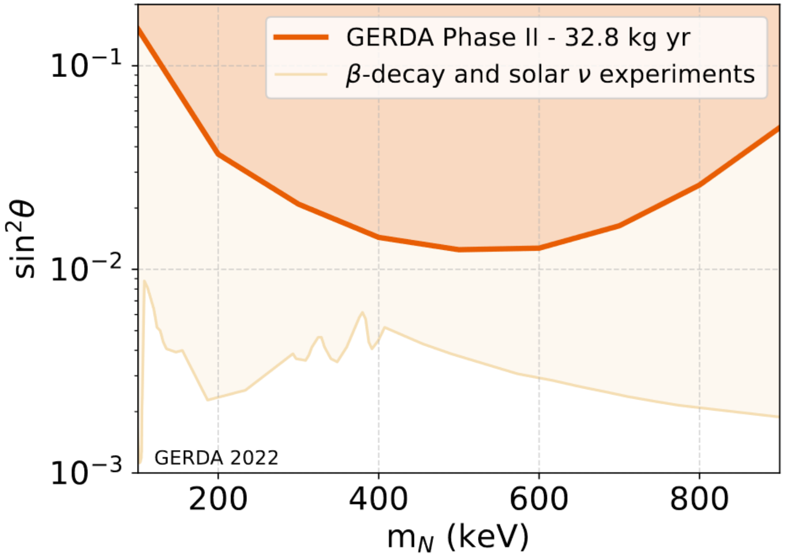

Lorentz Violation

Isotope	Limits on $\mathring{a}_{of}^{(3)}$ (GeV) at 90% C.L.	Ref.
^{76}Ge	$(-2.7 < \mathring{a}_{of}^{(3)} < 6.2)\cdot10^{-6}$	this work
^{136}Xe	$-2.65\cdot10^{-5} < \mathring{a}_{of}^{(3)} < 7.6\cdot10^{-6}$	EXO-200
^{116}Cd	$\mathring{a}_{of}^{(3)} < 4.0\cdot10^{-6}$	AURORA
^{100}Mo	$(-4.2 < \mathring{a}_{of}^{(3)} < 3.5)\cdot10^{-7}$	NEMO-3
^{82}Se	$\mathring{a}_{of}^{(3)} < 4.1\cdot10^{-6}$	CUPID-0
^{3}H (single-β decay)	$\lvert\mathring{a}_{of}^{(3)}\rvert < 2\cdot10^{-8}$	Díaz *et al.*
	$\lvert\mathring{a}_{of}^{(3)}\rvert < 3\cdot10^{-8}$	KATRIN

BSM decays

Comparison for inclusive tri-nucleon decays

Experiment	Decay	$\tau_b[x]$ (yr)
GERDA	$^{76}Ge \xrightarrow{ppp} {}^{73}Cu + X$	1.20×10^{26}
	$^{76}Ge \xrightarrow{ppn} {}^{73}Zn + X$	1.20×10^{26}
	$^{76}Ge \xrightarrow{pnn} {}^{73}Ga + X$	1.20×10^{26}
	$^{76}Ge \xrightarrow{nnn} {}^{73}Ge + X_{invisble}$	$k \times 10^{26}$
MAJORANA [19]	$^{76}Ge \xrightarrow{ppp} {}^{73}Cu + X$	1.08×10^{25}
	$^{76}Ge \xrightarrow{ppp} {}^{73}Cu\, e^+\pi^+\pi^+$	6.78×10^{25}
	$^{76}Ge \xrightarrow{ppn} {}^{73}Zn\, e^+\pi^+$	7.03×10^{25}
EXO-200 [20]	$^{136}Xe \xrightarrow{ppp} {}^{133}Sb + X$	3.3×10^{23}
	$^{136}Xe \xrightarrow{ppn} {}^{133}Te + X$	1.9×10^{23}
Hazama et al. [21]	$^{127}I \xrightarrow{nnn} {}^{124}I + X$	1.8×10^{23}

EPJ C 83 (2023) 778

Doppler Broadening effect in the electron semi-visible decay

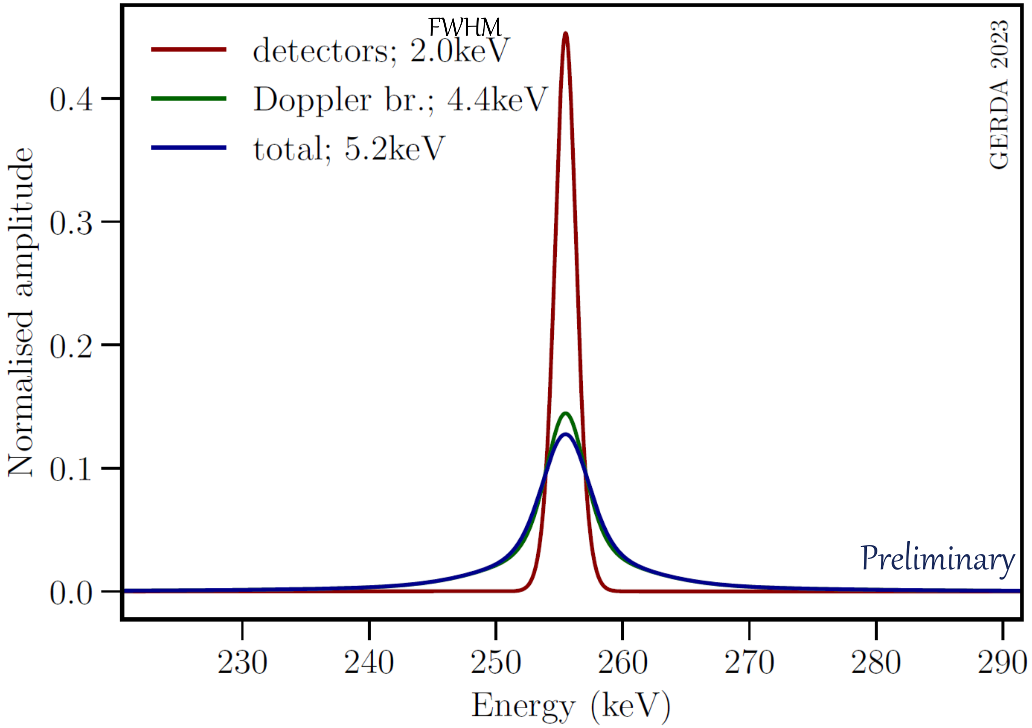

Bosonic Dark Matter Interactions

Two dark matter candidates:

- **vector DM** (*dark photons*), $\mathcal{L}_V = g_V V_\mu \bar{\psi}\gamma^\mu\psi$
- **pseudoscalar DM** (*axion-like particles*), $\mathcal{L}_a = g_a a\bar{\psi}i\gamma_5\psi$

Absorption

$$R_V^{abs} = \frac{4.7\cdot 10^{23}}{A}\cdot\frac{\sigma_{pe}}{m_V}\cdot\varepsilon_\beta\cdot\boldsymbol{\frac{\alpha'}{\alpha}}$$

$$R_a^{abs} = \frac{1.5\cdot 10^{19}}{A}\cdot\sigma_{pe}\cdot m_a\cdot\varepsilon_\beta\cdot\boldsymbol{g_{ae}^2}$$

Scattering

$$R_V^C = \frac{n_e\rho_{DM}}{\rho_T m_V}\cdot\frac{e^4}{24\pi m_e^2}\cdot\frac{(m_V^2+2m_e m_V+2m_e^2)(m_V+2m_e)}{(m_V+m_e)^3}\cdot\varepsilon_{\beta+\gamma}\cdot\boldsymbol{\frac{\alpha'}{\alpha}}$$

$$R_a^C = \frac{n_e\rho_{DM}}{\rho_T}\cdot\frac{e^2}{16\pi m_e^2}\cdot\frac{m_a(m_a+2m_e)^2}{(m_a+m_e)^4}\cdot\varepsilon_{\beta+\gamma}\cdot\boldsymbol{g_{ae}^2}$$

V = vector SW
a = pseudoscalar SW
A = Ge atomic mass
σ_{pe} = Ge photoelectric x-section

ε = detection efficiency
$m_{V/a}$ = V/a SW mass
$e^2 = 4\pi\alpha$
m_e = electron mass

ρ_T = target density
ρ_{DM} = DM density (0.3 Gev/cm^3)
n_e = target number density of electrons
g_{ae}, α'/α = SW couplings to electrons

$$\sigma_{pe} = \sqrt{\frac{32}{\gamma^7}}\alpha^4 Z^5\sigma_{Th}$$

$$\gamma = (2\pi\nu)/(m_e)$$

$$\sigma_{Th} = \frac{8}{3}\pi r_e^2$$

Vector DM

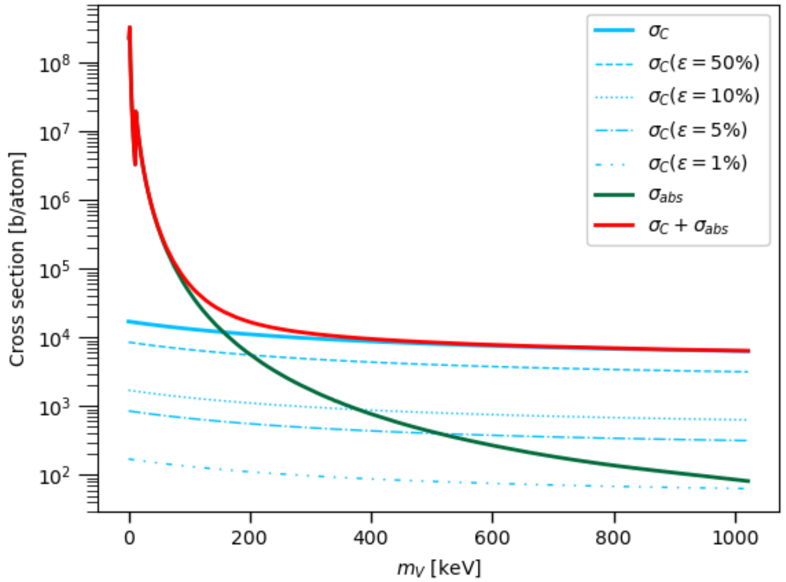

Pseudoscalar DM

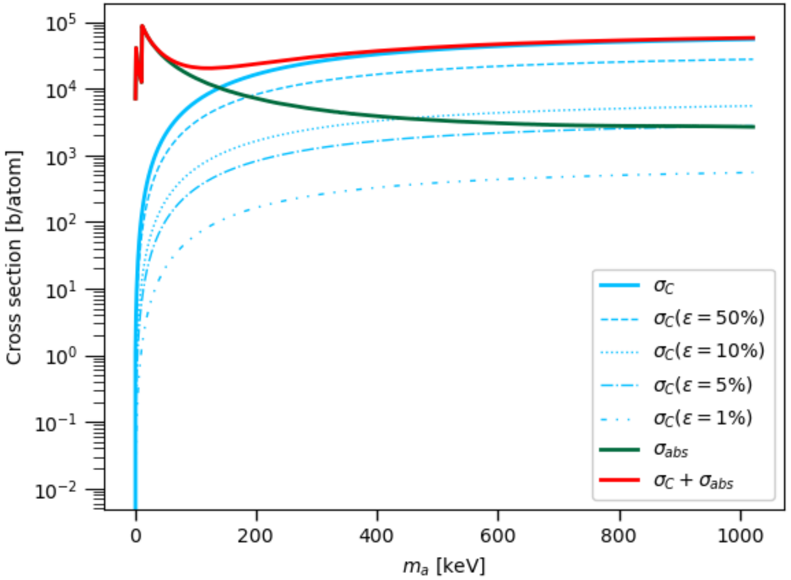

0ν2β Decay

$$\left(T_{1/2}^{0\nu}\right)^{-1} = G^{0\nu}(Q_{\beta\beta}, Z)|M^{0\nu}|^2 \left(\frac{m_{\beta\beta}}{m_e}\right)^2$$

Phase-space integral

arXiv: 1209.5722

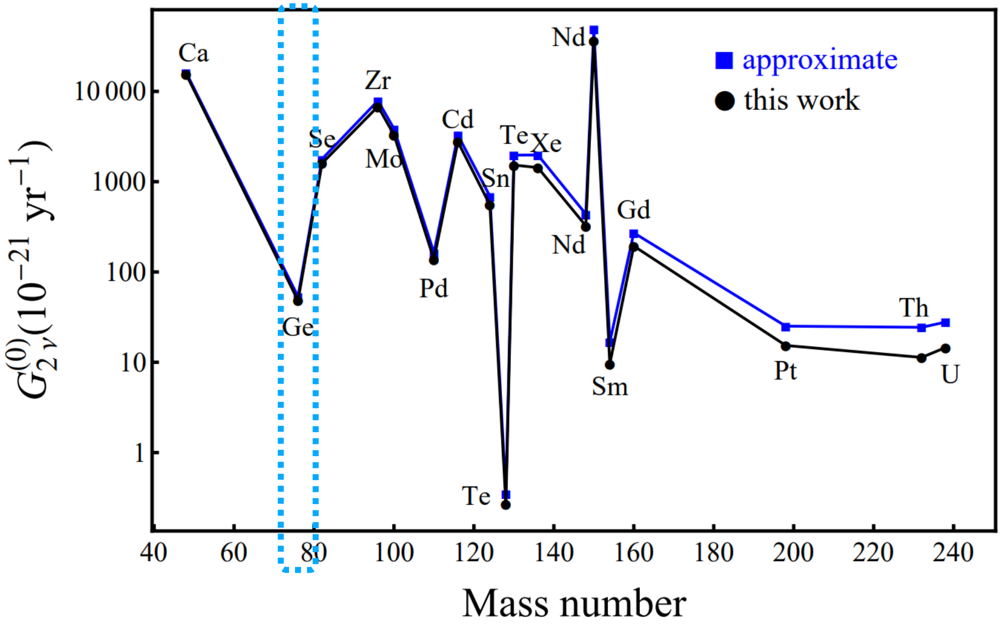

Nuclear Matrix Element

arXiv:2202.01787

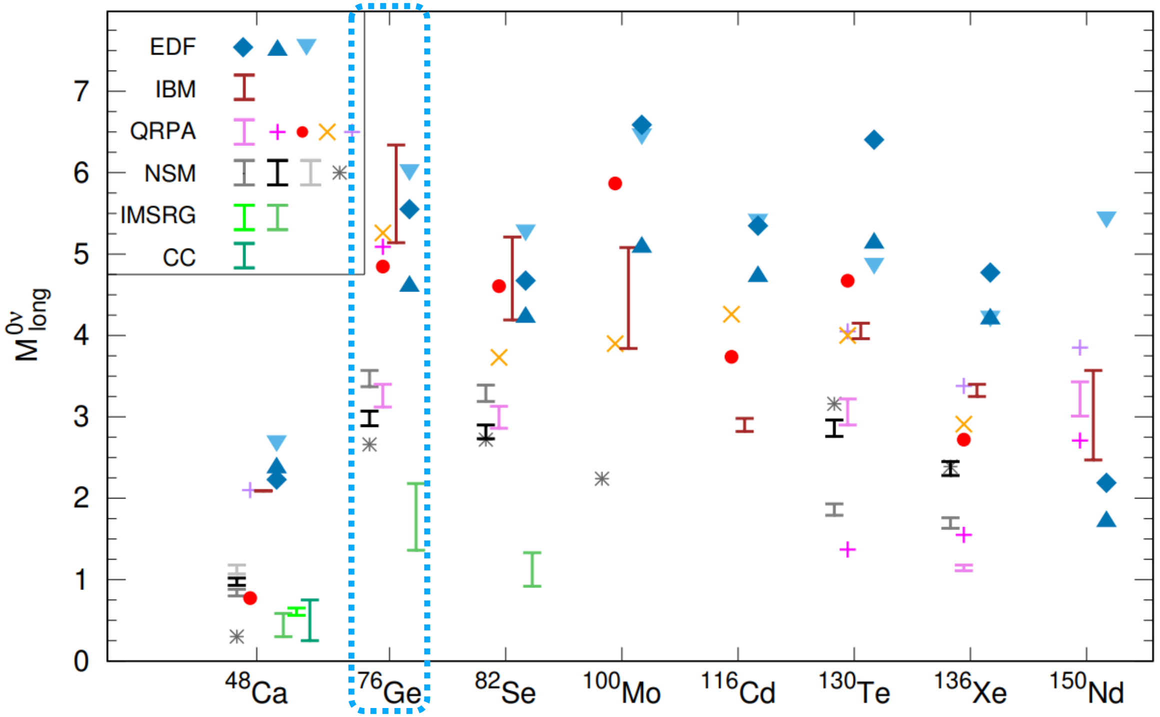

0ν2β Isotopes

arXiv:2202.01787

Isotope	Daughter	$Q_{\beta\beta}$ [a] [keV]	f_{nat} [b] [%]	f_{enr} [c] [%]	$T_{1/2}^{2\nu\beta\beta}$ [d] [yr]	$T_{1/2}^{0\nu\beta\beta}$ [e] [yr]
^{48}Ca	^{48}Ti	4 267.98(32)	0.187(21)	16	$(6.4^{+0.7}_{-0.6}(\text{stat})^{+1.2}_{-0.9}(\text{syst})) \cdot 10^{19}$	$> 5.8 \cdot 10^{22}$
^{76}Ge	^{76}Se	2 039.061(7)	7.75(12)	92	$(1.926 \pm 94) \cdot 10^{21}$	$> 1.8 \cdot 10^{26}$
^{82}Se	^{82}Kr	2 997.9(3)	8.82(15)	96.3	$(8.60 \pm 0.03(\text{stat})^{+0.19}_{-0.13}(\text{syst})) \cdot 10^{19}$	$> 3.5 \cdot 10^{24}$
^{96}Zr	^{96}Mo	3 356.097(86)	2.80(2)	86	$(2.35 \pm 0.14(\text{stat}) \pm 0.16(\text{syst})) \cdot 10^{19}$	$> 9.2 \cdot 10^{21}$
^{100}Mo	^{100}Ru	3 034.40(17)	9.744(65)	99.5	$(7.12^{+0.18}_{-0.14}(\text{stat}) \pm 0.10(\text{syst})) \cdot 10^{18}$	$> 1.5 \cdot 10^{24}$
^{116}Cd	^{116}Sn	2 813.50(13)	7.512(54)	82	$(2.63^{+0.11}_{-0.12}) \cdot 10^{19}$	$> 2.2 \cdot 10^{23}$
^{130}Te	^{130}Xe	2 527.518(13)	34.08(62)	92	$(7.71^{+0.08}_{-0.06}(\text{stat})^{+0.12}_{0.15}(\text{syst})) \cdot 10^{20}$	$> 2.2 \cdot 10^{25}$
^{136}Xe	^{136}Ba	2 457.83(37)	8.857(72)	90	$(2.165 \pm 0.016(\text{stat}) \pm 0.059(\text{syst})) \cdot 10^{21}$	$> 1.1 \cdot 10^{26}$
^{150}Nd	^{150}Sm	3 371.38(20)	5.638(28)	91	$(9.34 \pm 0.22(\text{stat})^{+0.62}_{-0.60}(\text{syst})) \cdot 10^{18}$	$> 2.0 \cdot 10^{22}$

0ν2β Experiments

arXiv:2202.01787

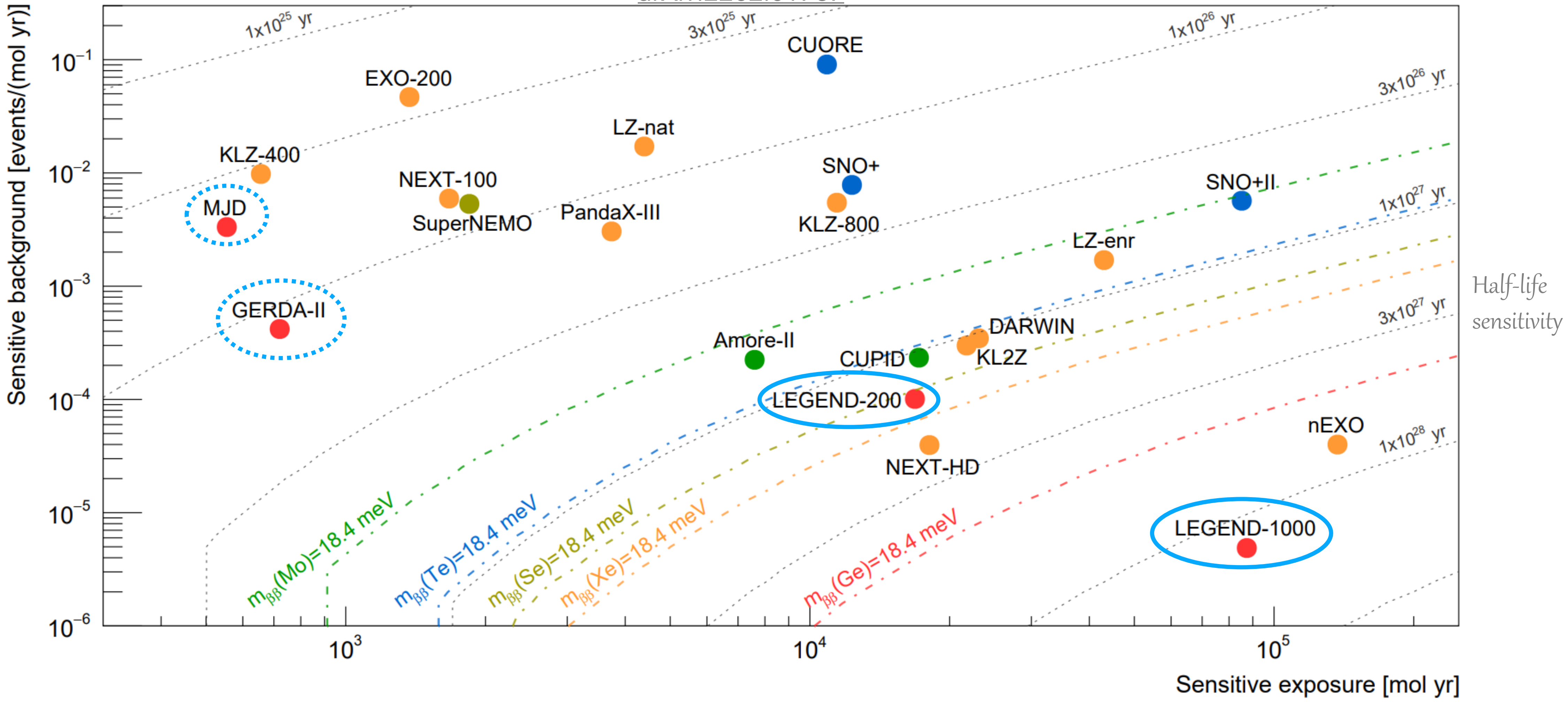

LEGEND-200: $T_{1/2}^{0\nu} > 10^{27}$ yr @ 90% CL

LEGEND-1000: $T_{1/2}^{0\nu} > 1.6 \cdot 10^{28}$ yr @ 90% CL

- Assumption: 10 yr of data acquisition for all experiments, but for those that already finished to operate (*)
- The colourful-dashed lines correspond to the half-life sensibility requested to test the inverted hierarchy with isotopes Mo-100, Te-130, Se-82, Xe-136, Ge-76

Inverted or Normal Hierarchy?

arXiv:2202.01787

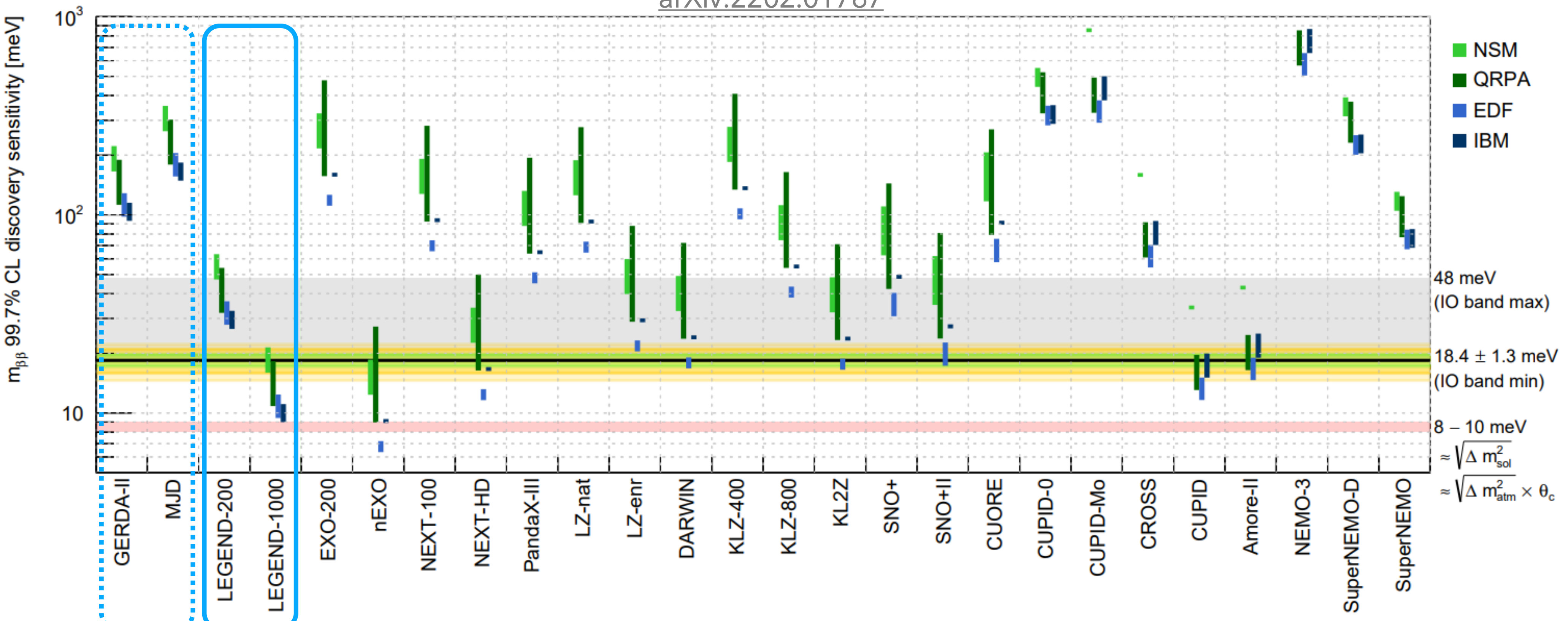

LEGEND-200: $m_{\beta\beta} < 34 - 78$ meV

LEGEND-1000: $m_{\beta\beta} < 8.5 - 19.4$ meV

- Gray band: range of $m_{\beta\beta}$ values for the inverted order (IO) and $m_{light} \rightarrow 0$
- **$m_{\beta\beta}$=18.4 meV: minimum value allowed for the IO**
- 1σ, 2σ, 3σ uncertainty bands for $m_{\beta\beta}$=18.4 meV are shown in green, orange and yellow, respectively
- **Red band at 8-10 meV: future aim for 0νββ next-generation experiments**
- NSM (*Nuclear Shell Model*), QRPA (*Quasiparticle Random-Phase Approximation*), EDF (*Energy-Density Functional*), IBM (*Interacting Boson Model*): models and nuclear theories used in extracting the *Nuclear Matrix Elements* (NMEs)

The GERDA Collaboration

GERDA = GERmanium Detector Array